LBL-7057
UC-66b

CATALOGUE OF MAGNETOTELLURIC APPARENT RESISTIVITY PSEUDO-SECTIONS OVER TWO-DIMENSIONAL MODELS

Ki Ha Lee, Victor Labson,
Michael Wilt, and Norman Goldstein

August 1978

Prepared for the Division of Geothermal
Energy of the U. S. Department of Energy
under Contract W-7405-ENG-48

LBL-7057

LBL-7057

CATALOGUE OF MAGNETOTELLURIC APPARENT RESISTIVITY PSEUDO-SECTIONS OVER TWO-DIMENSIONAL MODELS*

Ki Ha Lee
Victor Labson

Engineering Geoscience
University of California
Berkeley, California 94720

Michael Wilt
Norman Goldstein

Earth Sciences Division
Lawrence Berkeley Laboratory
University of California
Berkeley, California 94720

*Work supported by Division of Geothermal Energy of the U.S. Department of Energy.

INTRODUCTION

As part of the LBL program on geothermal exploration technique evaluation and development, the magnetotelluric method was evaluated in a Basin and Range environment (Beyer et al., 1976). One development from this effort is an improved two-dimensional magnetotelluric resistivity computer algorithm, called TEM, capable of calculating the transverse electric (TE) and transverse magnetic (TM) soundings over an arbitrary two-dimensional body. Using this program the first author (KHL) generated a series of magnetotelluric pseudo-sections over a set of two-dimensional models which in a gross sense typify structure and resistivities of northern Nevada.

This catalogue may be used for qualitative evaluation of existing MT data or for planning future surveys.

METHOD AND PROGRAM

The basic algorithm used in TEM was developed by Ryu (1971) at U.C. Berkeley Engineering Geoscience Group and later improved by one of the authors (KHL). The algorithm is based on the finite element method for calculating the response of an arbitrary two-dimensional earth to a vertically incident plane wave at specified frequencies. From the calculated electromagnetic fields, the program computes soundings for the electric field oriented parallel to strike (transverse electric, TE-mode) and for the electric field perpendicular to strike (transverse magnetic, TM-mode). The ratio of vertical to horizontal magnetic fields (tipper) is also computed for the TE case (there is no vertical magnetic field in the TM response).

For the TE response the electric fields are calculated from the incident plane wave source over the resistivity model using the finite element method. The corresponding magnetic fields are then computed by numerical differentiation of the electric fields via Maxwell's equations. In this case the following relation holds:

$$\rho_{yx}(\omega) = \frac{1}{\omega\mu} \left|\frac{E_y}{H_x}\right|^2 ,$$

where $\rho_{yx}(\omega)$ is the TE-mode apparent resistivity at angular frequency ω; μ is the magnetic permeability; E_y and H_x are the orthogonal electric and magnetic field strengths, respectively.

The tipper is calculated as:

$$T(\omega) = \left|\frac{H_z}{H_x}\right| e^{j\phi(\omega)} ,$$

where $\phi(\omega)$ is the tipper phase.

For the TM response the magnetic fields are calculated from the finite element method and the electric fields are computed via Maxwell's equations from the magnetic fields. In this case the TM-mode apparent resistivity is defined as:

$$\rho_{xy}(\omega) = \frac{1}{\omega\mu} \left|\frac{E_x}{H_y}\right|^2 .$$

With the TEM program, the user inputs the earth resistivity model with a grid of data values; either a small grid of size 55 x 36 or a large grid of size 101 x 56 may be used. Each grid is composed of two regions. The inhomogeneities are restricted to an internal region surrounded by a one-dimensional external region. The size of the internal inhomogeneous region is determined by the geometry of the body to be modeled and the average resistivity of the external region. The resistivity of the external region is important in these calculations because the outermost nodal points must not be affected by the secondary fields generated by inhomogeneities within the internal region. The internal region is therefore restricted to a size controlled by "skin depths" computed by using the average resistivity of the external region. Skin depth is the distance over which an electromagnetic wave of period T, traveling through a medium of average resistivity ρ, is attenuated to approximately one third of its original value. It is expressed as

$$\delta = 0.5\sqrt{\rho T} ,$$

where δ is the skin depth in kilometers and ρ and T are in ohm-meters and seconds, respectively. With the small grid the inhomogeneous region may be 3 x 2.4 skin depths in dimension; the large grid allows 5.2 x 4 for the internal region.

The program is capable of generating an unlimited number of MT resistivity sounding curves for points over the section.

Another program, PSDPLT, written by one of the authors (VL) takes the TEM program output and plots pseudo-sections of apparent resistivities and tippers as shown in the appendices.

The major drawback to program TEM, as with any other highly accurate numerical solution over a large grid, is the high cost of computer runs. Using the LBL CDC 7600 computer, we find that a run on the small grid costs approximately $7 per frequency or approximately $120 for a suite of 17 frequency soundings or profiles. The large grid costs $40 per frequency or $700 for 17 frequency soundings.

THE CATALOGUE

This catalogue is presented without analysis or discussion of 16 two-dimensional resistivity pseudo-sections.

For each model section, apparent resistivity vs. period is plotted for the TE-mode and TM-mode. In addition, tipper amplitude vs. period is plotted for the TE-mode. The plots were constructed from 55 to 100 soundings made at 17 frequencies. Models have been divided into six types:

1. Semi-infinite vertical contact, Models 1-a, 1-b and 1-c (Appendix 1).
2. Vertical contact in surface layer, Models 2-a and 2-b (Appendix 2).

3. Vertical contact concealed by a surface layer, Models 3-a, 3-b, and 3-c (Appendix 3).
4. Shallow basin, Models 4-a, 4-b, 4-c and 4-d (Appendix 4).
5. Vertical inhomogeneity beneath a surface layer, Model 5-a (Appendix 5).
6. Two-layer basin overlying deep conductor, Models 6-a, 6-b and 6c (Appendix 6).

A version of this program will be available with documentation in the Fall of 1978. Information will be available through the Engineering Geosciences Department, University of California, Berkeley.

REFERENCES

Beyer, H., A. Dey, A. Liaw, T.V. McEvilly, H.F. Morrison and H. Wollenberg, 1976. Preliminary Open File Report: Geological and Geophysical Studies in Grass Valley, Nevada, Lawrence Berkeley Laboratory LBL-5262, 144 p.

Ryu, Jisoo, 1971. Low-Frequency Electromagnetic Scattering, Ph.D. thesis, Engineering Geoscience, University of California, Berkeley, 108 p.

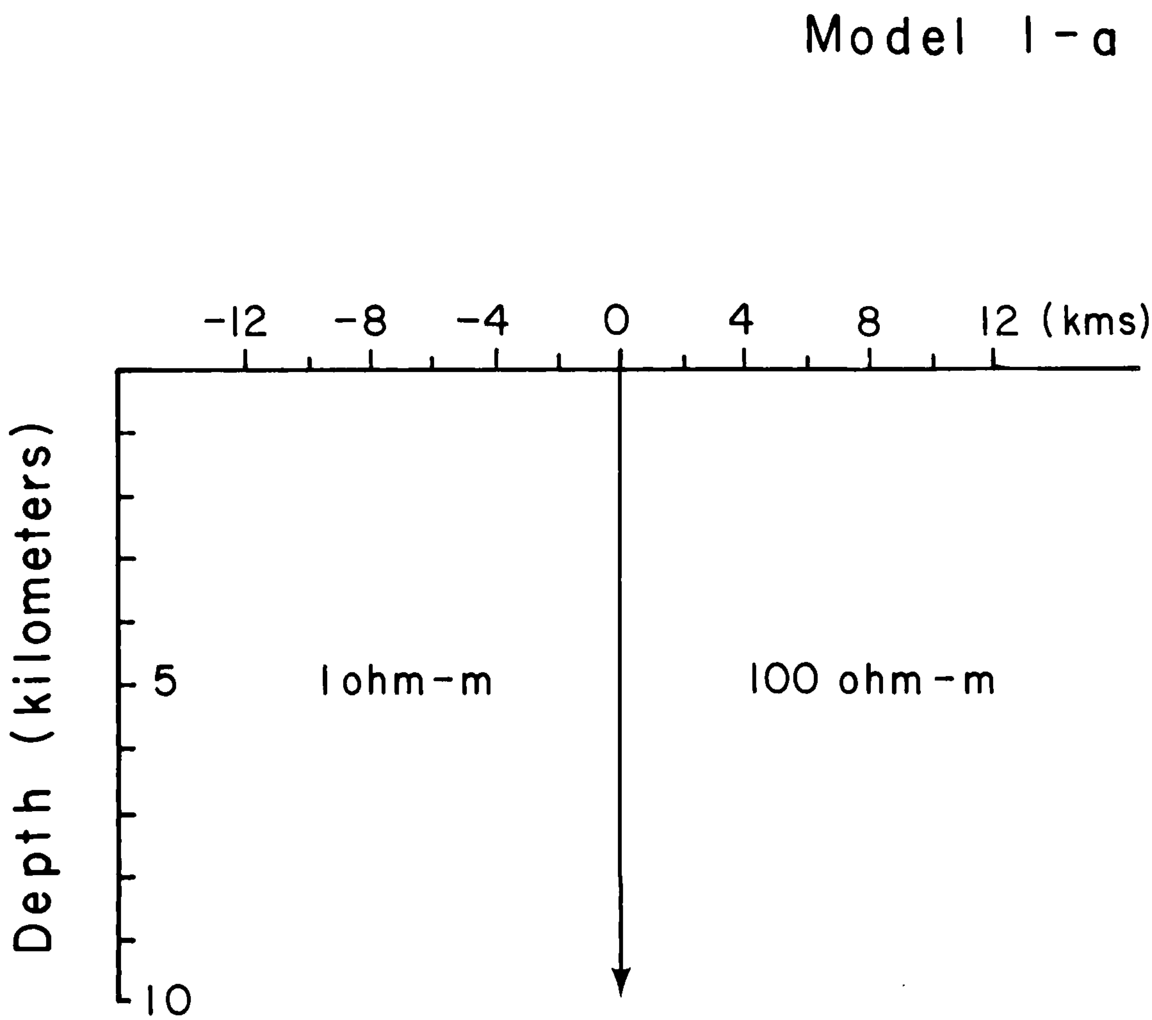

XBL 786-1957

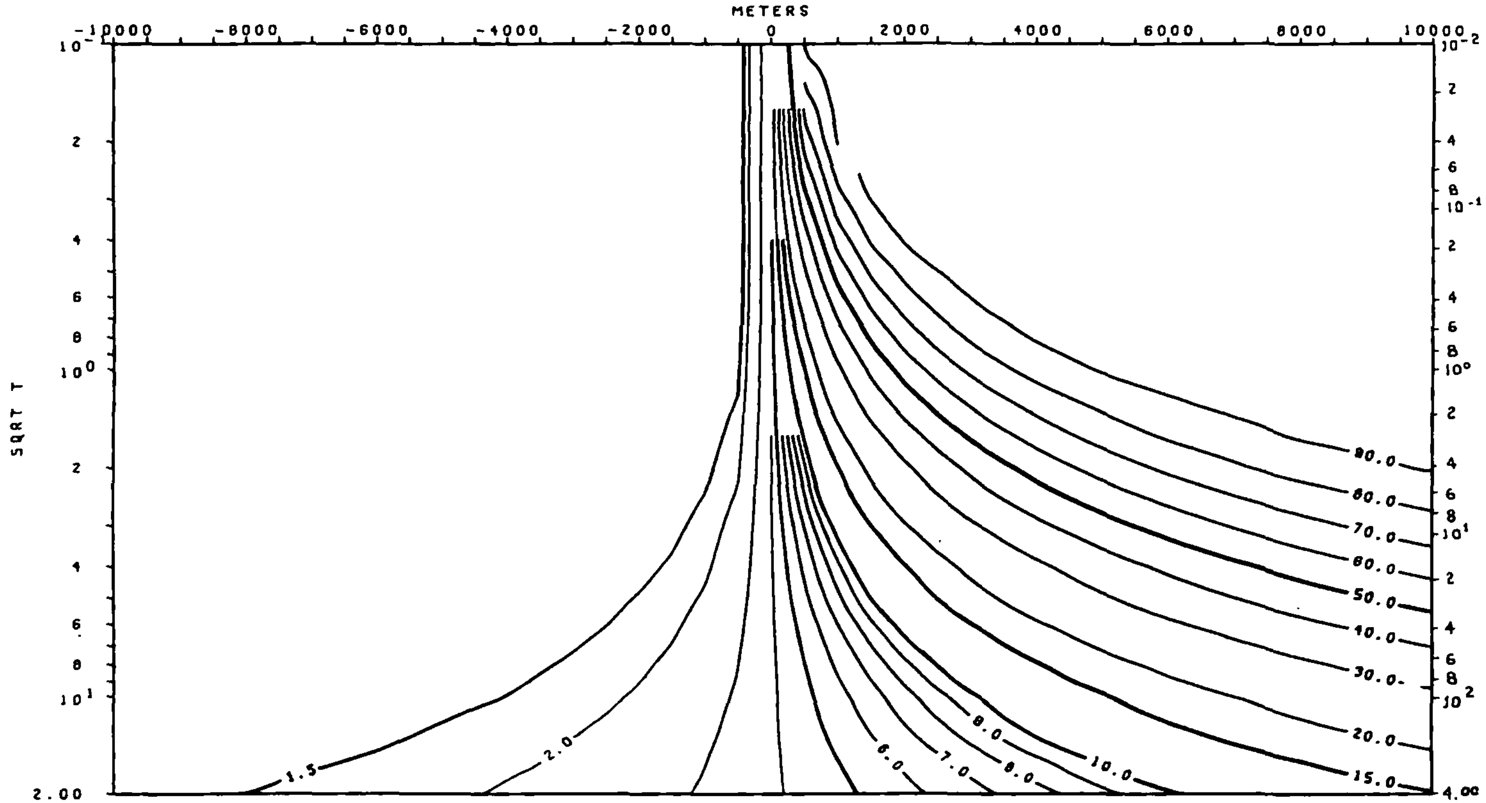

TE MODE
APPARENT RESISTIVITY VS. PERIOD (T)
MODEL 1-a

XBL 786-1903

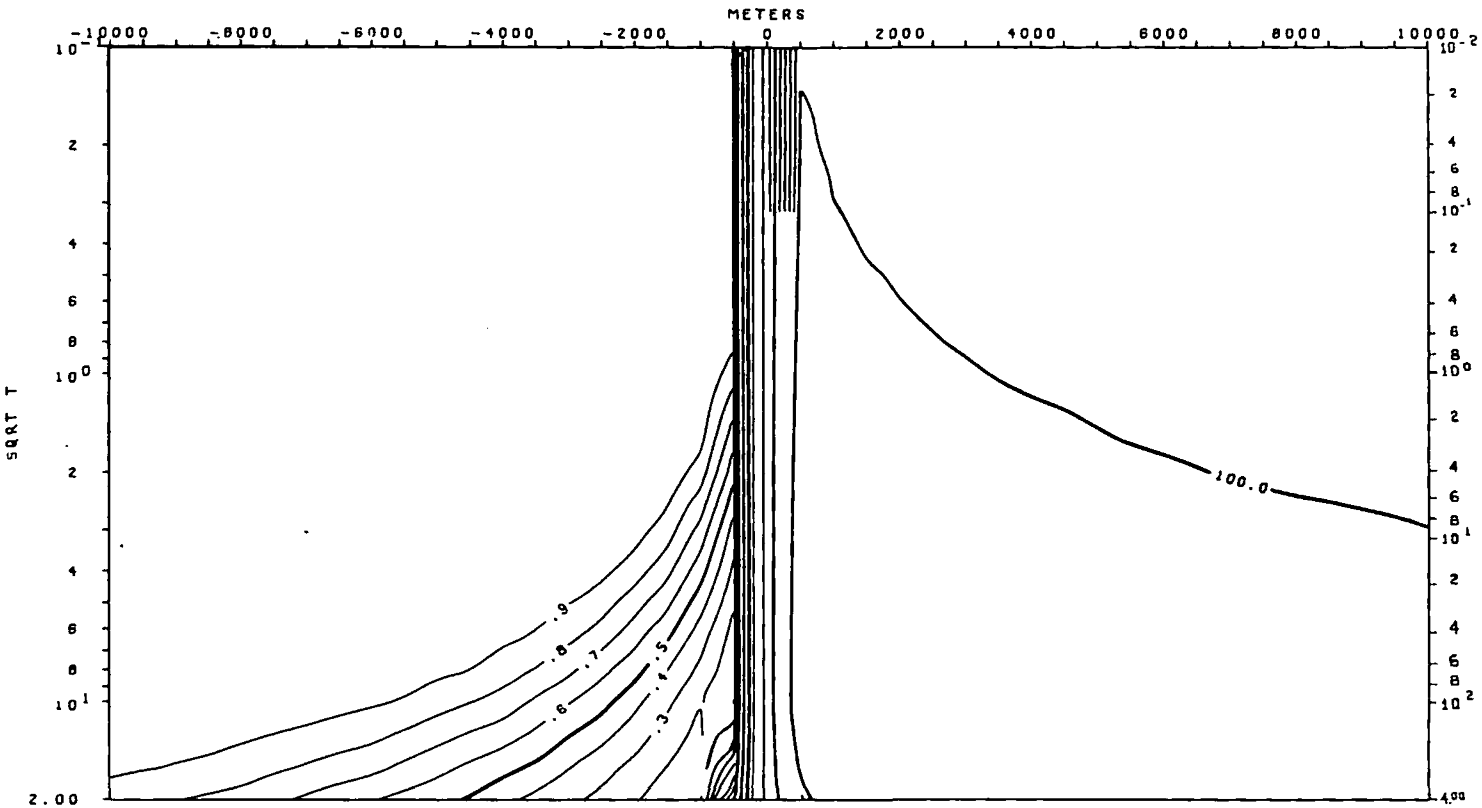

TM MODE
APPARENT RESISTIVITY VS. PERIOD (T)
MODEL 1-a

XBL 786-1929

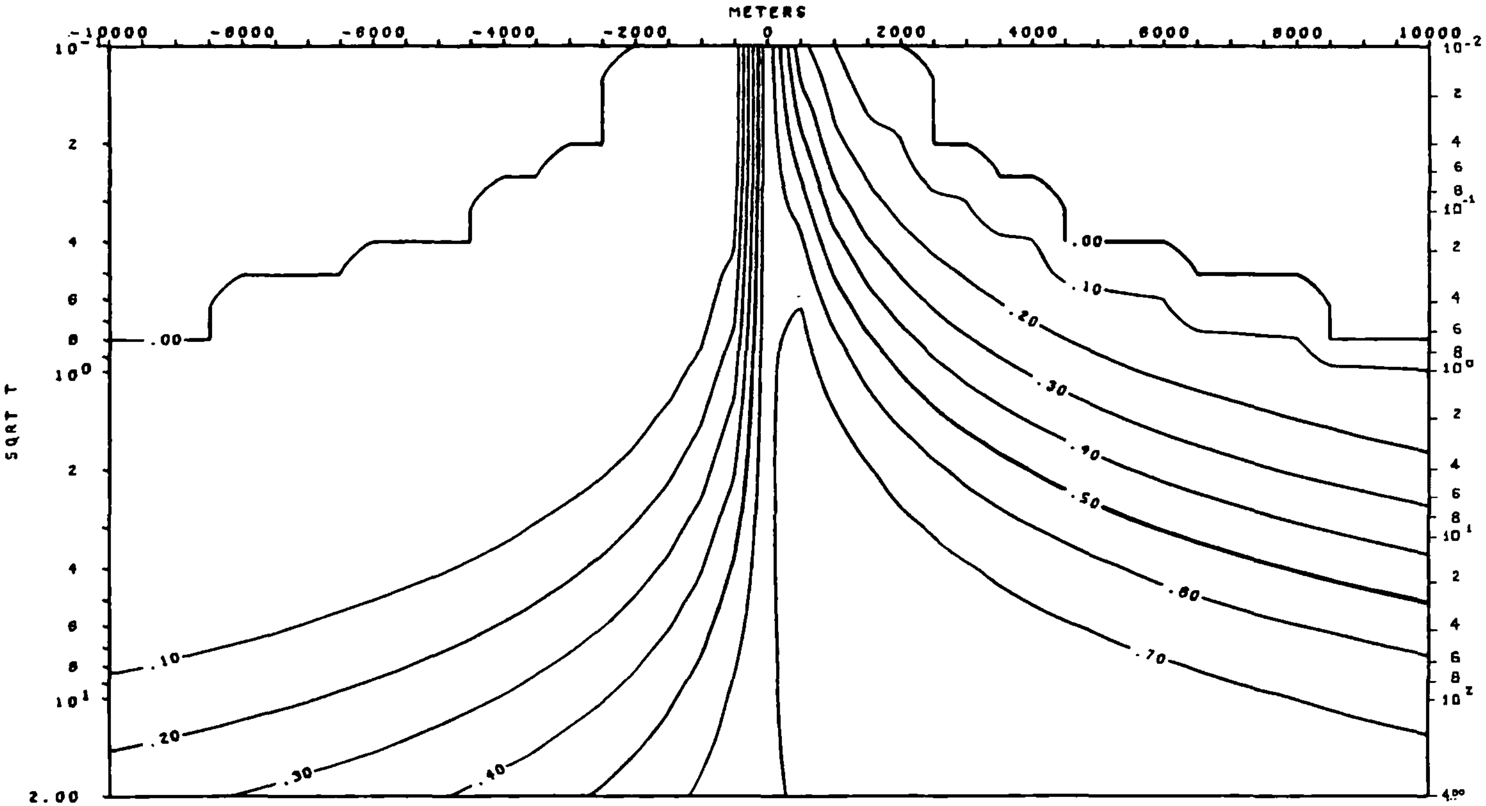

TIPPER VS. PERIOD (T)
MODEL 1-a

XBL 786-1904

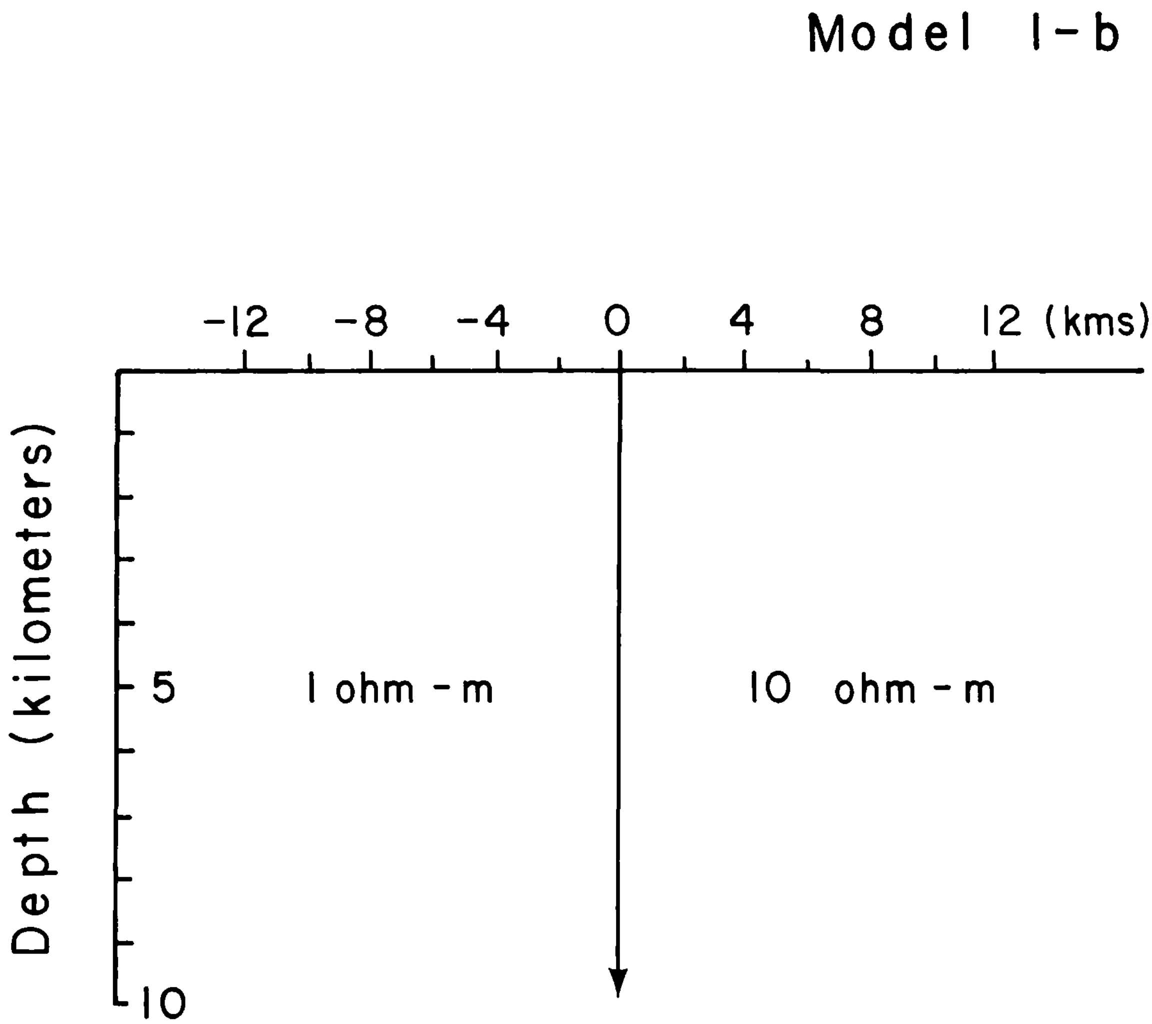

XBL 786-1958

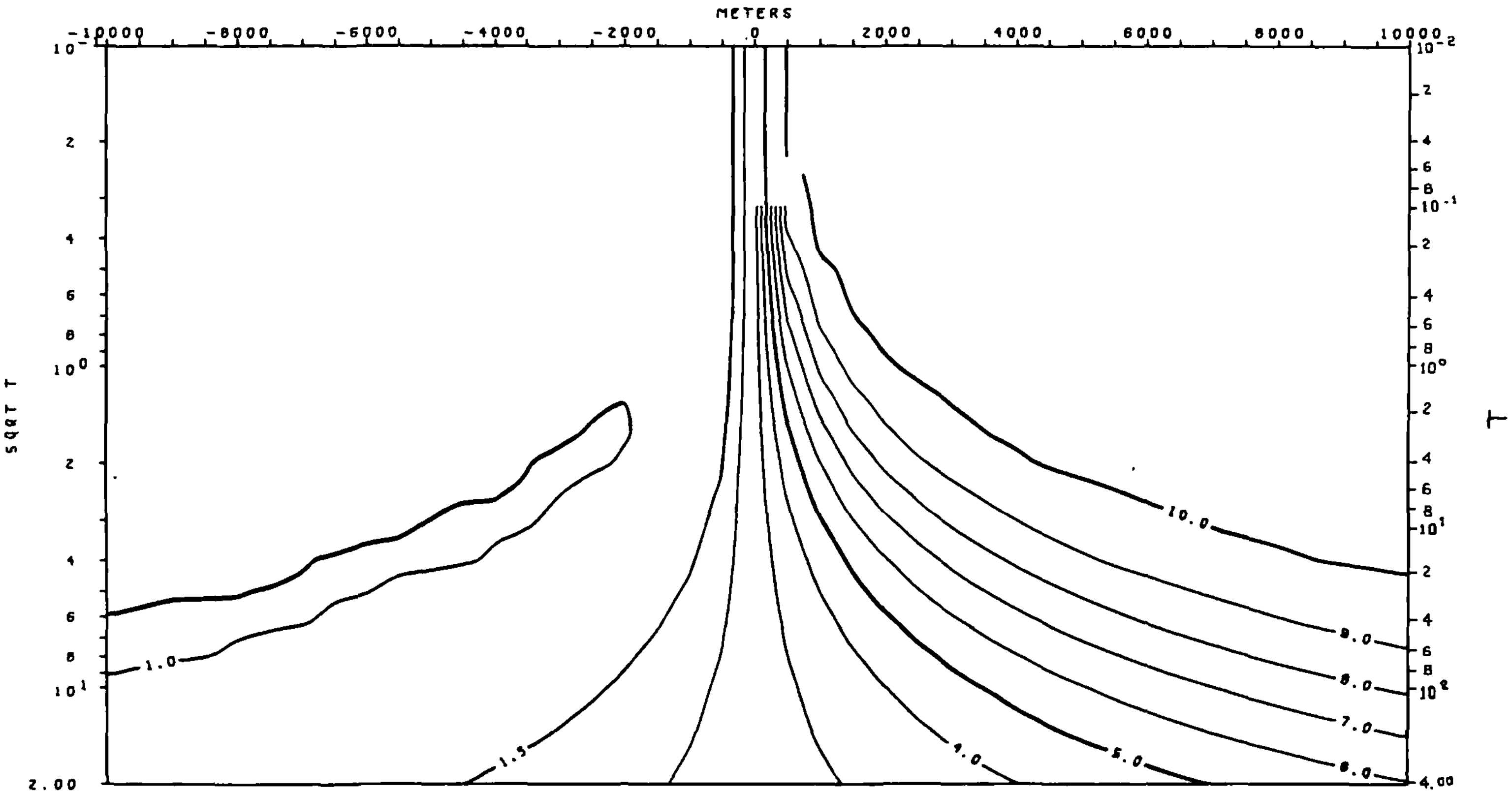

TE MODE
APPARENT RESISTIVITY VS. PERIOD (T)
MODEL 1-b

XBL 786-1916

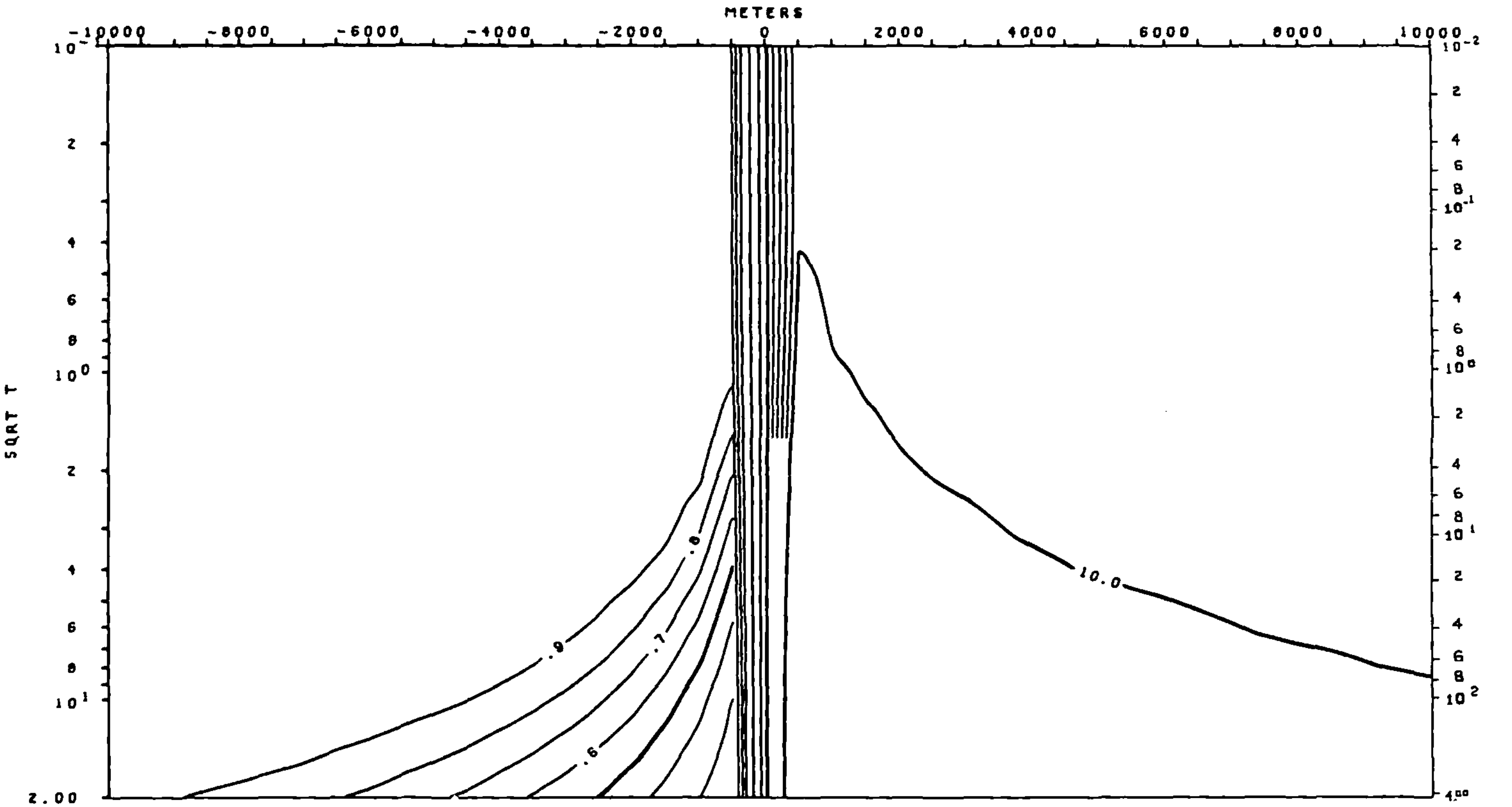

TM MODE
APPARENT RESISTIVITY VS. PERIOD (T)
MODEL 1-b

XBL 786-1915

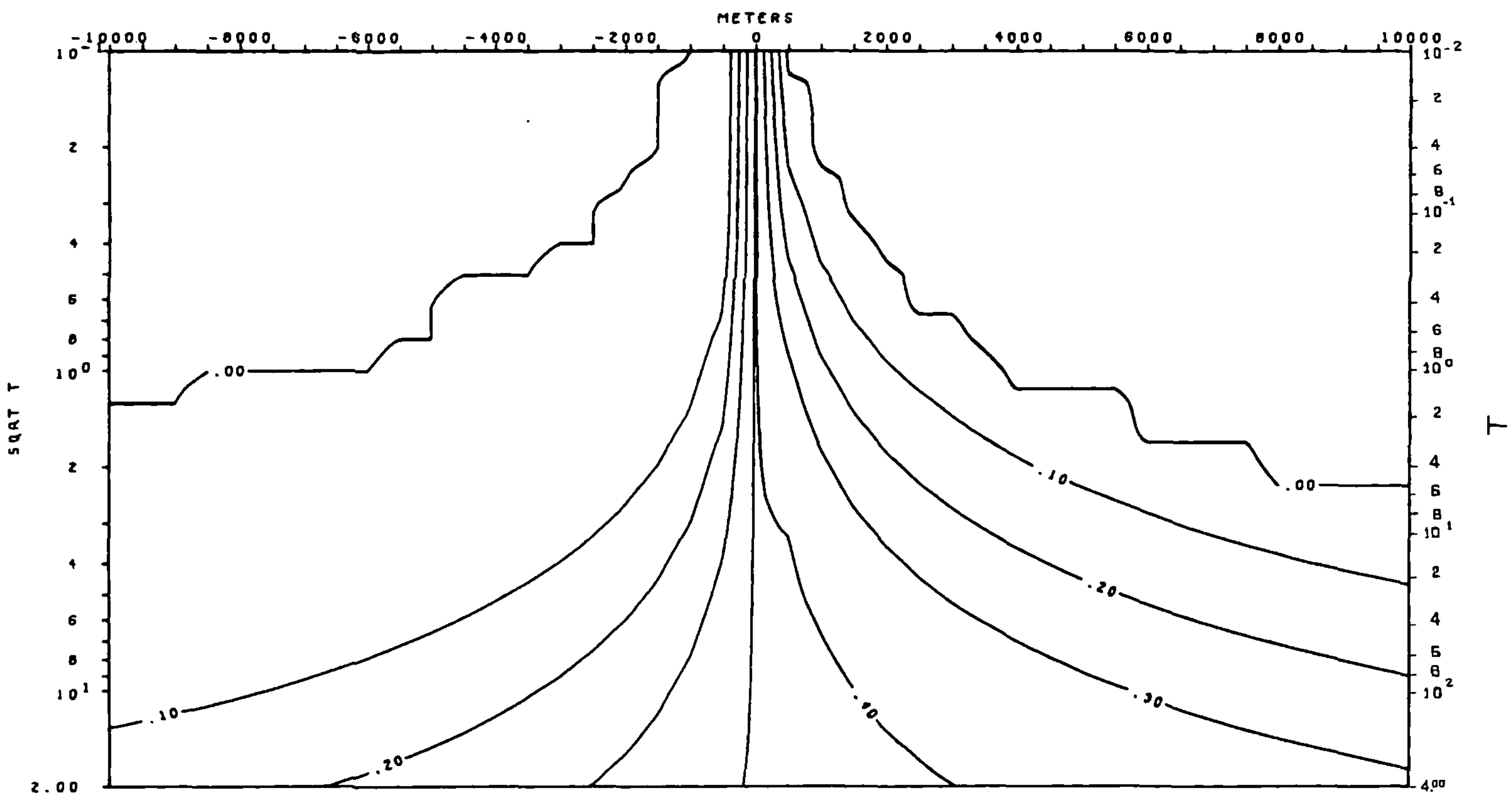

TIPPER VS. PERIOD (T)
MODEL 1-b

XBL 786-1930

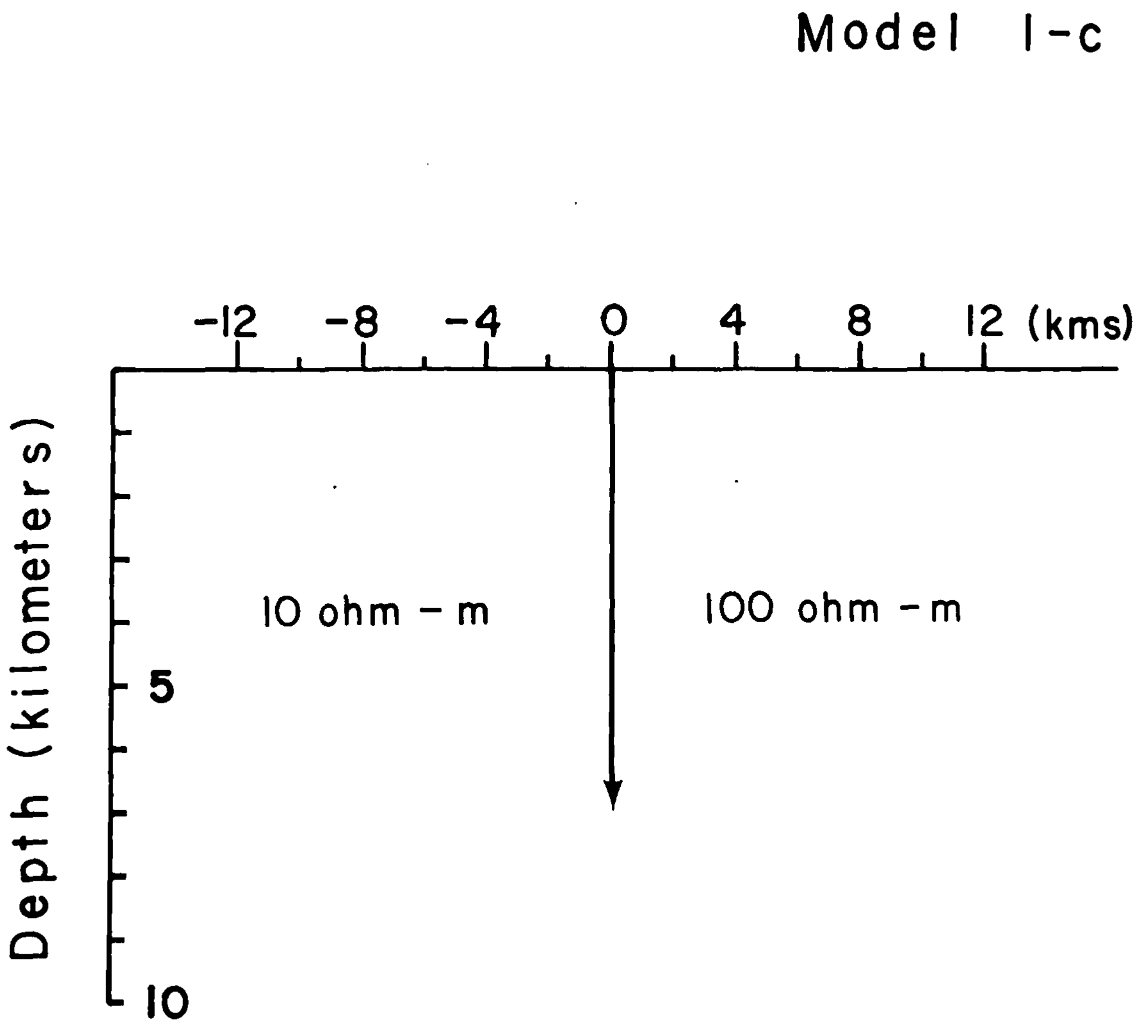
Model I-c
-12
-8
-4
0
4
8
12 (kms)
Depth (kilometers)
5
10
10 ohm - m
100 ohm - m

XBL 786-1947

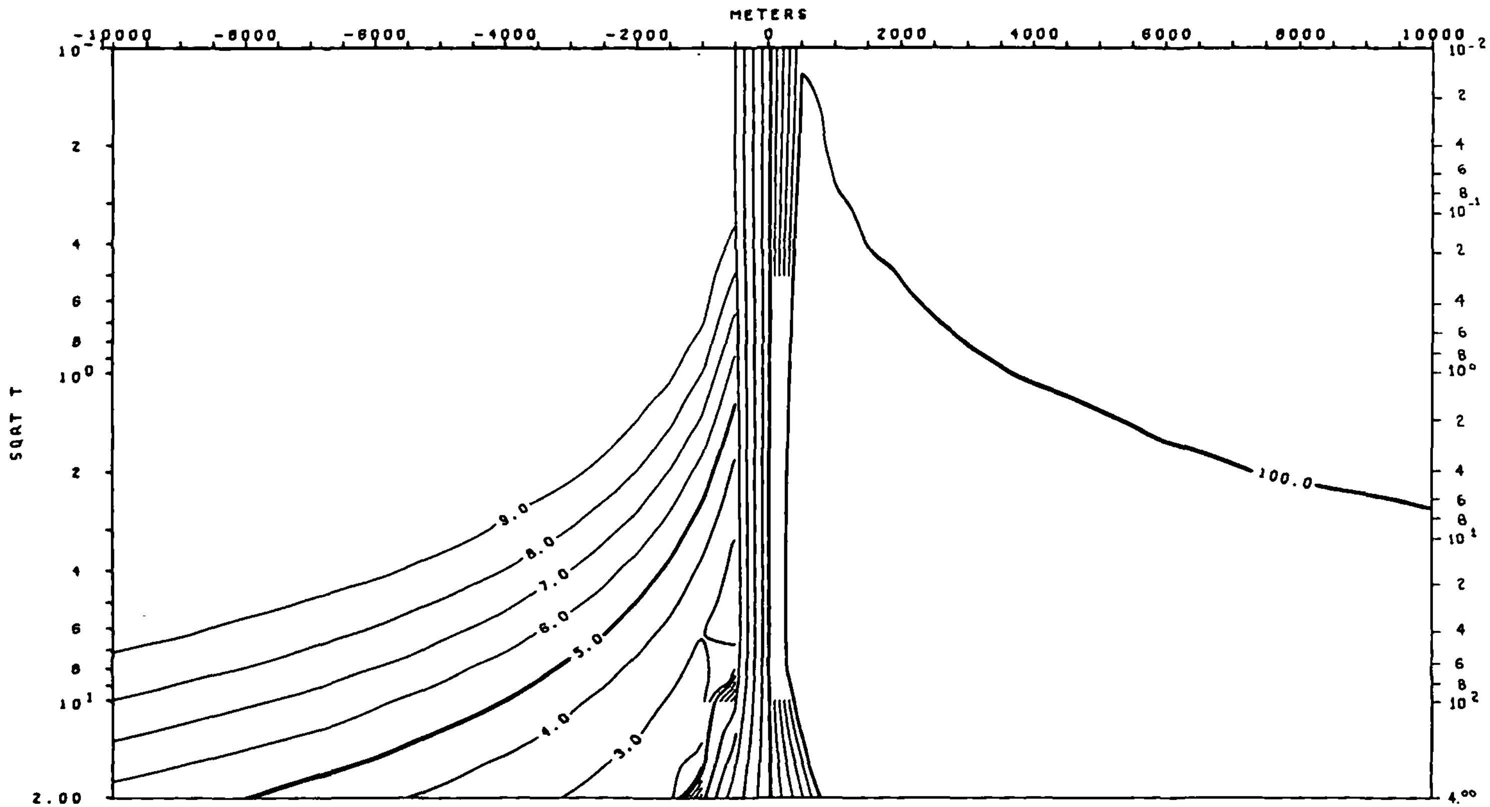

TE MODE
APPARENT RESISTIVITY VS. PERIOD (T)
MODEL 1-c

XBL 786-1906

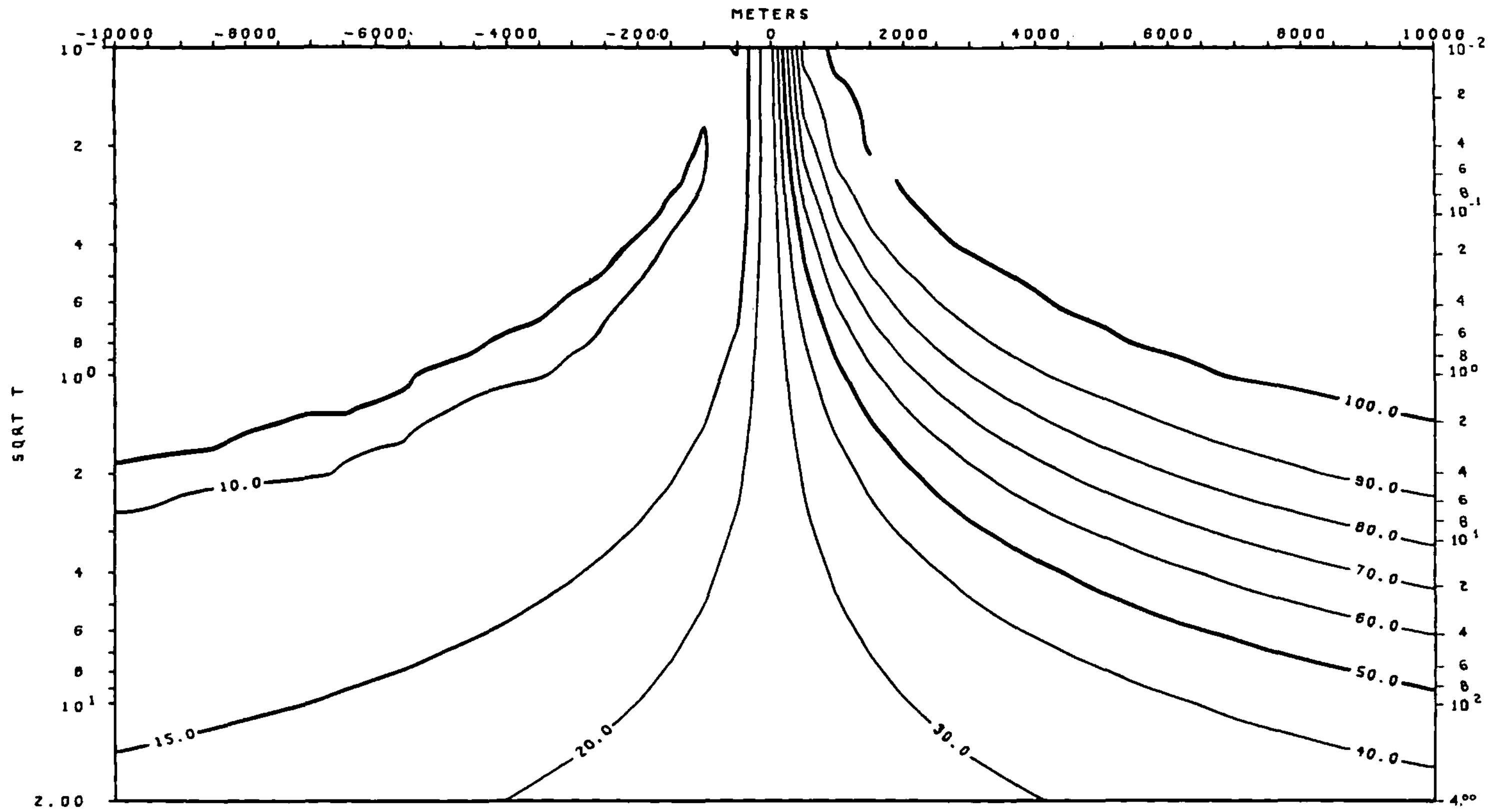

TM MODE
APPARENT RESISTIVITY VS. PERIOD (T)
MODEL 1-c

XBL 786-1902

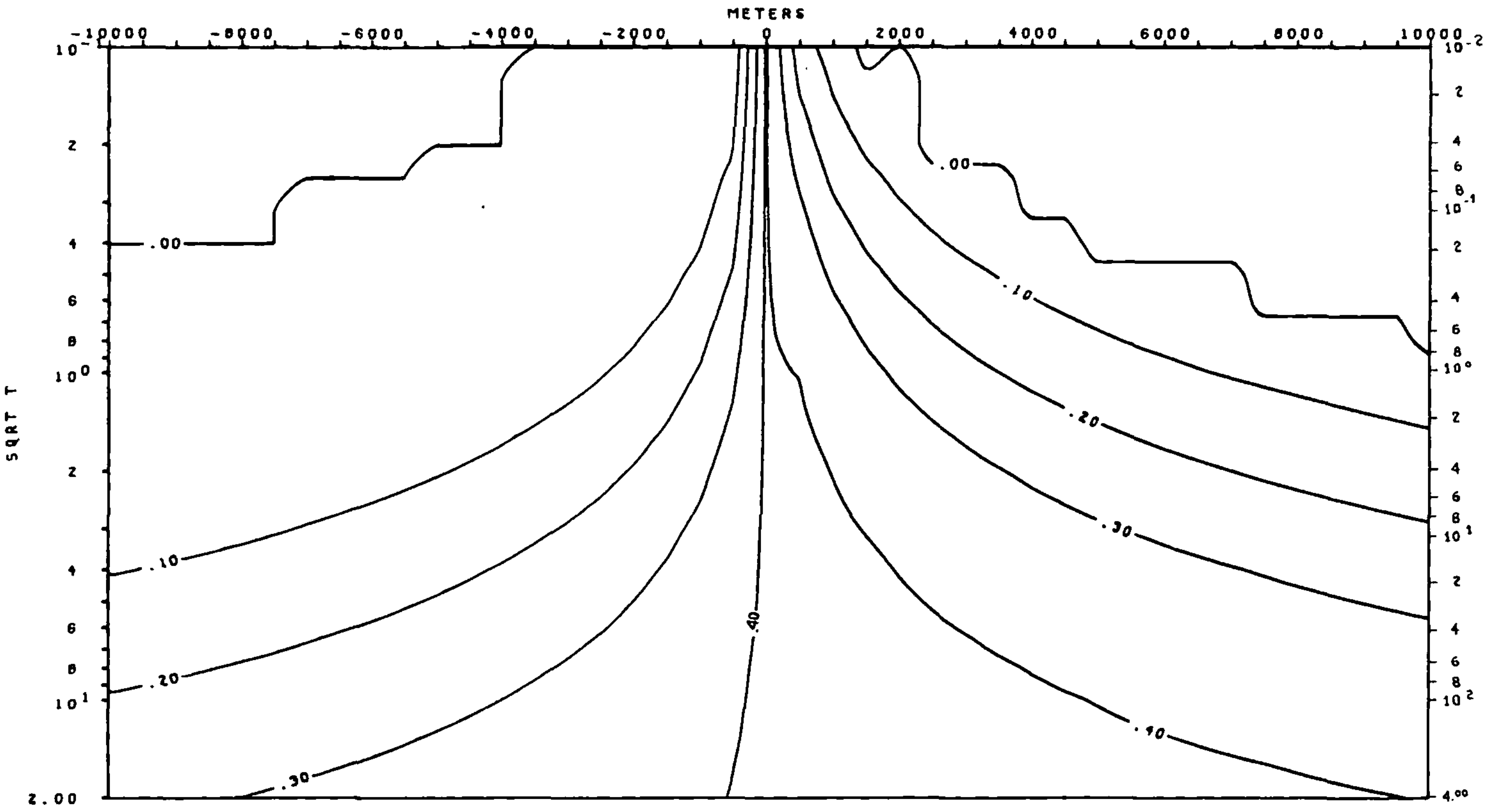

TIPPER VS. PERIOD (T)
MODEL 1-c

XBL 786-1932

Appendix 2

Model 2-a

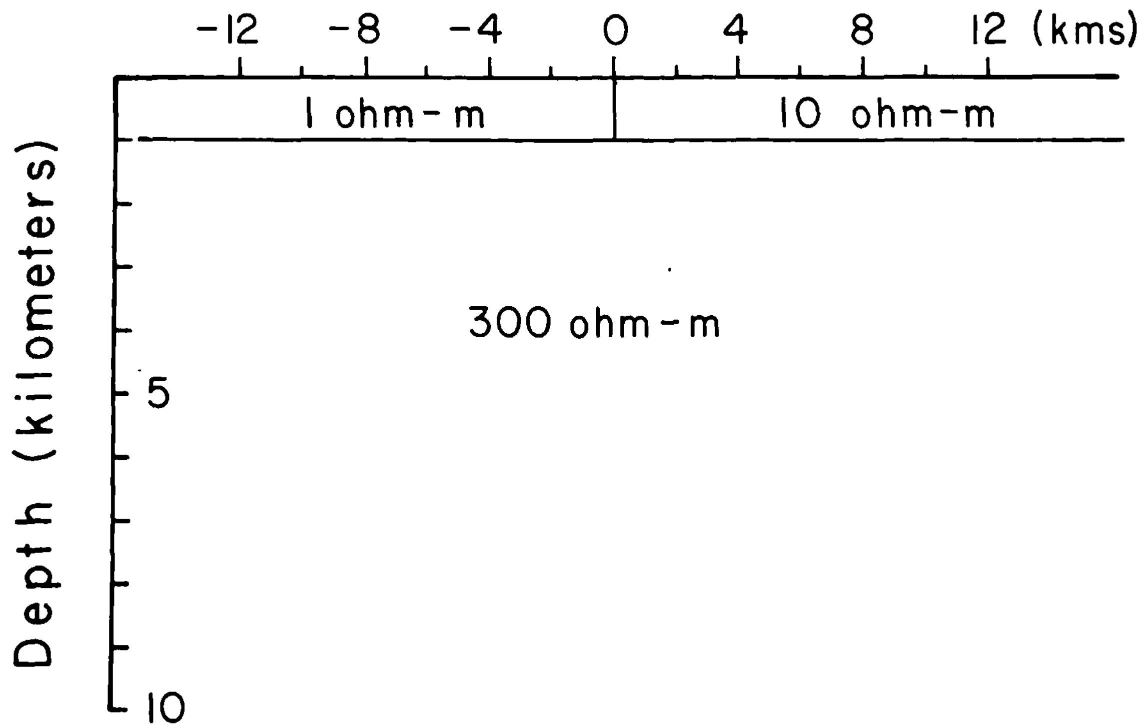

XBL 786-1948

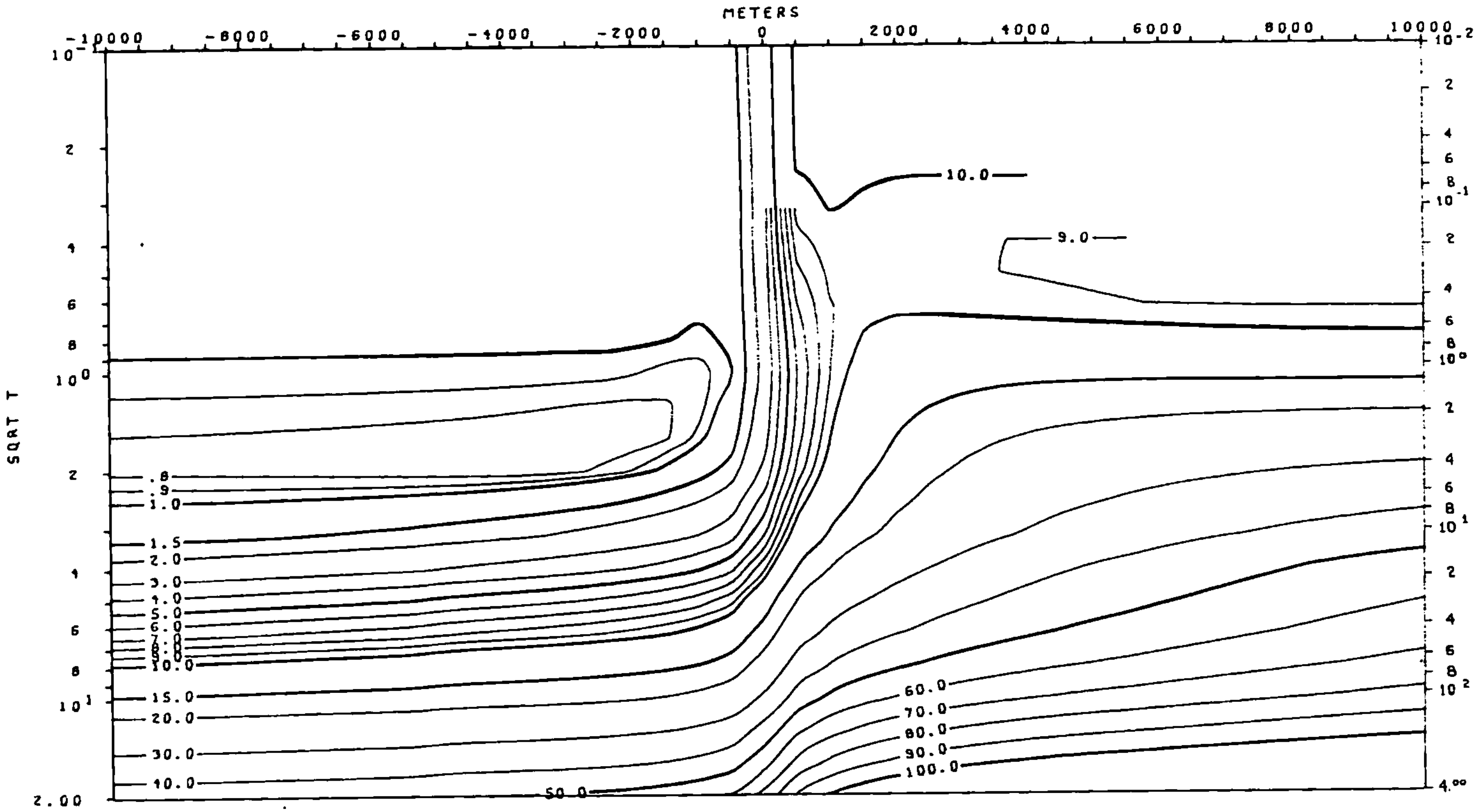

TE MODE
APPARENT RESISTIVITY VS. PERIOD (T)
MODEL 2-a

XBL 786-1943

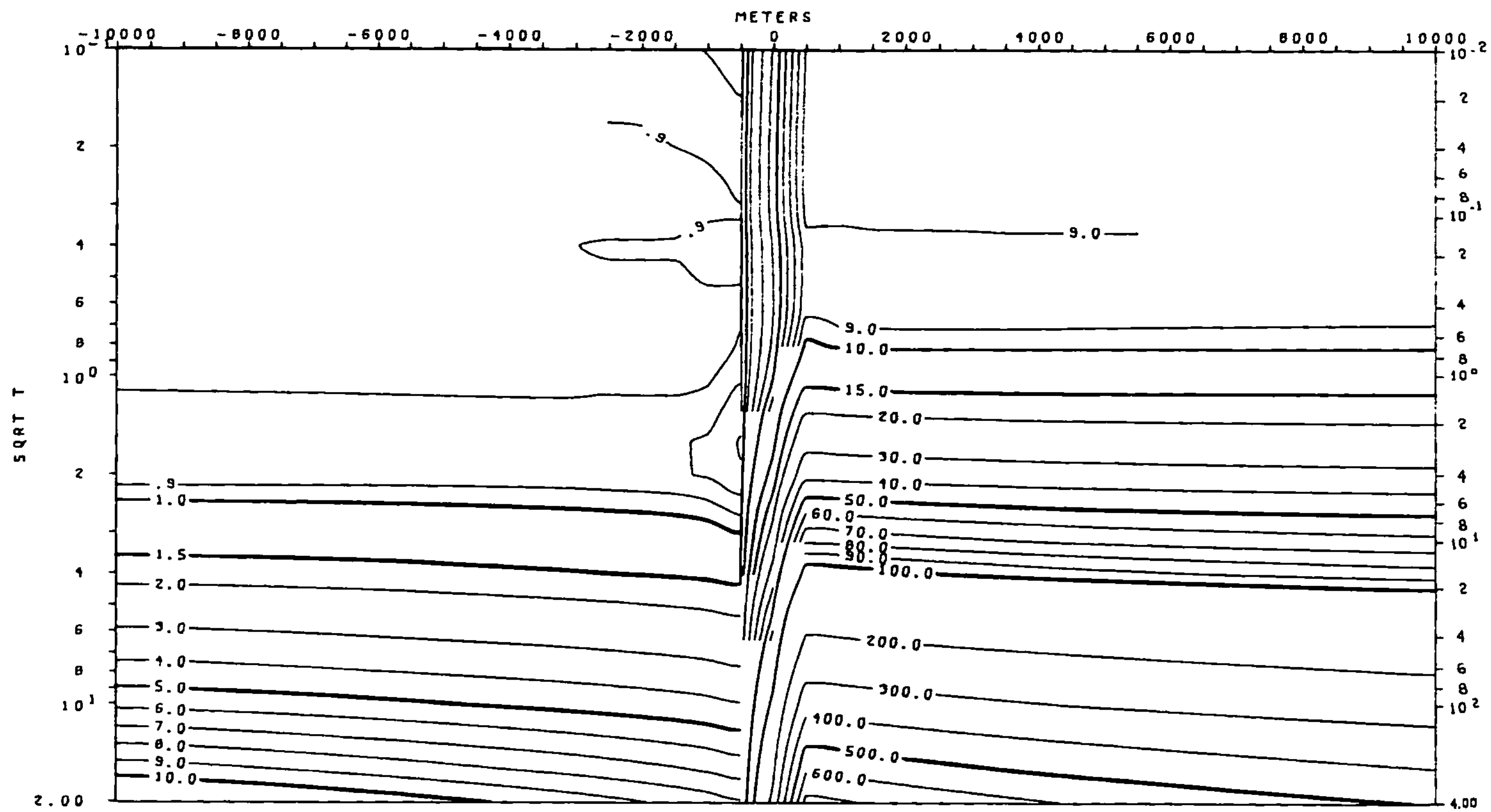

TM MODE
APPARENT RESISTIVITY VS. PERIOD (T)
MODEL 2-a

XBL 786-1925

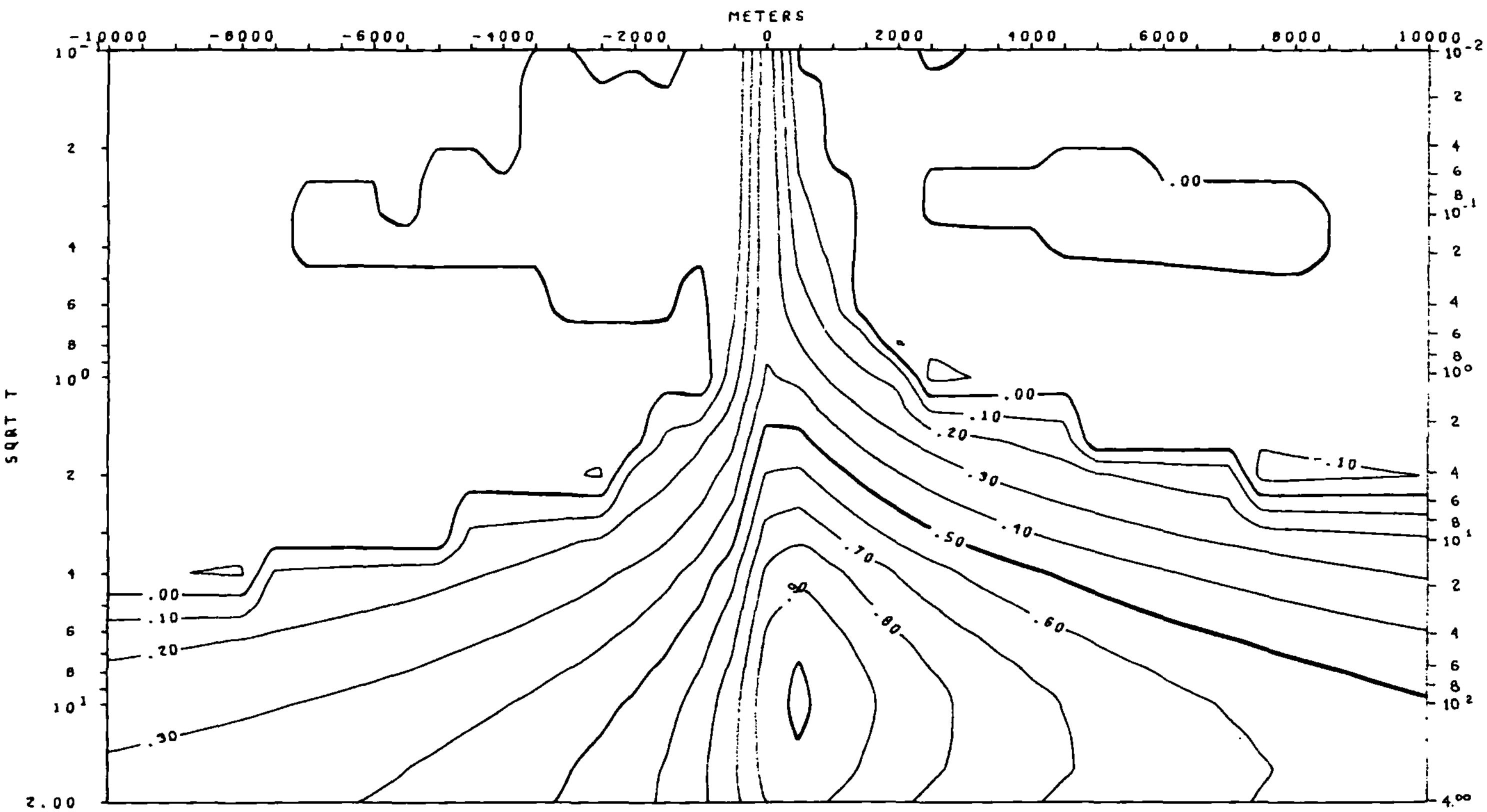

TIPPER VS. PERIOD (T)
MODEL 2-a

XBL 786-1900

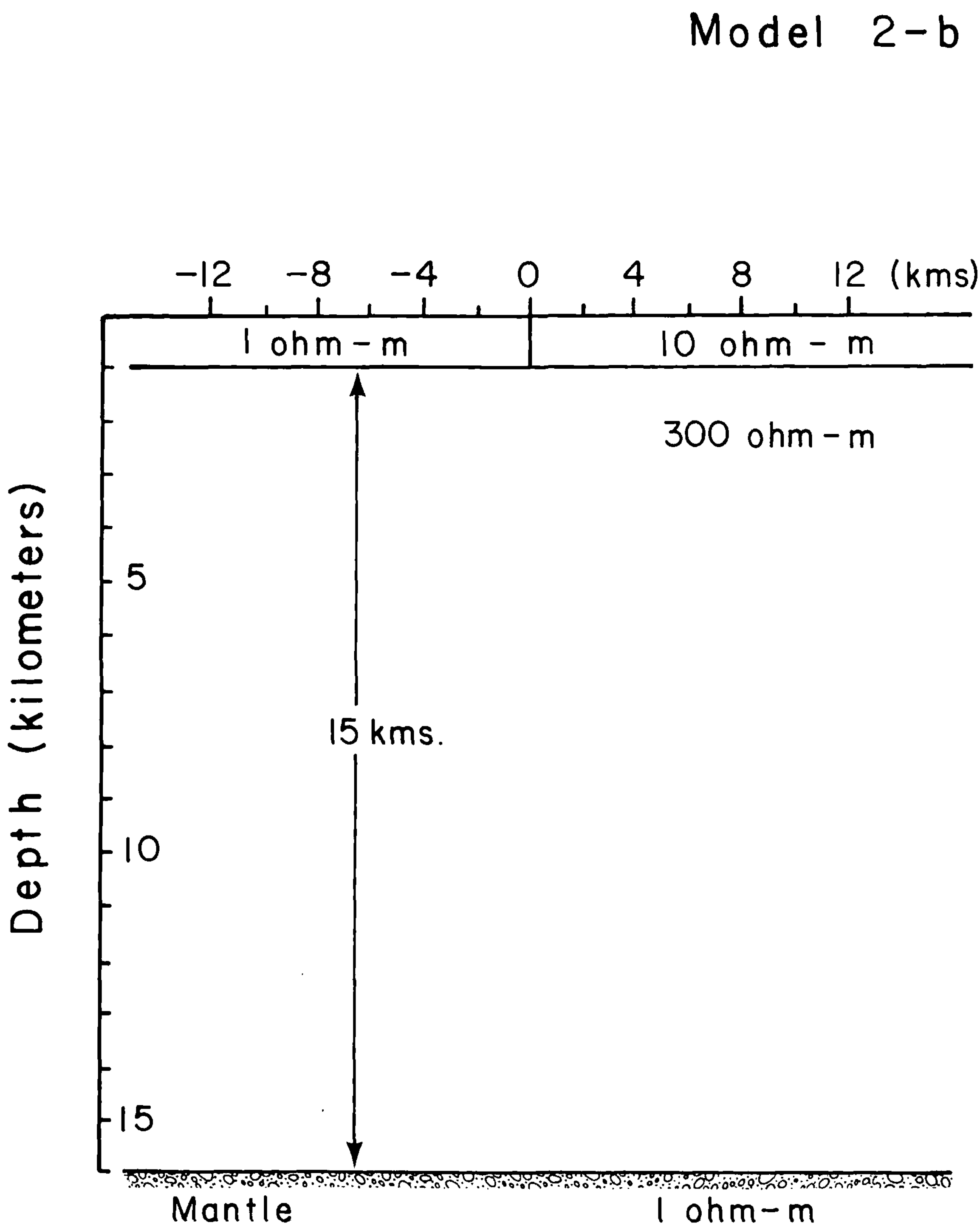

Model 2-b
-12
-8
-4
0
4
8
12
(kms)
1 ohm-m
10 ohm - m
300 ohm-m
Depth (kilometers)
5
10
15
15 kms.
Mantle
1 ohm-m

XBL 786-1954

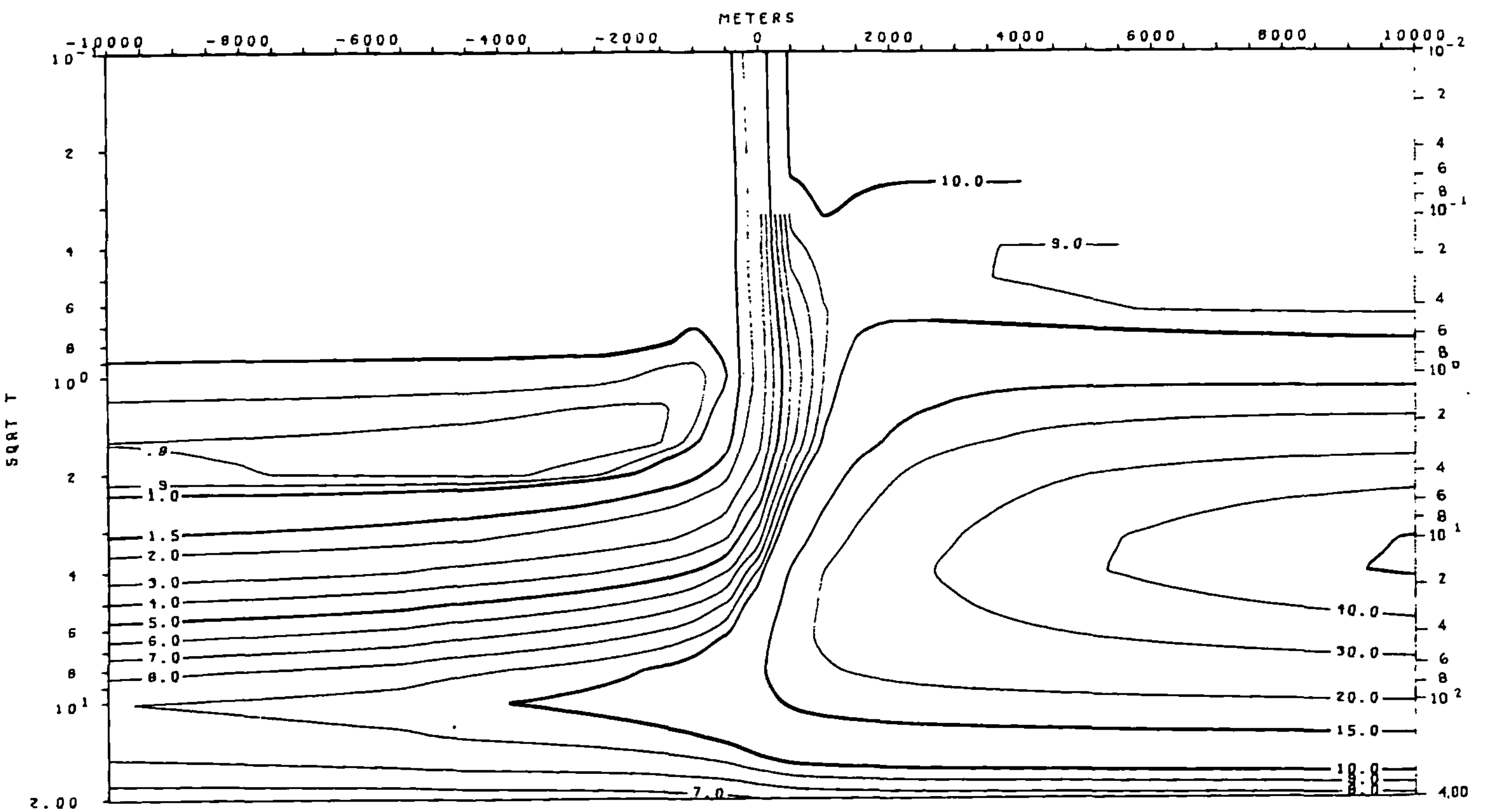

TE MODE
APPARENT RESISTIVITY VS. PERIOD (T)
MODEL 2-b

XBL 786-1926

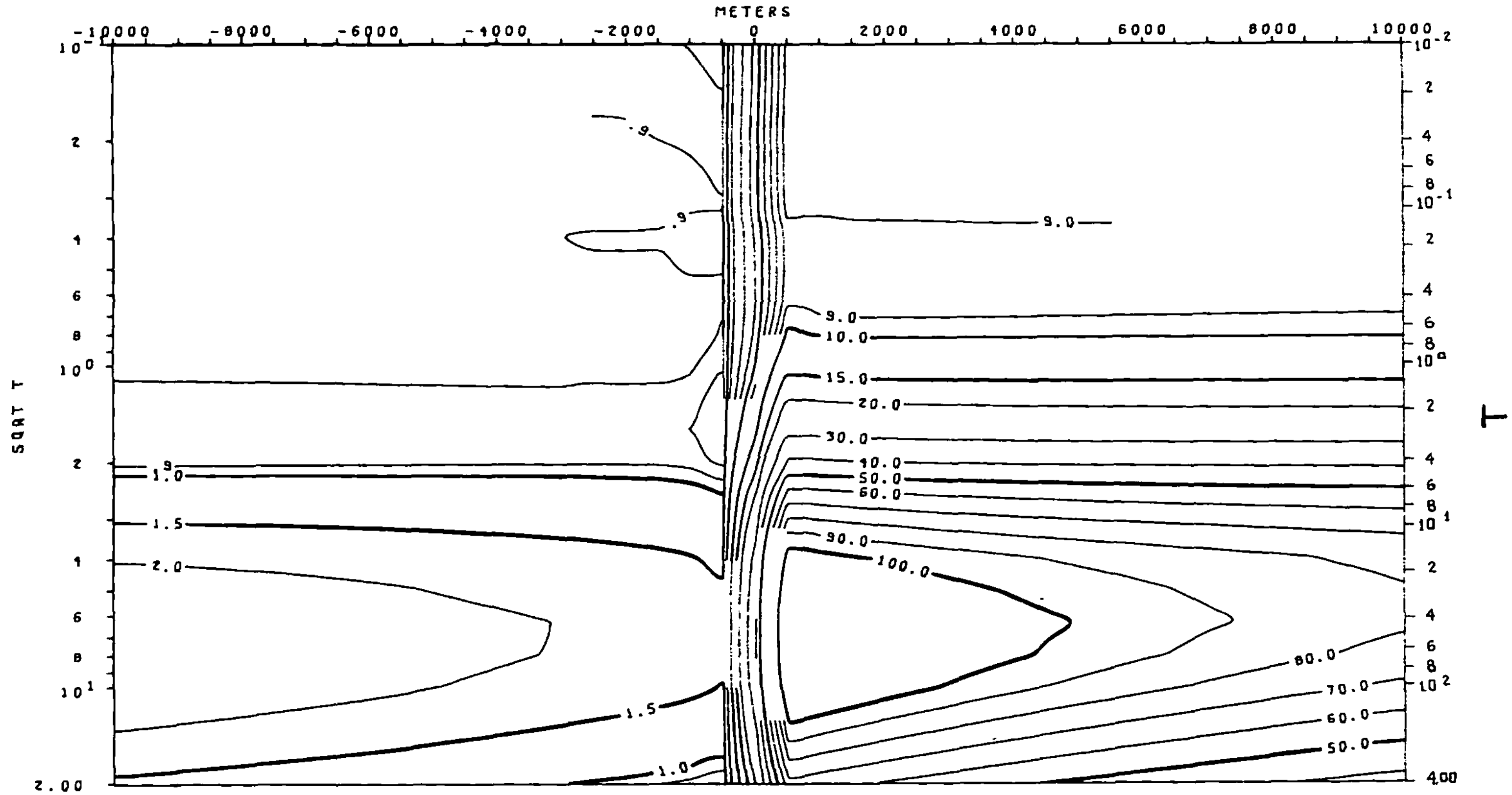

TM MODE
APPARENT RESISTIVITY VS. PERIOD (T)
MODEL 2-b

XBL 786-1913

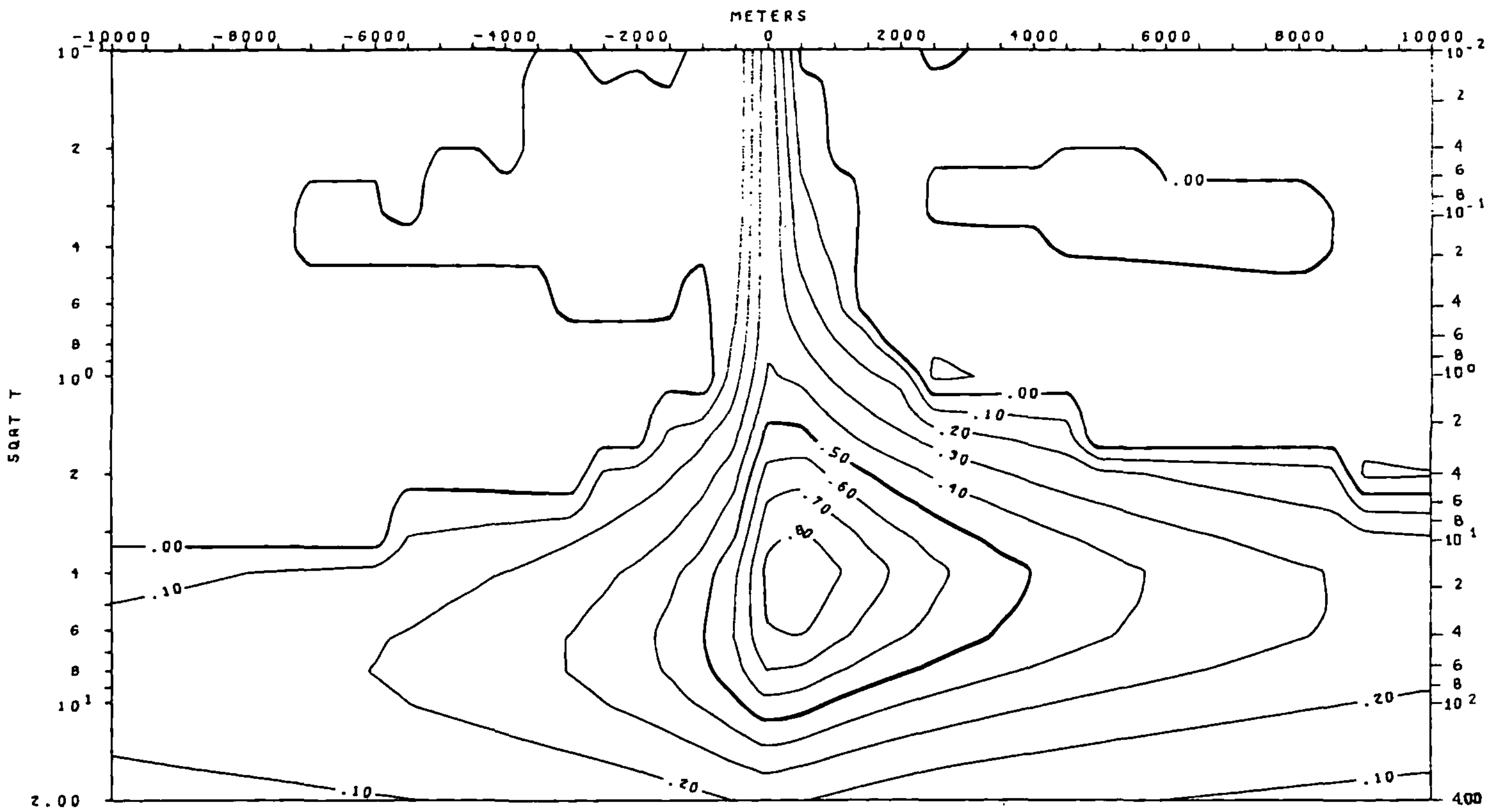

TIPPER VS. PERIOD (T)
MODEL 2-b

XBL 786-1912

Model 3-a

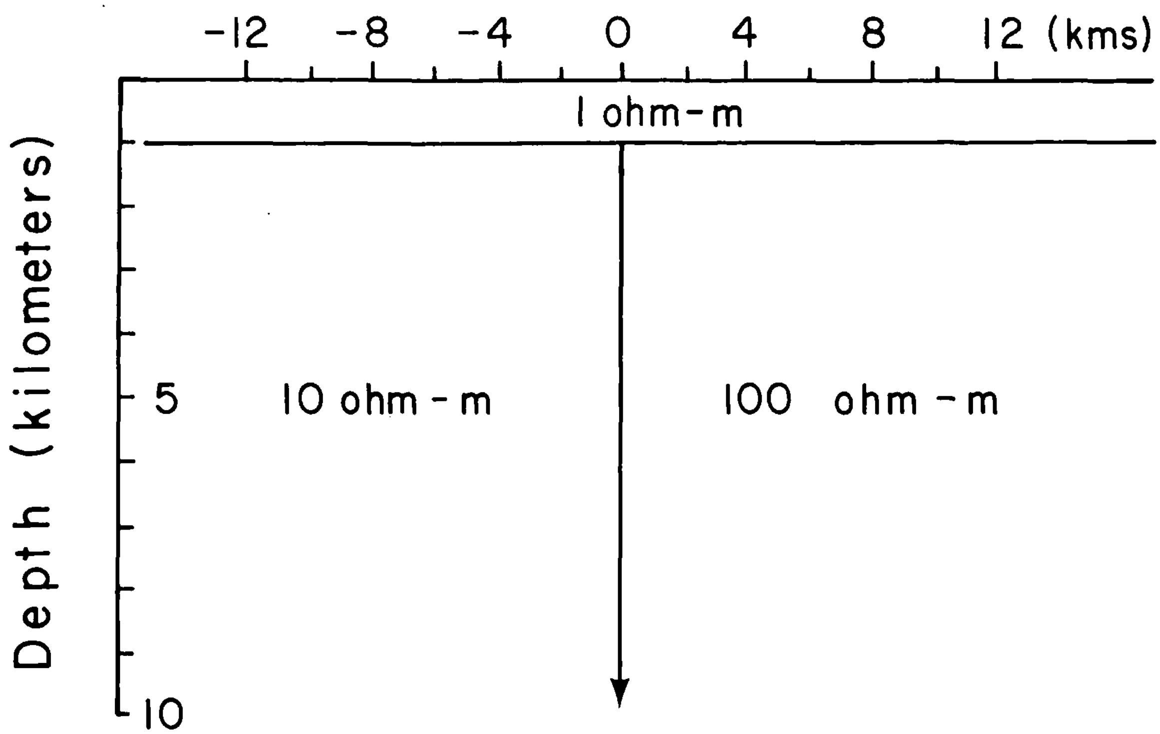

XBL 786-1959

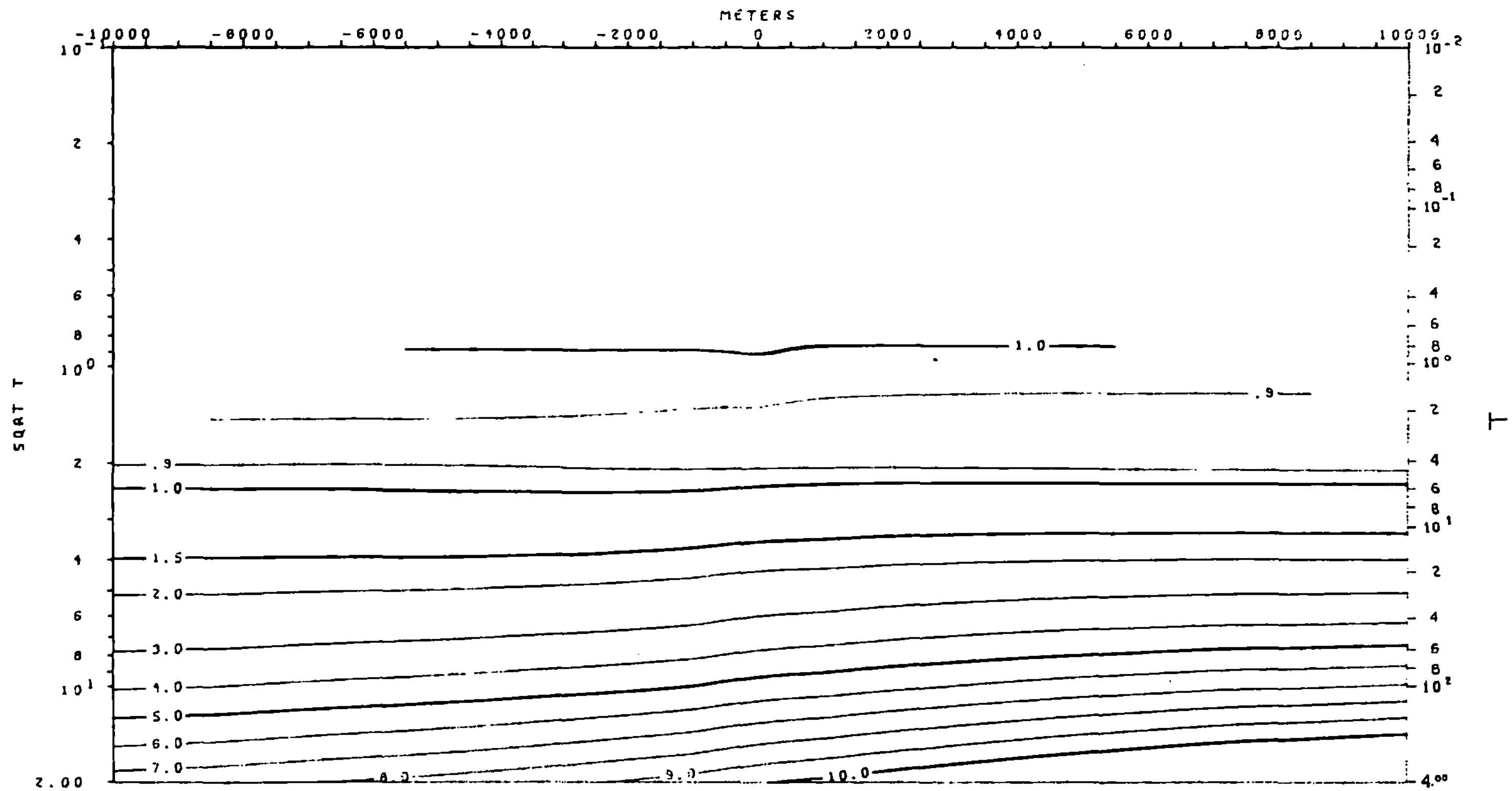

TE MODE
APPARENT RESISTIVITY VS. PERIOD (T)
MODEL 3-a

XBL 786-1936

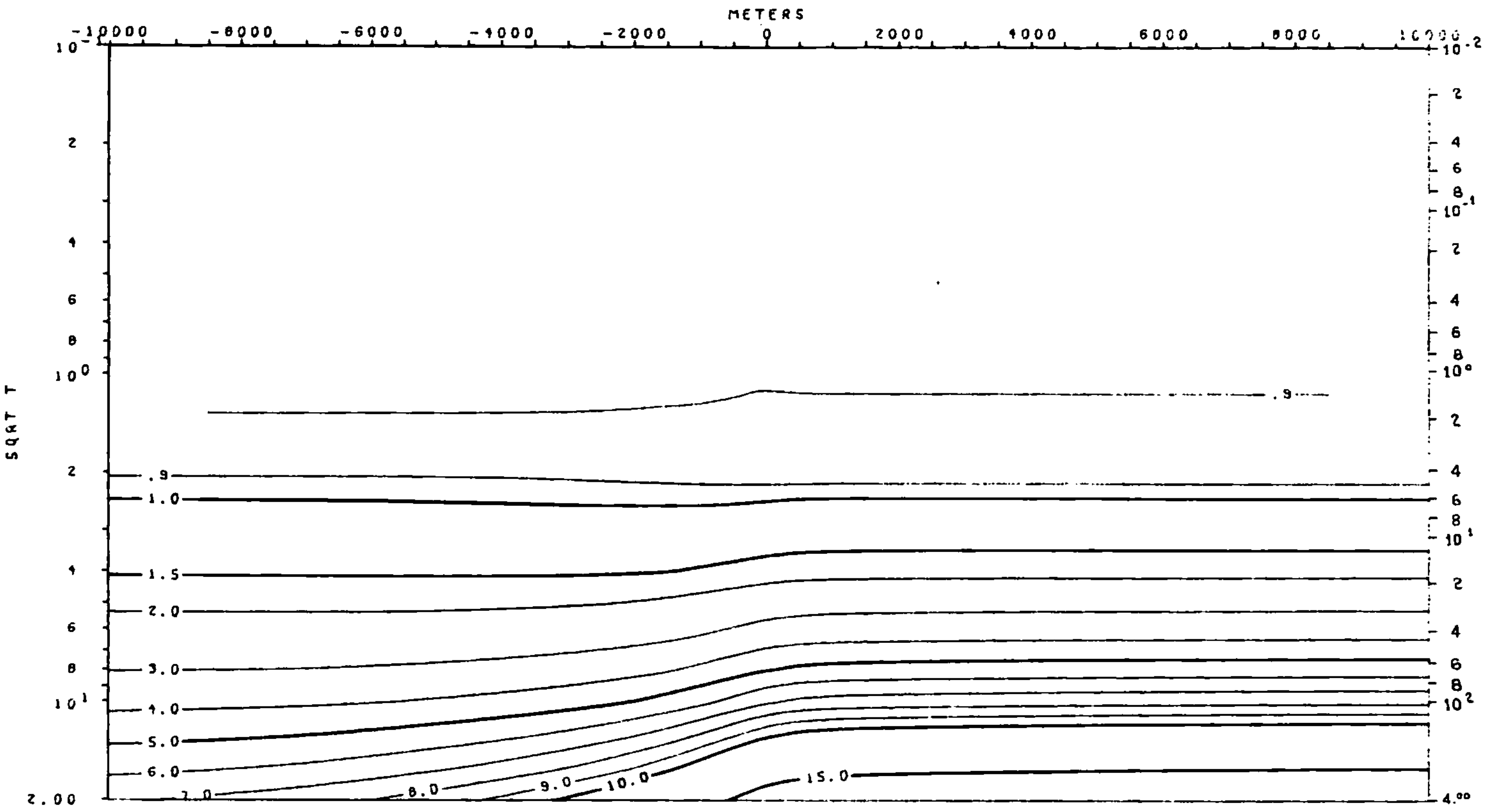

TM MODE
APPARENT RESISTIVITY VS. PERIOD (T)
MODEL 3-a

XBL 786-1919

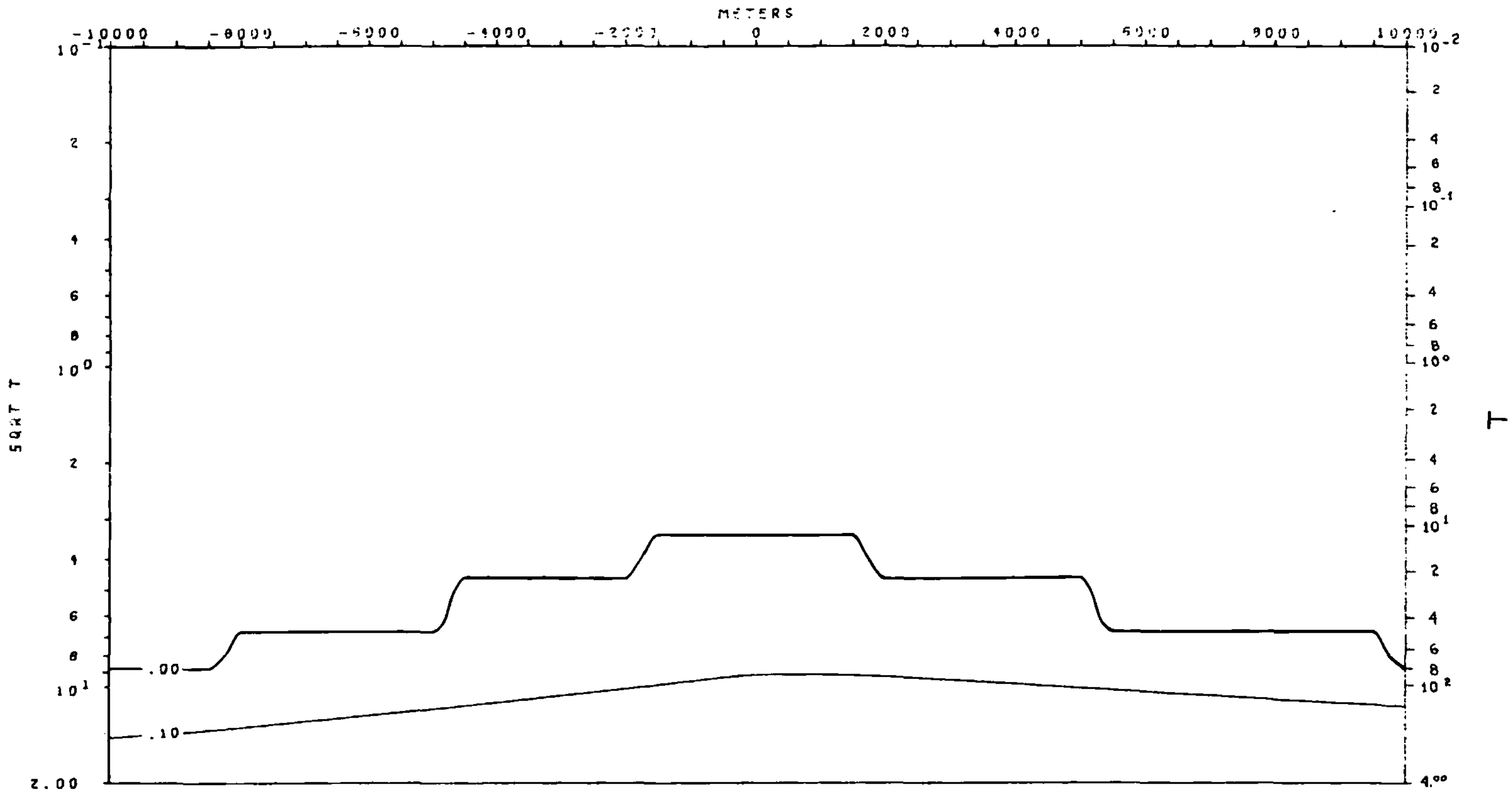

TIPPER VS. PERIOD (T)
MODEL 3-a

XBL 786-1918

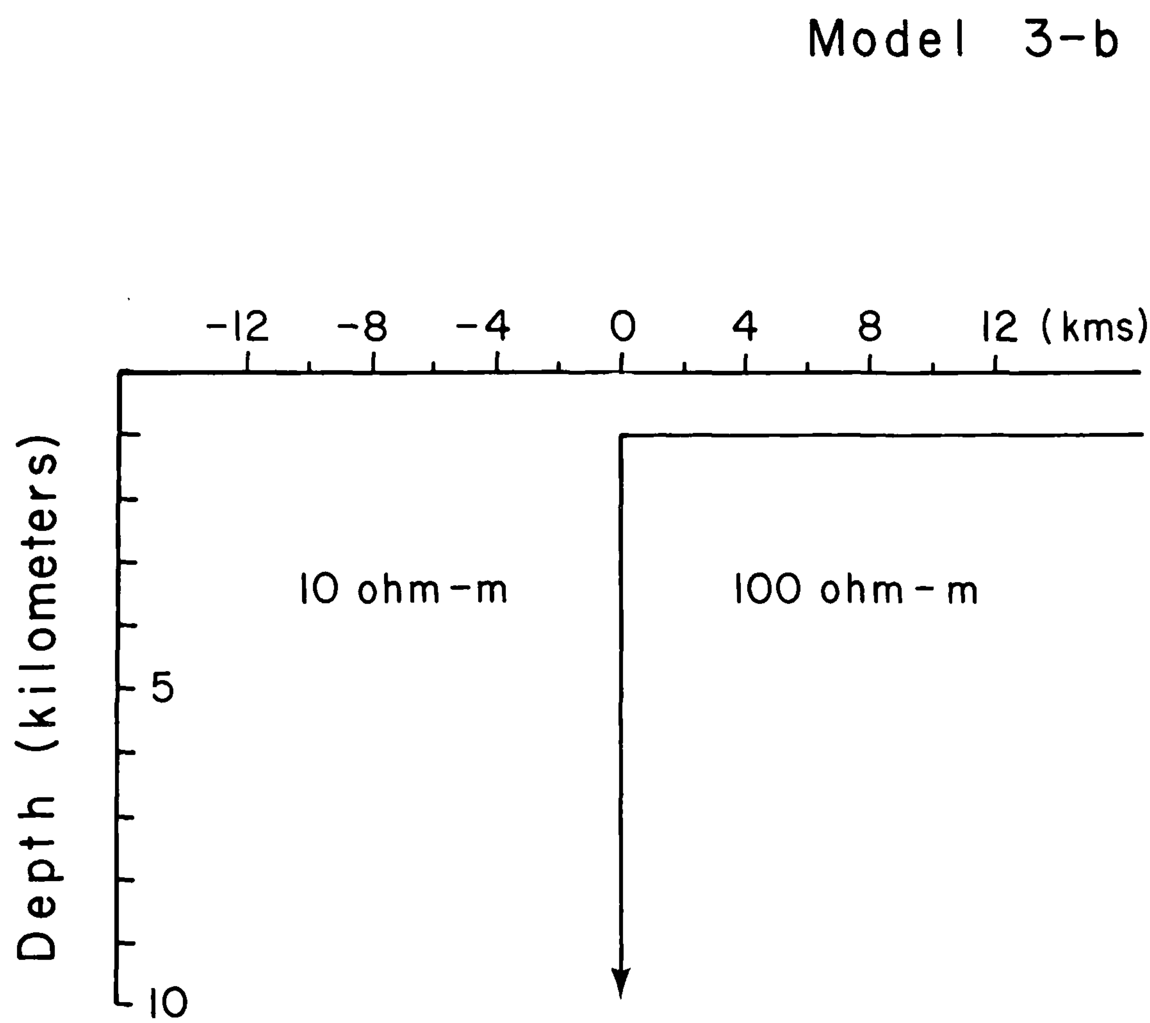
Model 3-b
-12
-8
-4
0
4
8
12 (kms)
Depth (kilometers)
5
10
10 ohm-m
100 ohm-m

XBL 786-1949

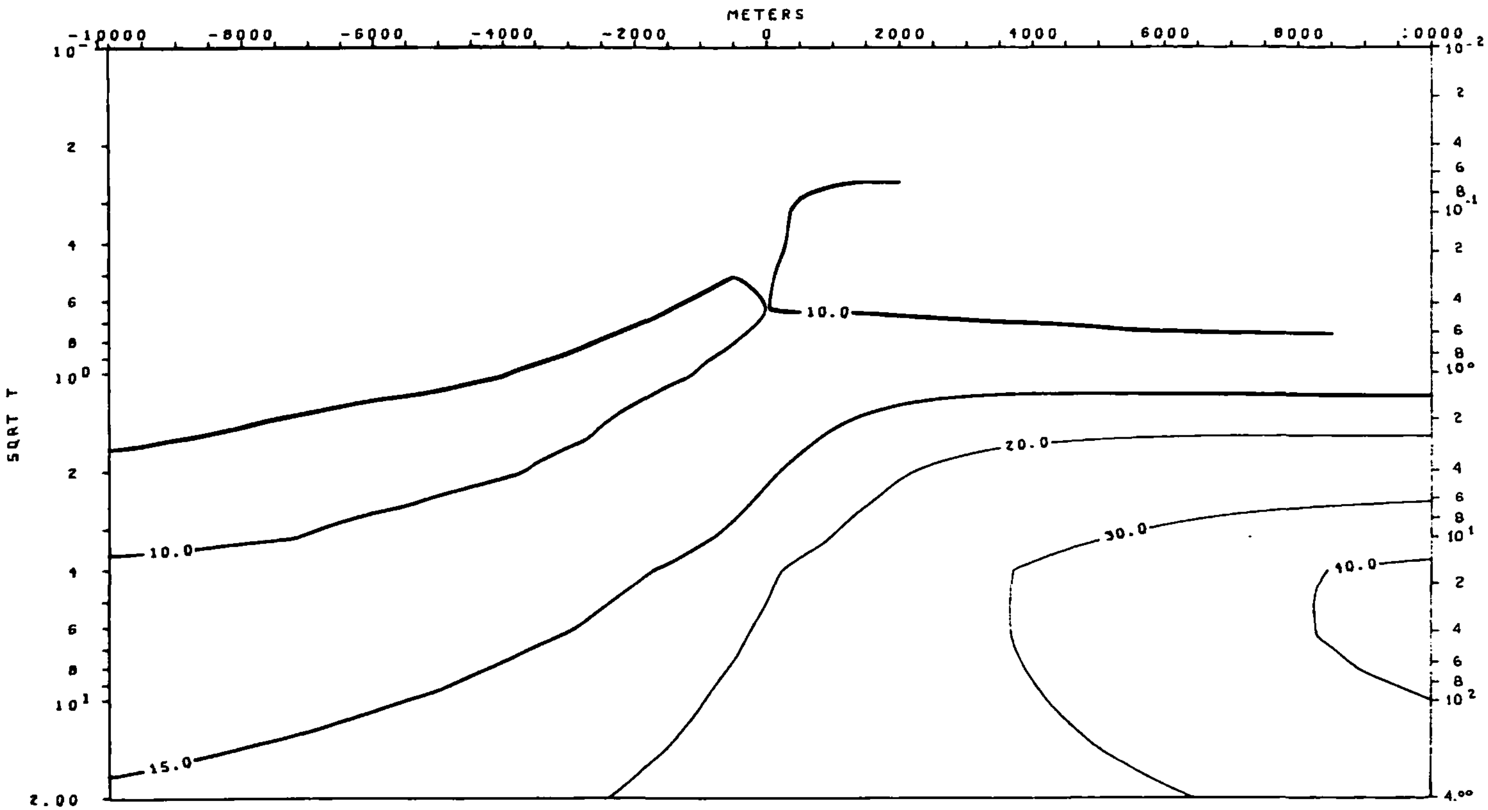

TE MODE
APPARENT RESISTIVITY VS. PERIOD (T)
MODEL 3-b

XBL 786-1907

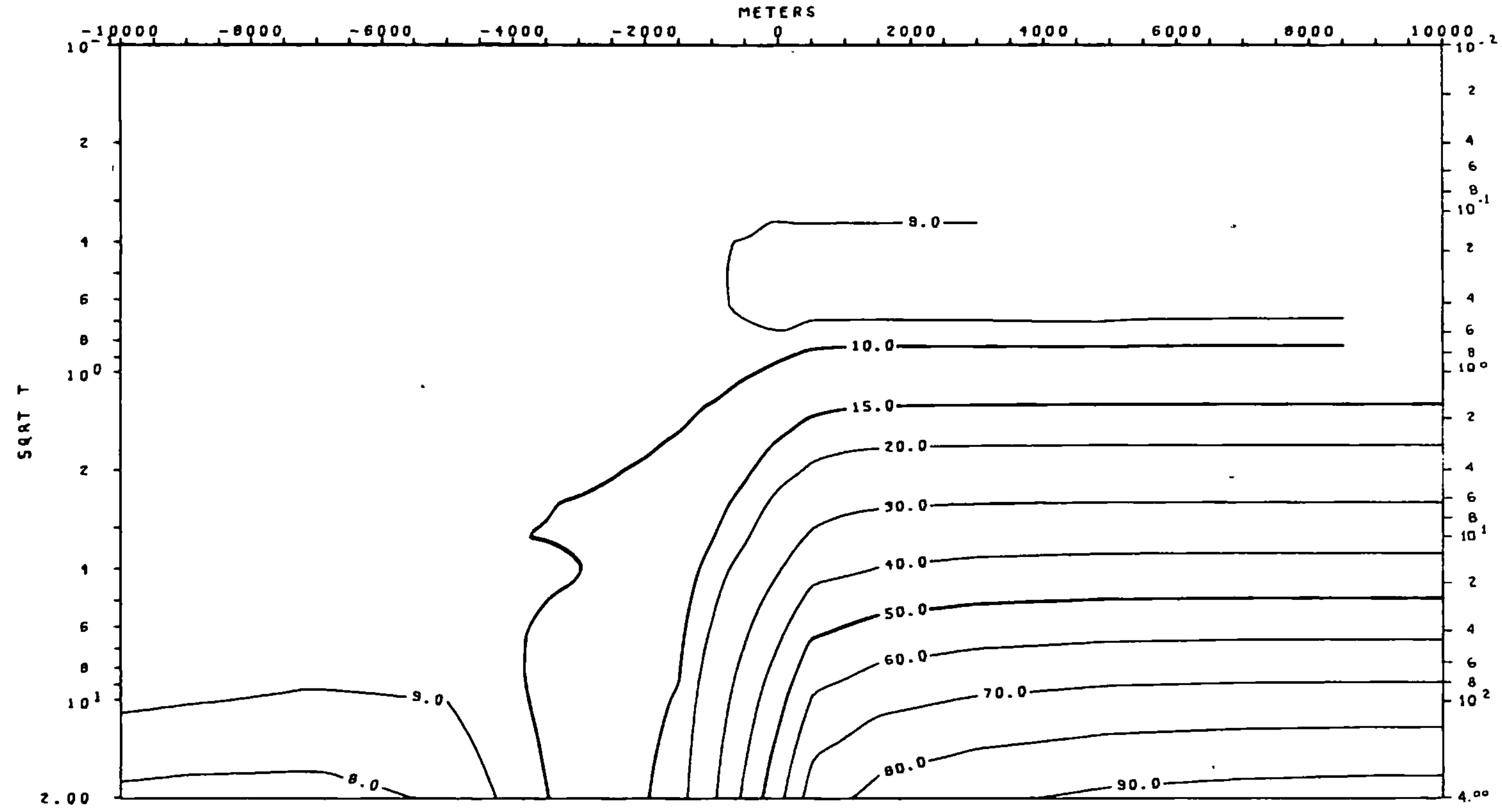

TM MODE
APPARENT RESISTIVITY VS. PERIOD (T)
MODEL 3-b

XBL 786-1909

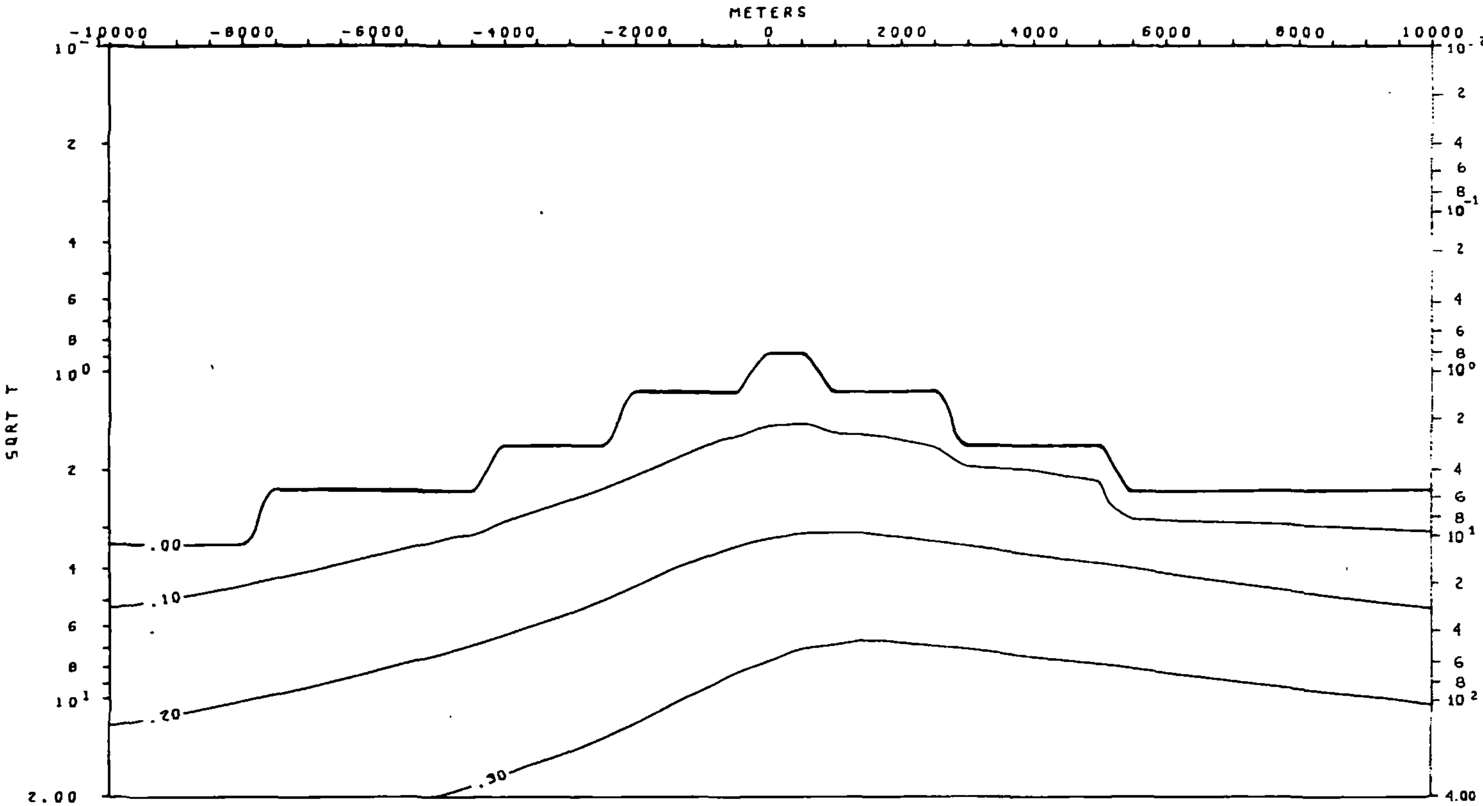

TIPPER VS. PERIOD (T)
MODEL 3-b

XBL 786-1944

Model 3-c

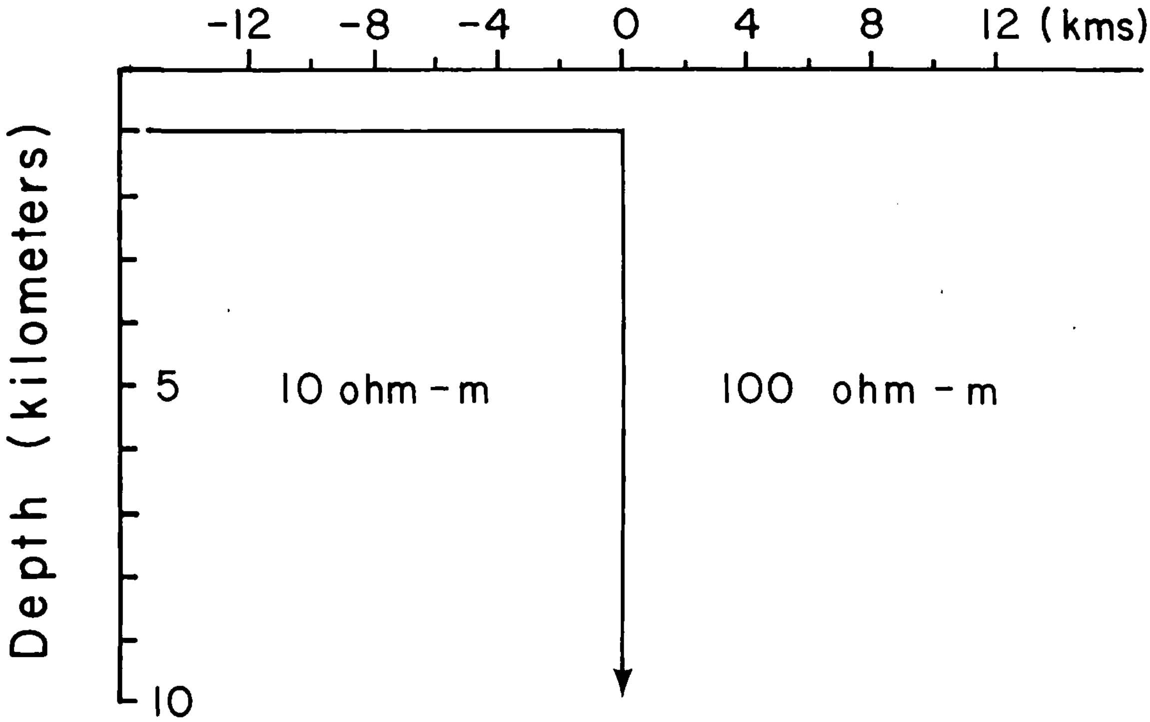

XBL 786-1951

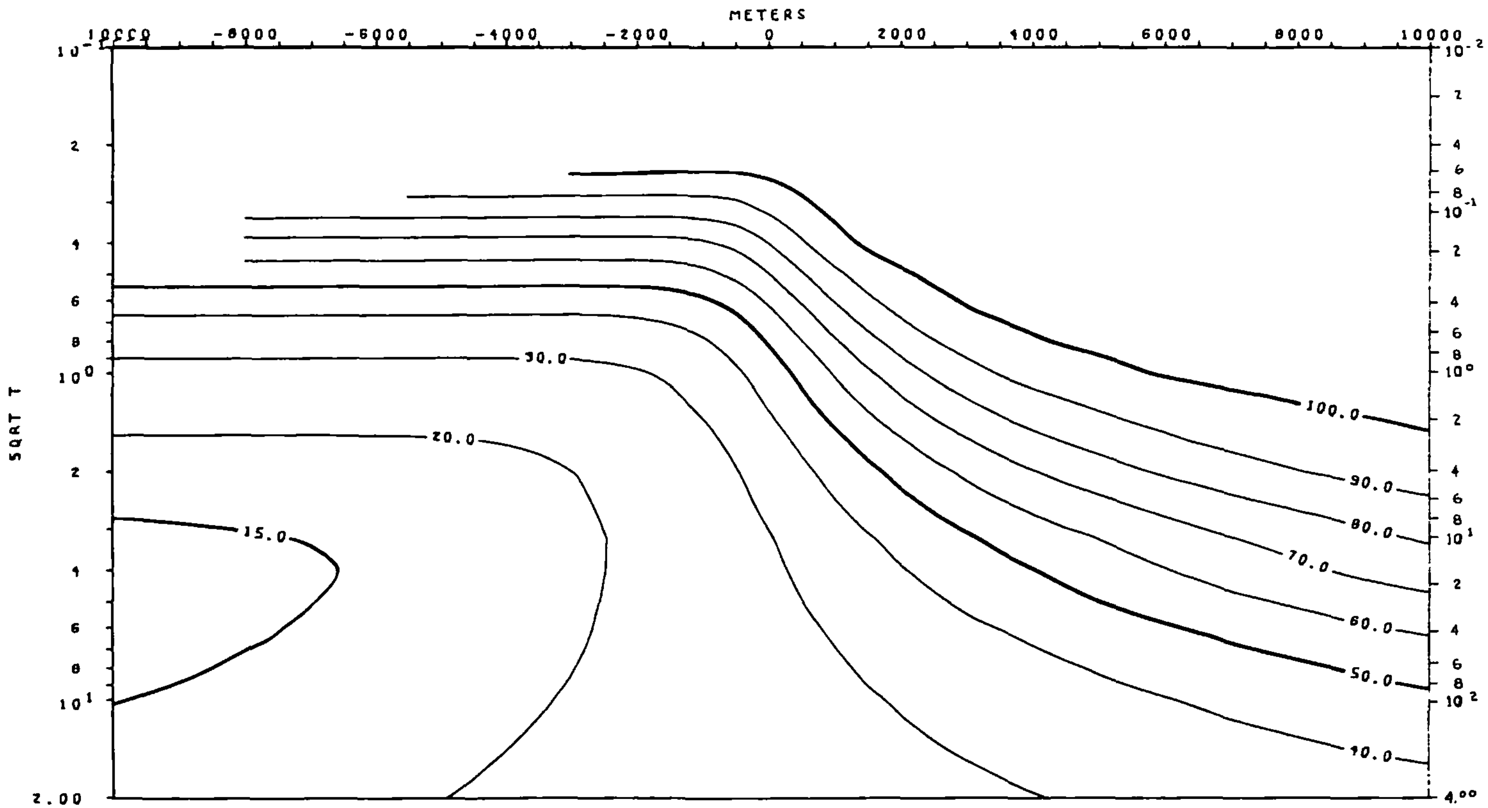

TE MODE
APPARENT RESISTIVITY VS. PERIOD (T)
MODEL 3-c

XBL 786-1908

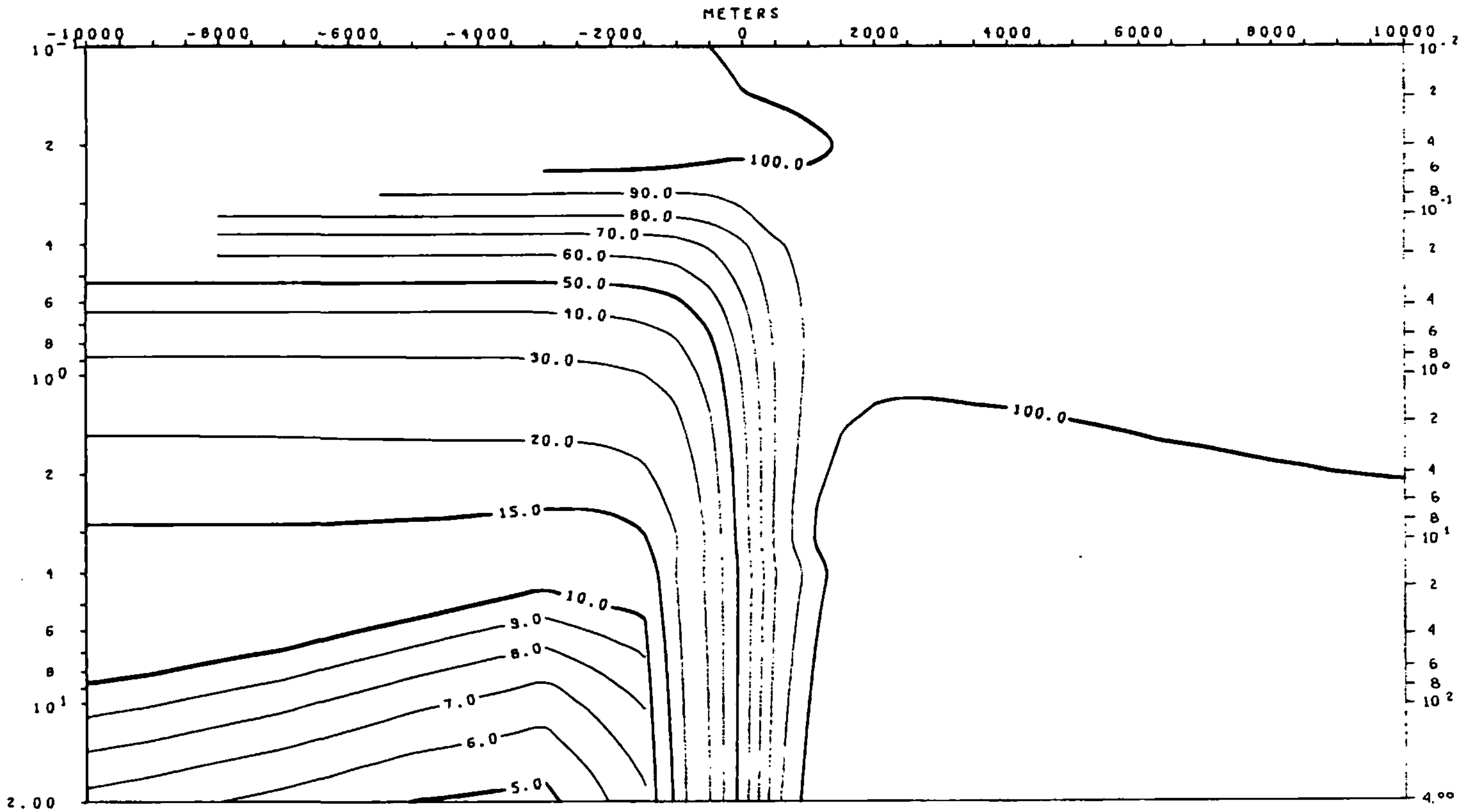

TM MODE
APPARENT RESISTIVITY VS. PERIOD (T)
MODEL 3-c

XBL 786-1928

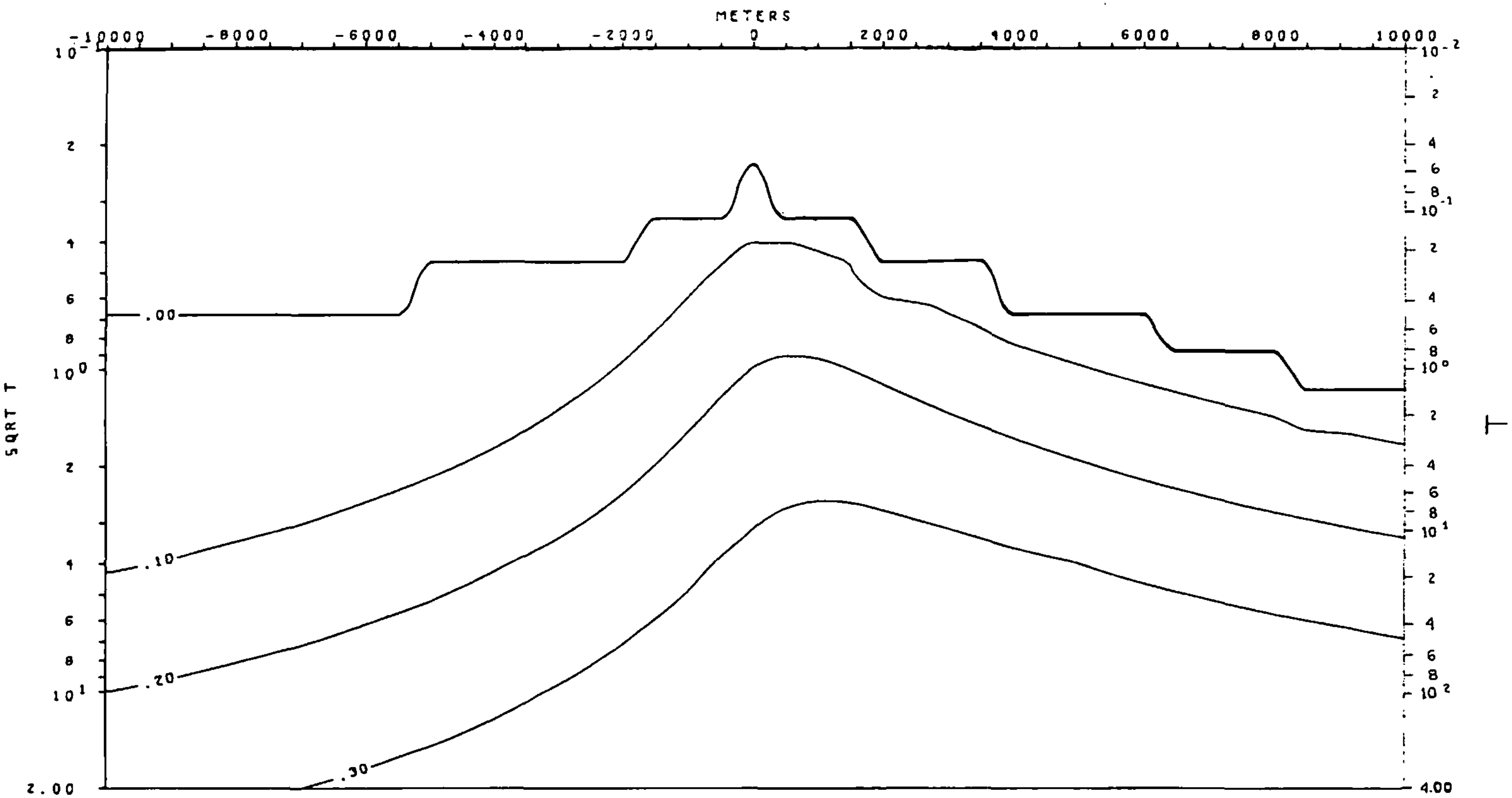

TIPPER VS. PERIOD (T)
MODEL 3-c

XBL 786-1923

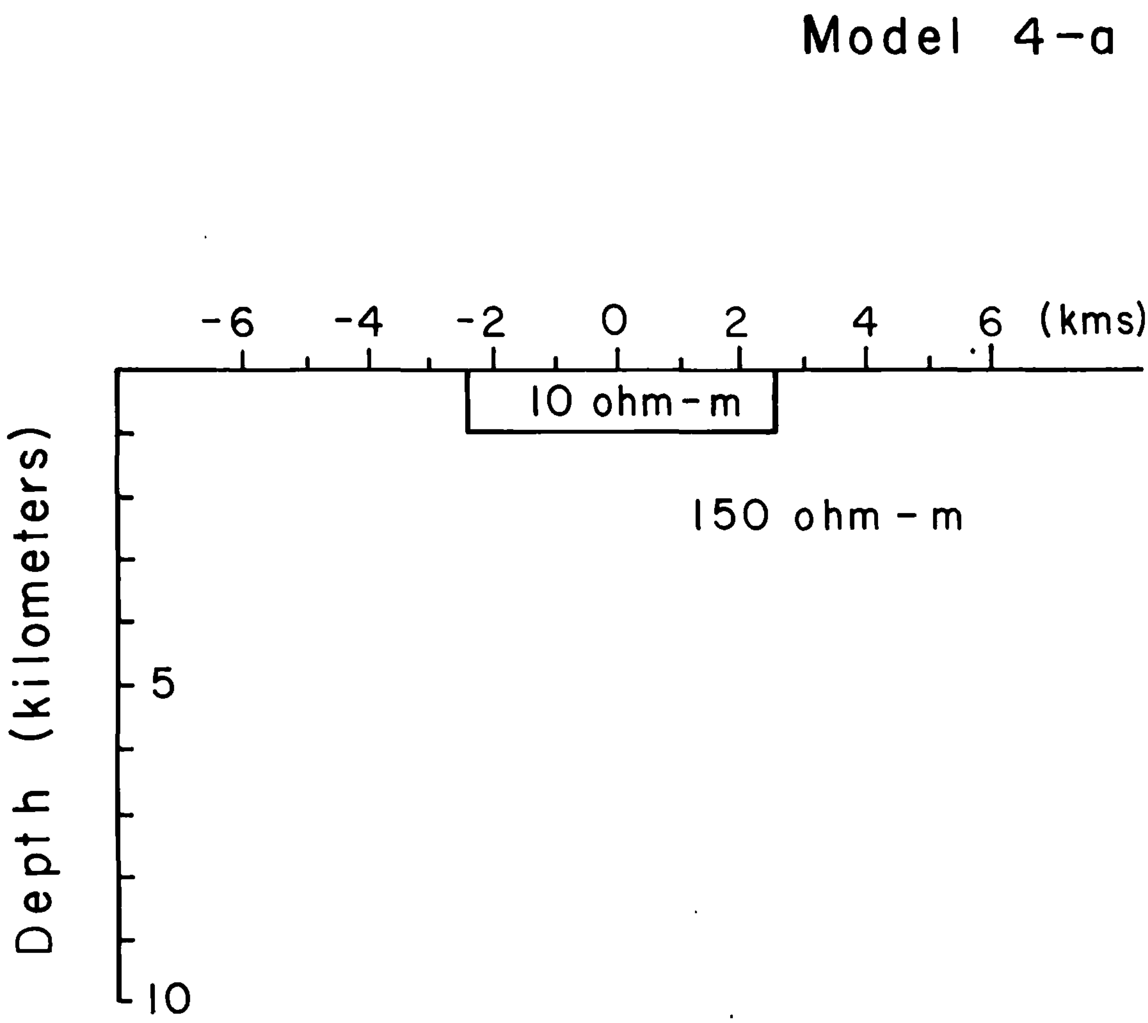

XBL 786-1953

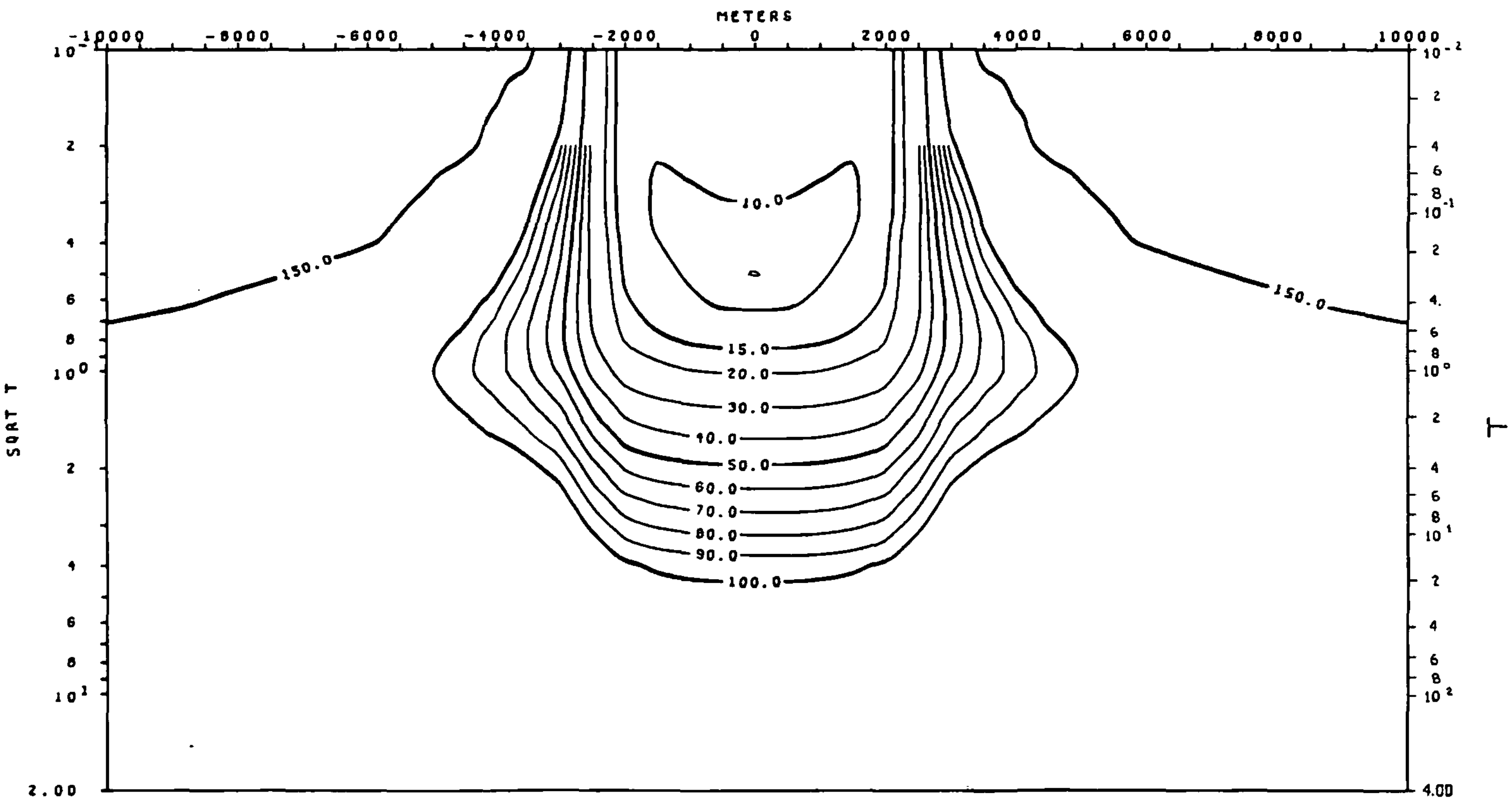

TE MODE
APPARENT RESISTIVITY VS. PERIOD (T)
MODEL 4-a

XBL 786-1901

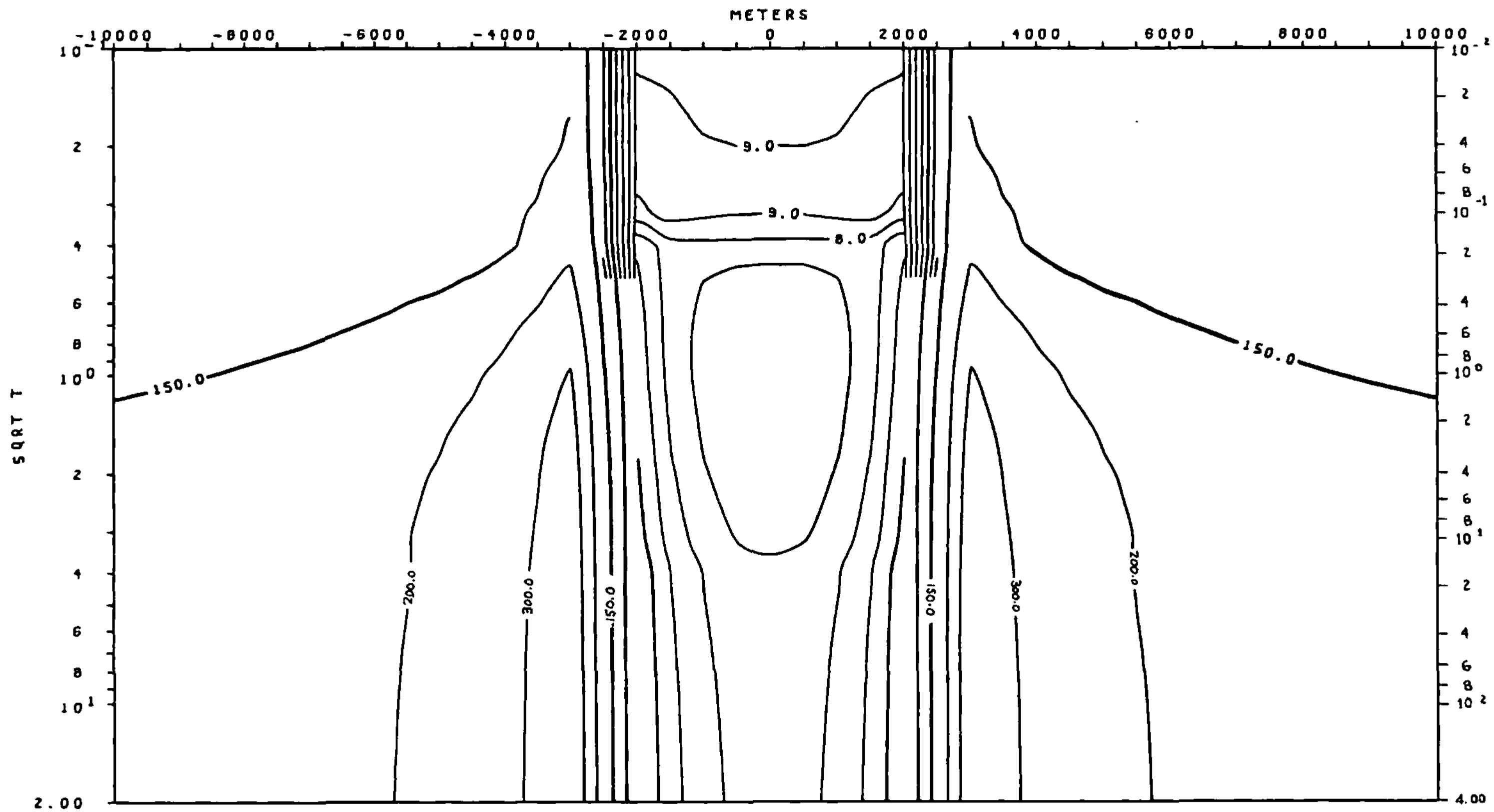

TM MODE
APPARENT RESISTIVITY VS. PERIOD (T)
MODEL 4-a

XBL 786-1946

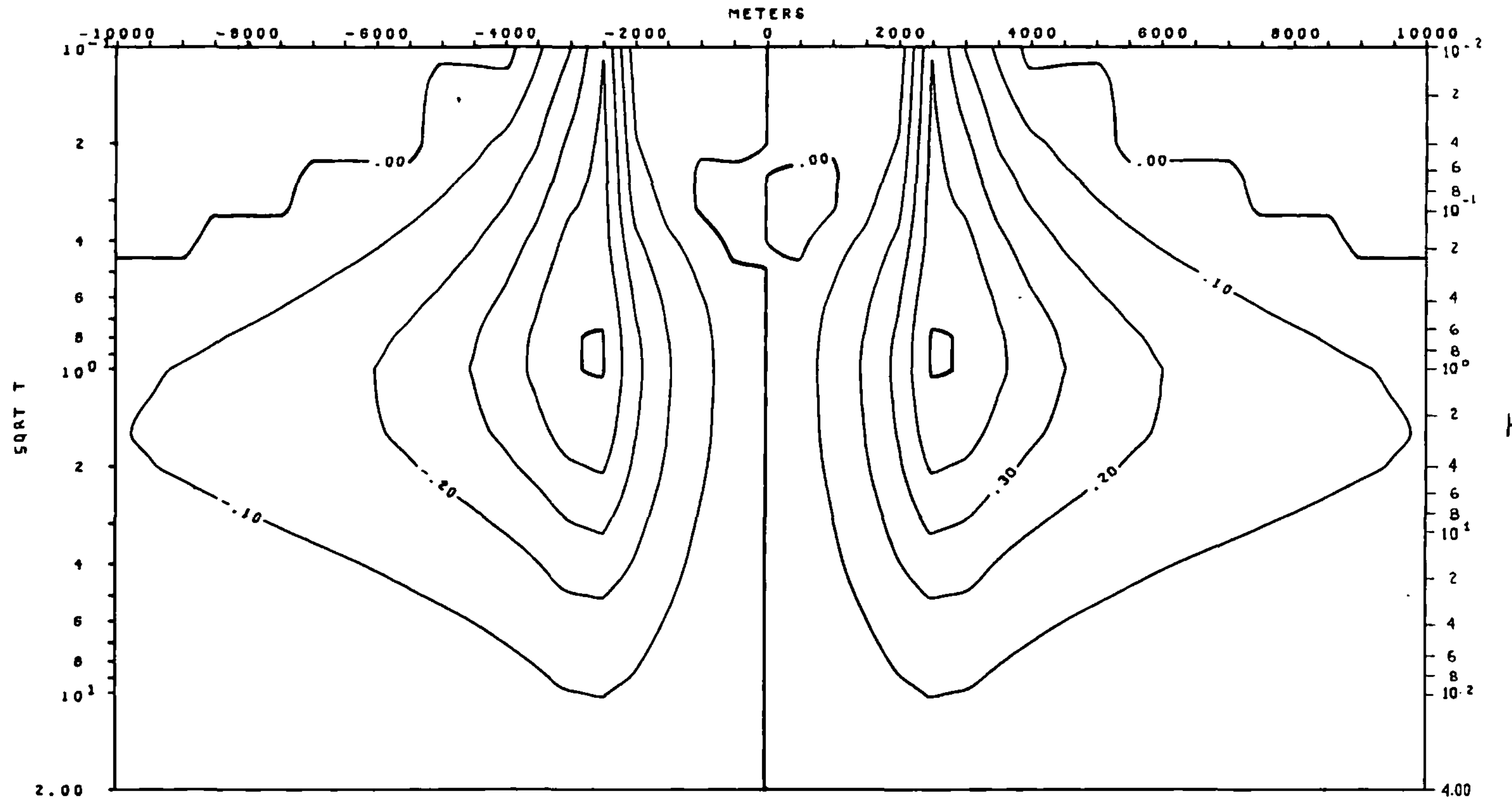

TIPPER VS. PERIOD (T)
MODEL 4-a

XBL 786-1933

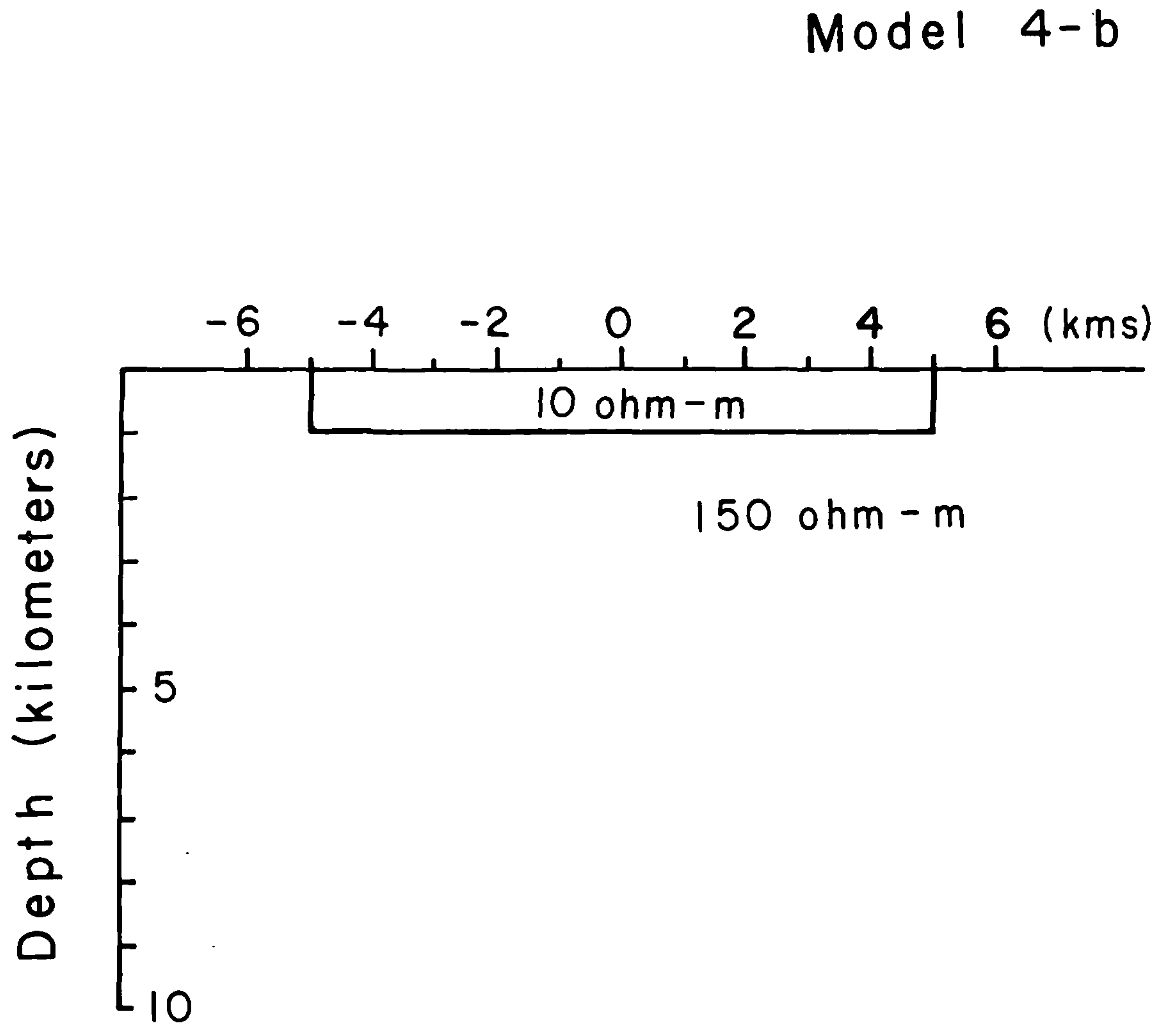

XBL 786-1952

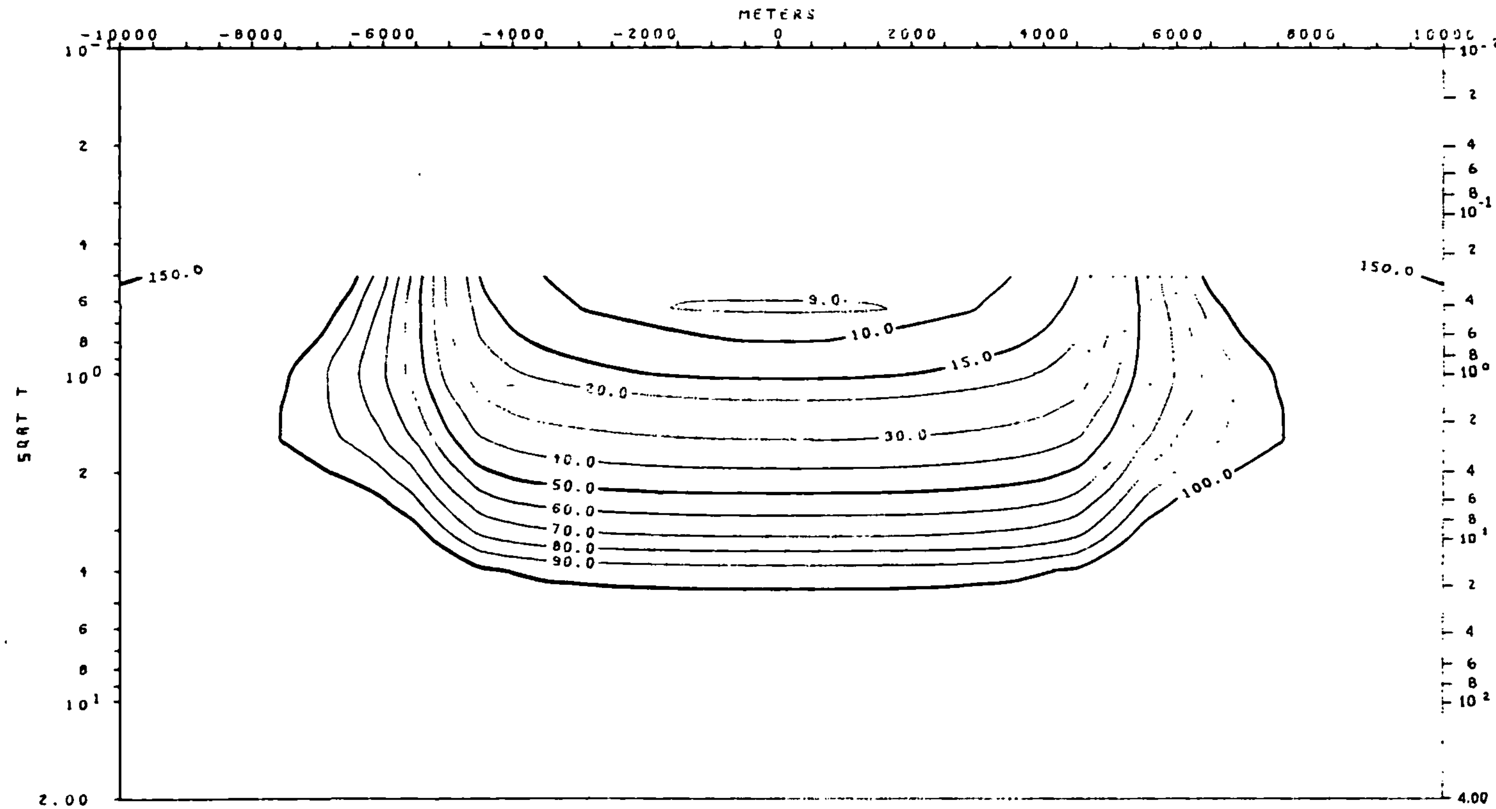

TE MODE
APPARENT RESISTIVITY VS. PERIOD (T)
MODEL 4-b

XBL 786-1935

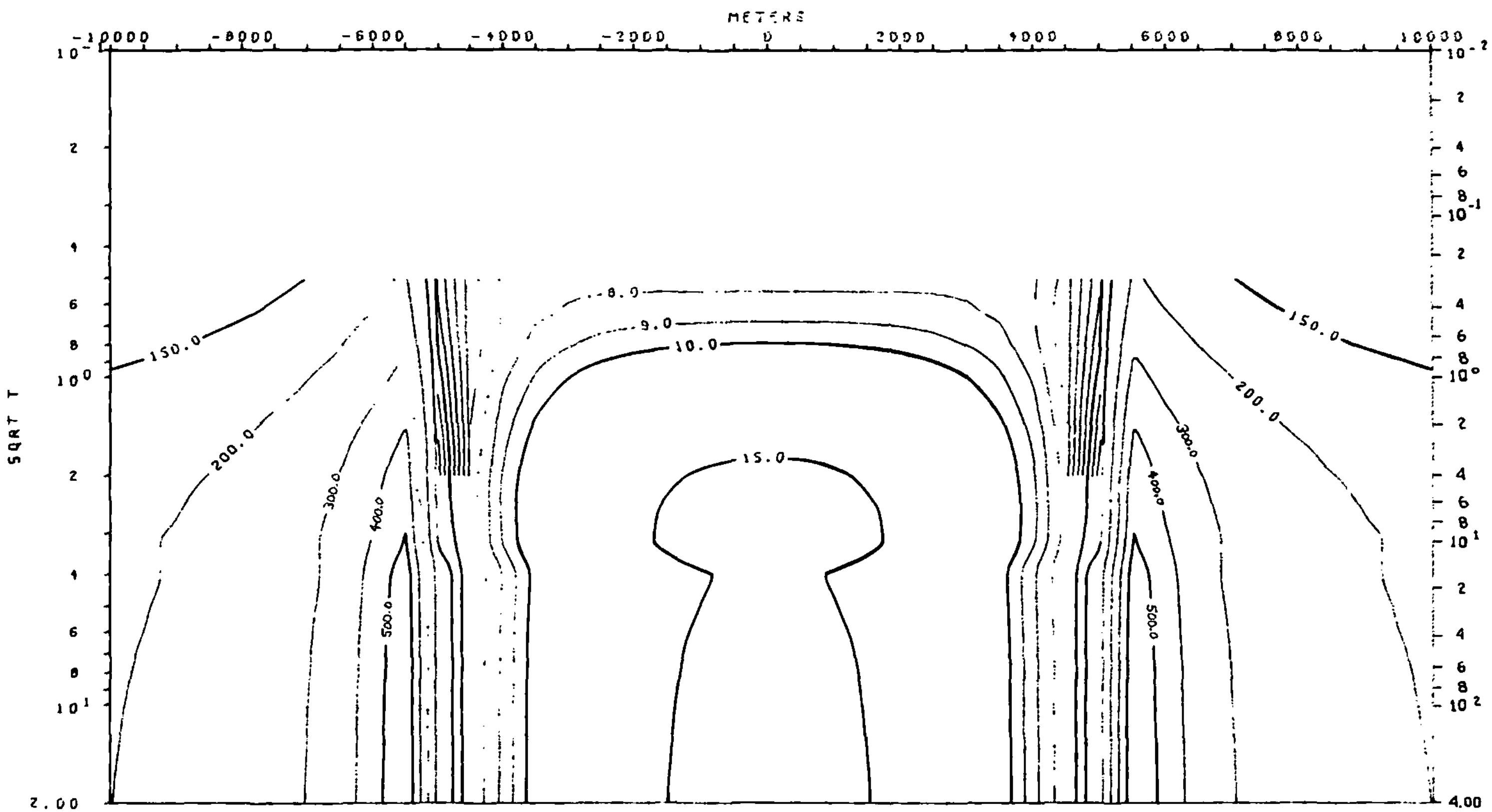

TM MODE
APPARENT RESISTIVITY VS. PERIOD (T)
MODEL 4-b

XBL 786-1934

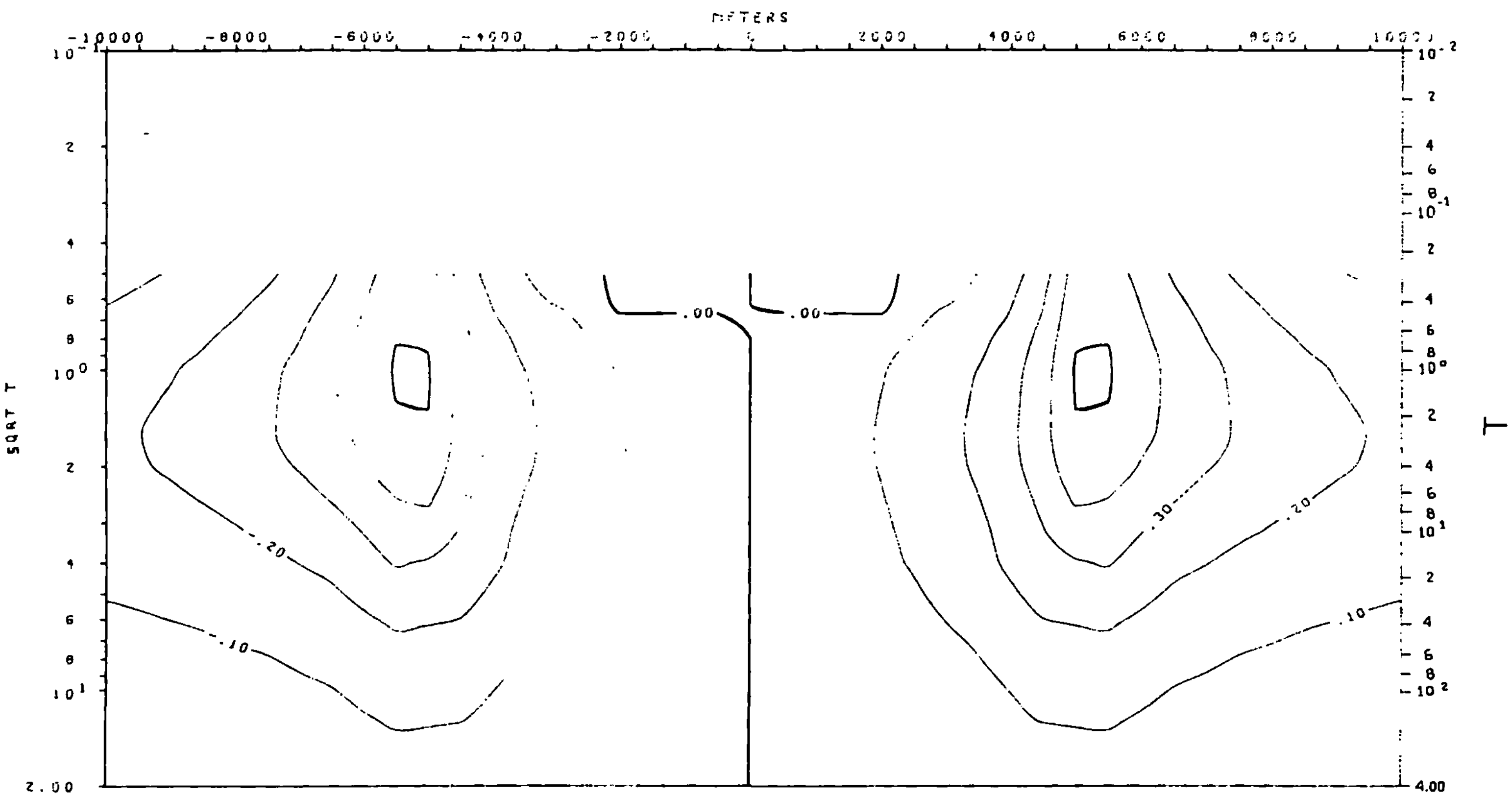

TIPPER VS. PERIOD (T)
MODEL 4-b

XBL 786-1937

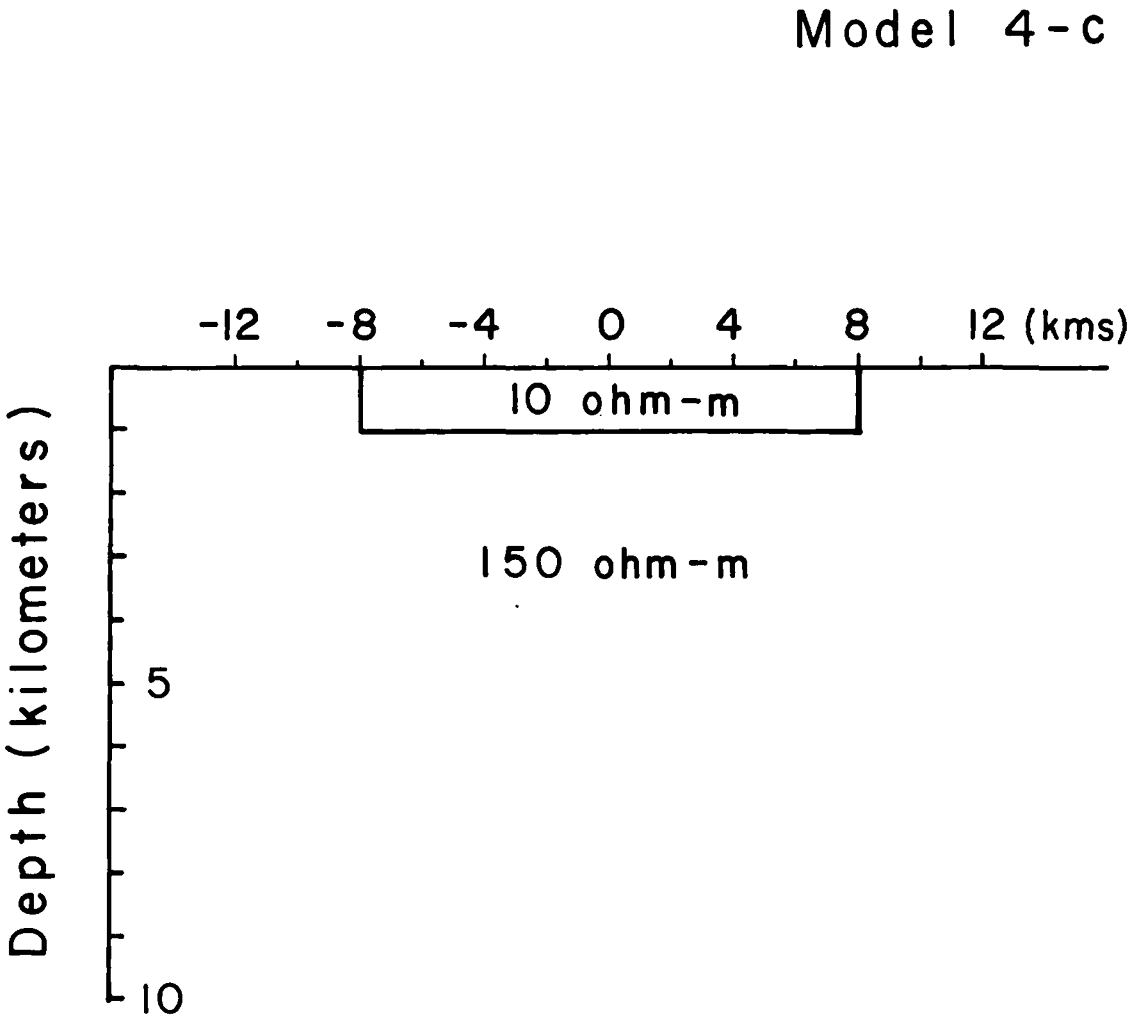

Model 4-c
-12
-8
-4
0
4
8
12 (kms)
10 ohm-m
150 ohm-m
Depth (kilometers)
5
10

XBL 786-1880

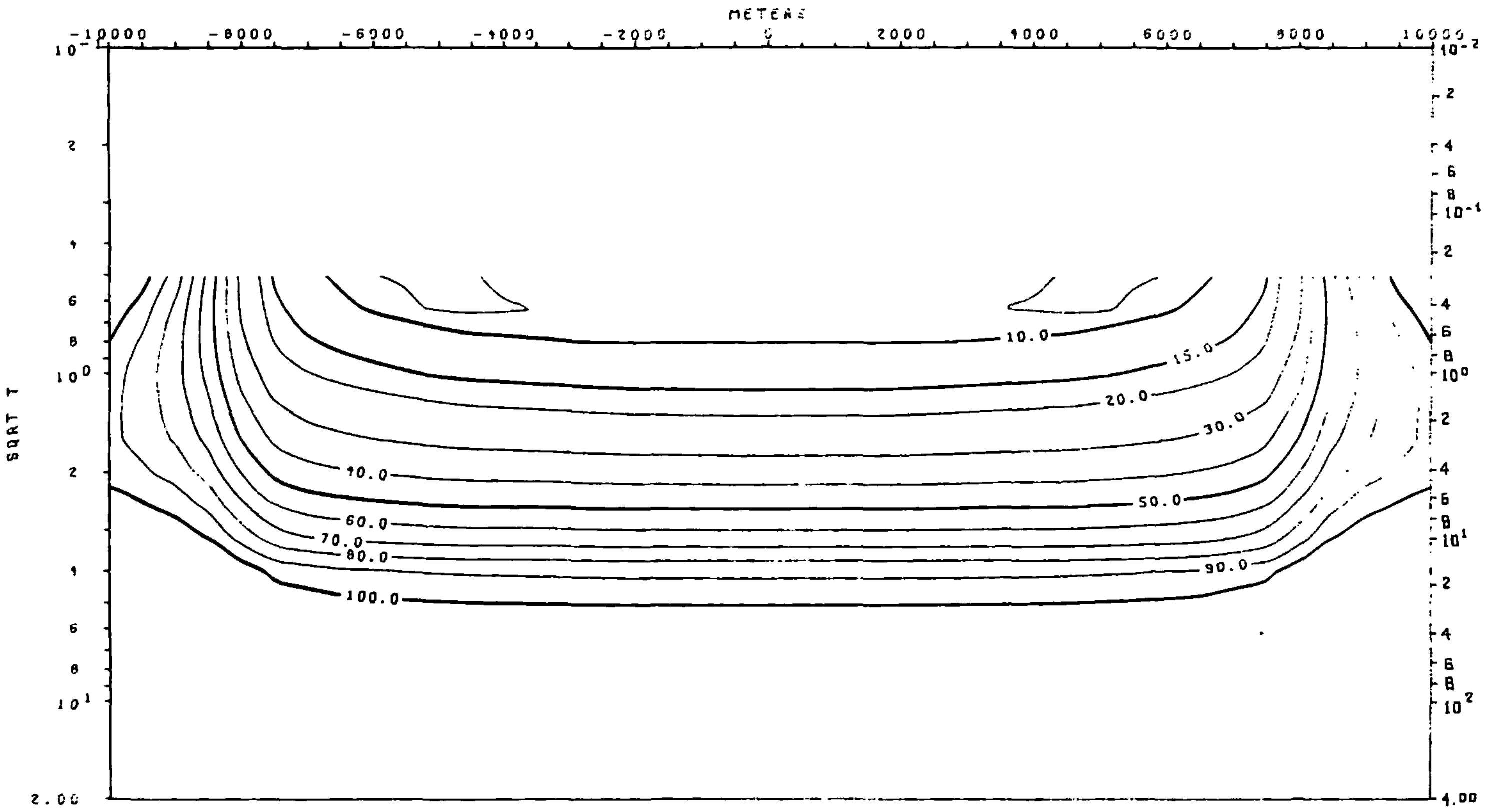

TE MODE
APPARENT RESISTIVITY VS. PERIOD (T)
MODEL 4-c

XBL 786-1911

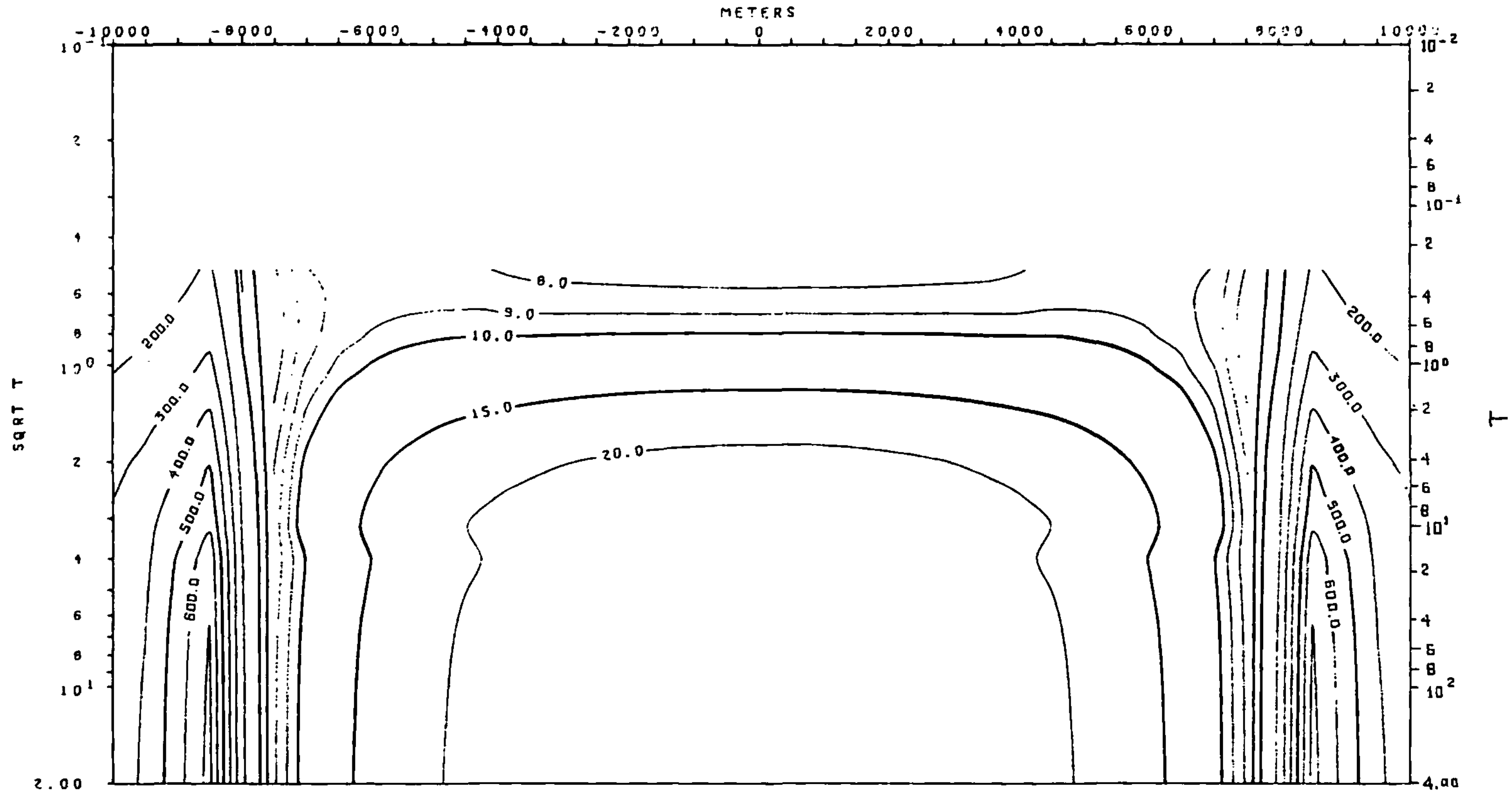

TM MODE
APPARENT RESISTIVITY VS. PERIOD (T)
MODEL 4-c

XBL 786-1910

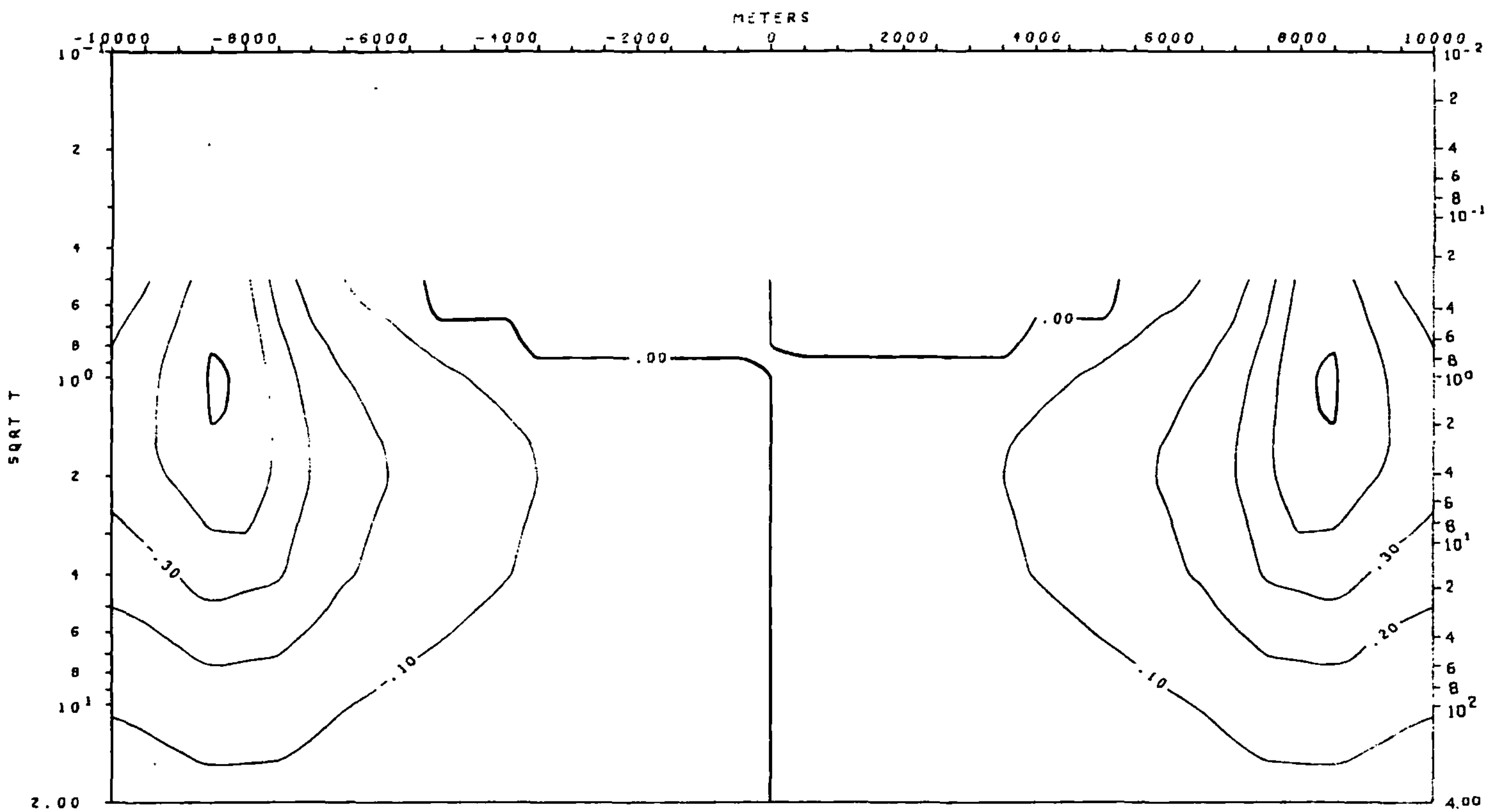

TIPPER VS. PERIOD (T)
MODEL 4-c

XBL 786-1917

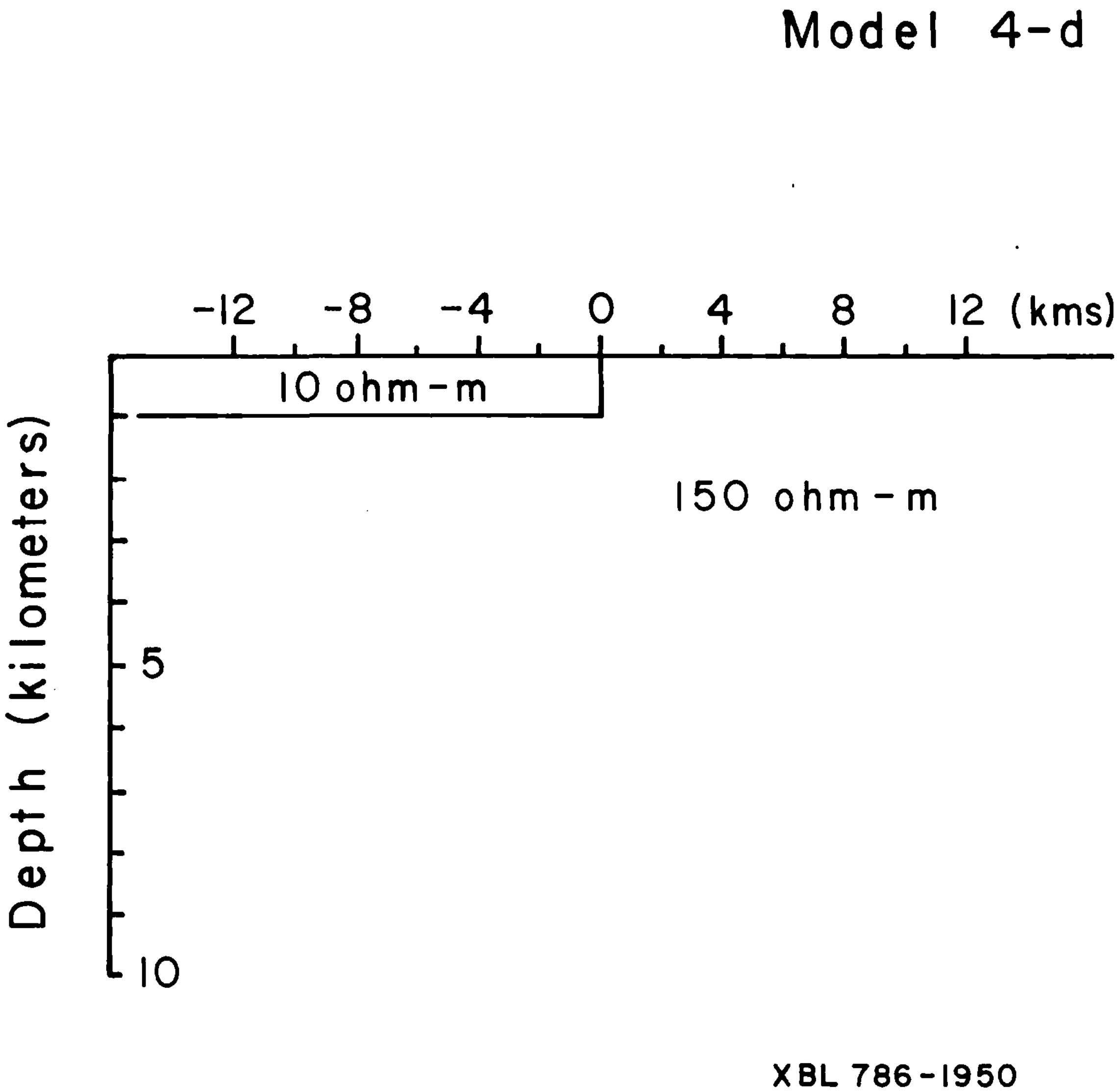
Model 4-d
-12
-8
-4
0
4
8
12 (kms)
10 ohm-m
150 ohm-m
Depth (kilometers)
5
10
XBL 786-1950

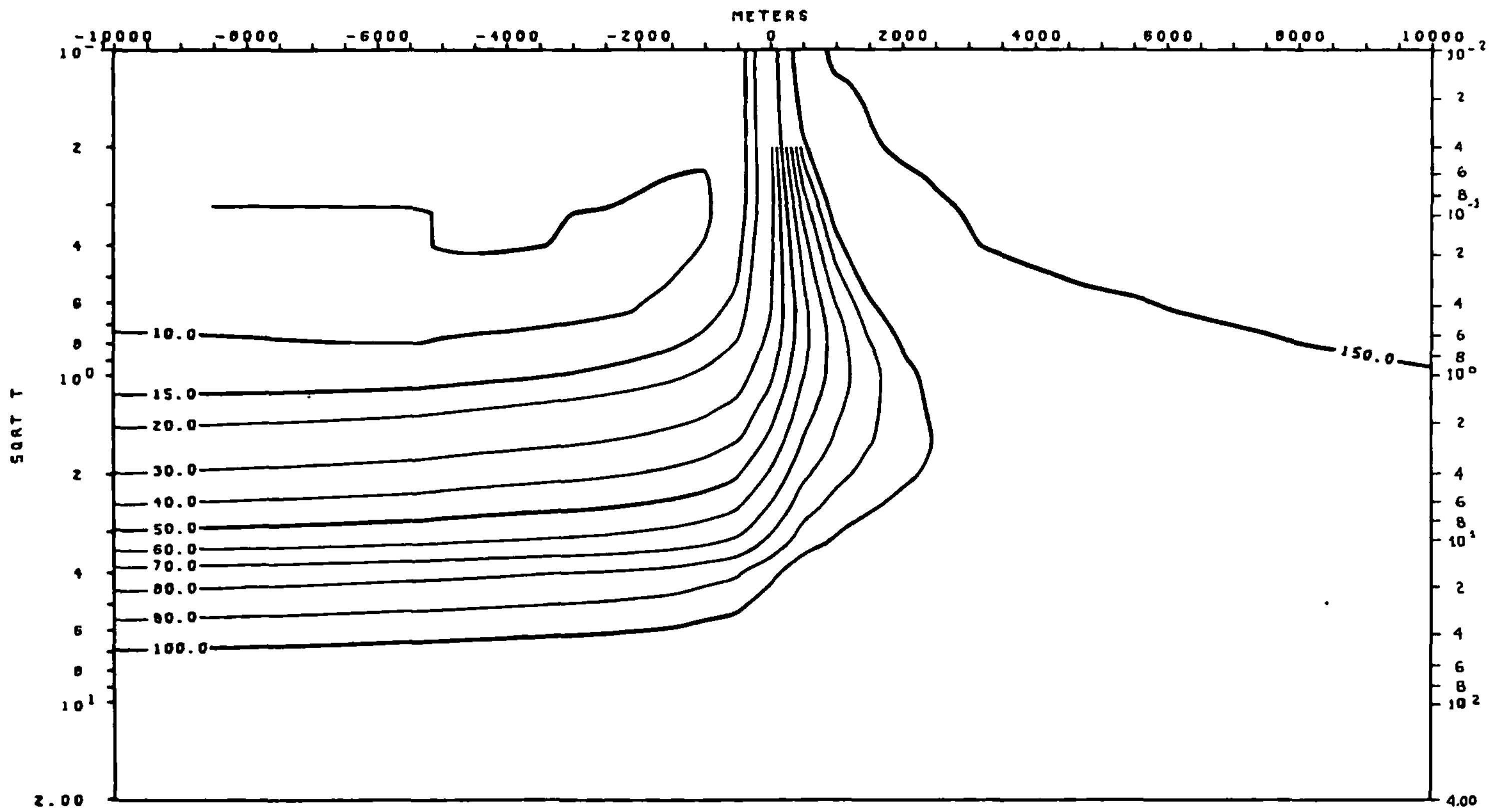

TE MODE
APPARENT RESISTIVITY VS. PERIOD (T)
MODEL 4-d

XBL 786-1905

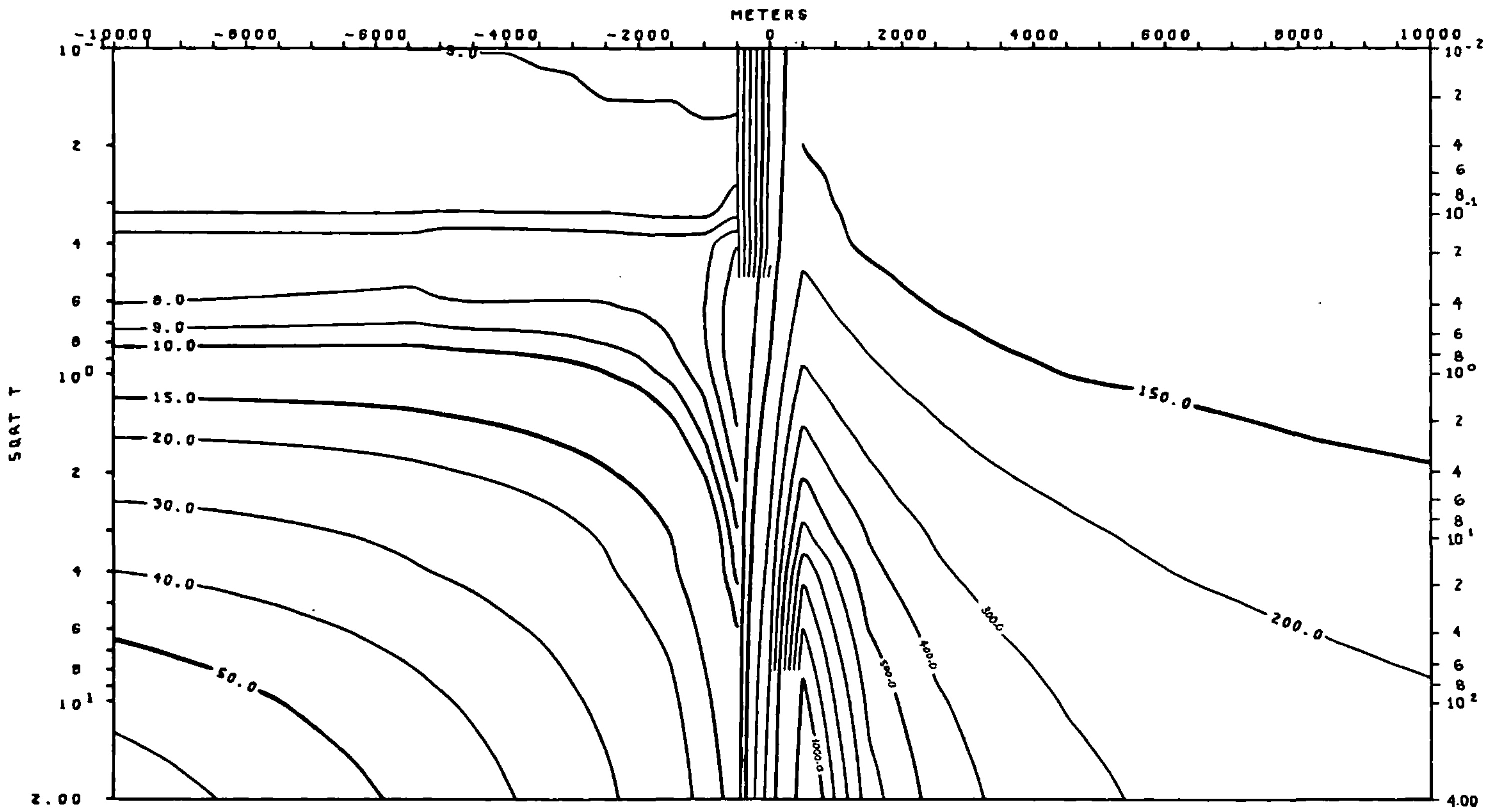

TM MODE
APPARENT RESISTIVITY VS. PERIOD (T)
MODEL 4-d

XBL 786-1931

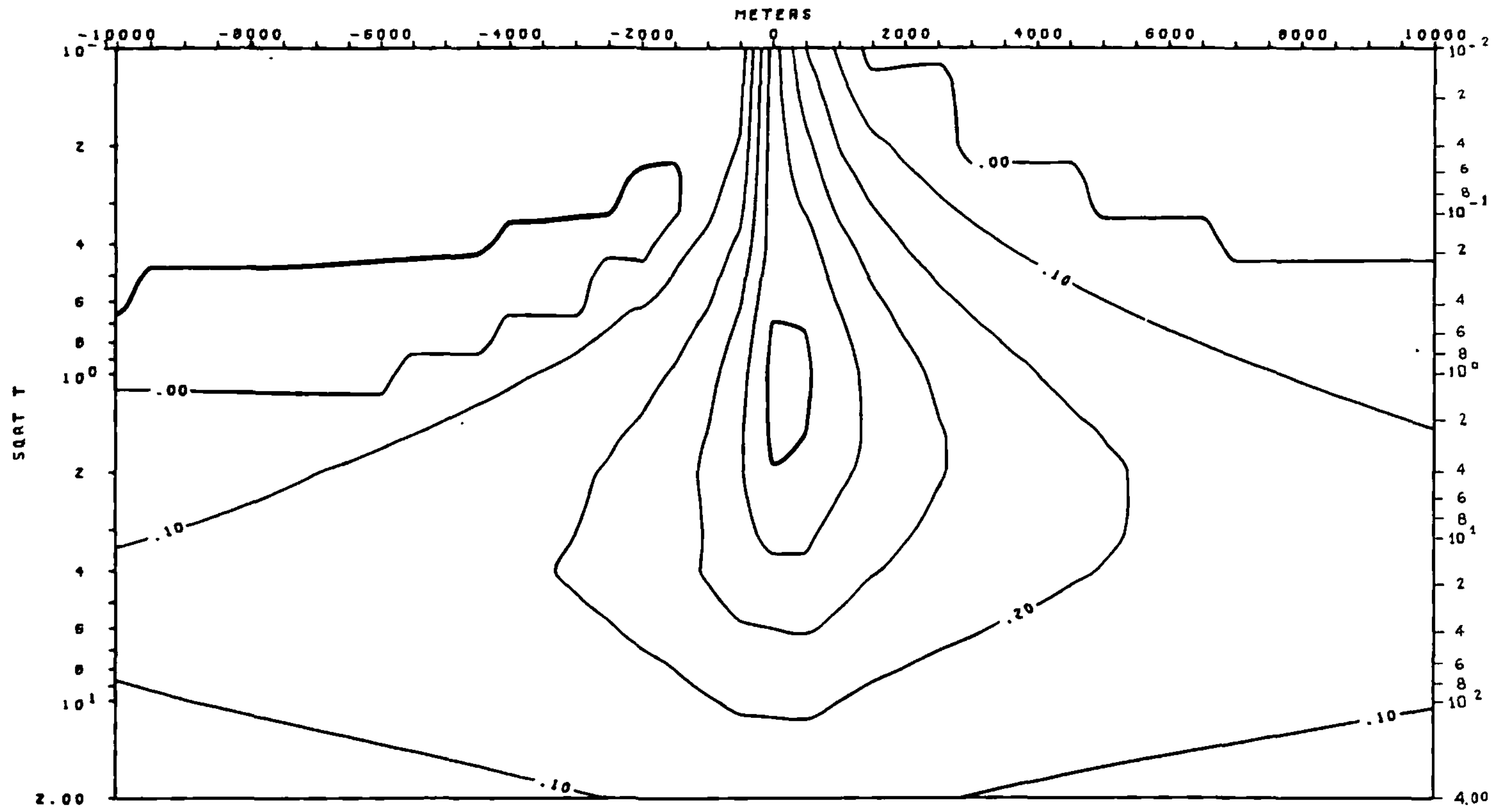

TIPPER VS. PERIOD (T)
MODEL 4-d

XBL 786-1945

Appendix 5

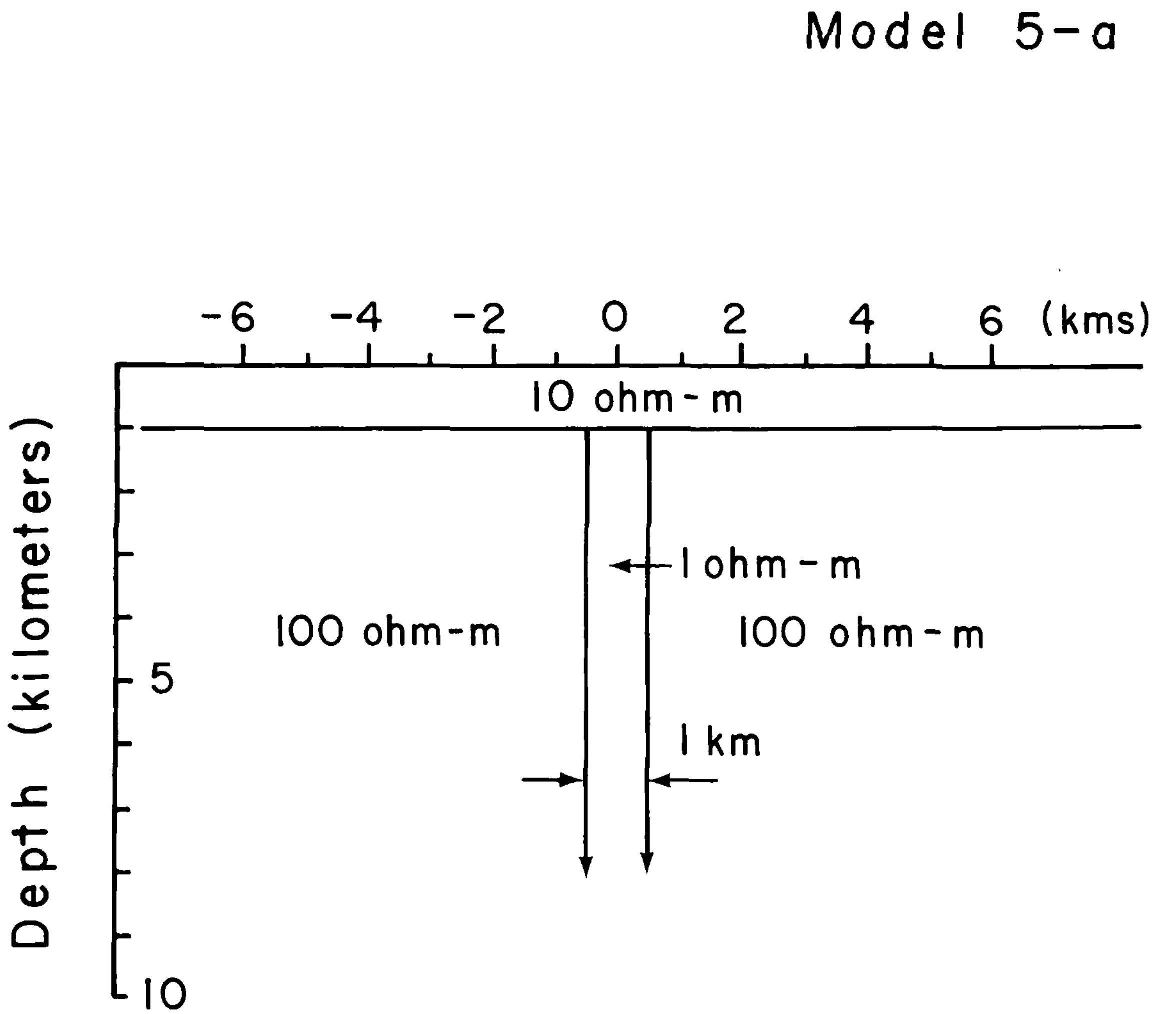
Model 5-a
-6
-4
-2
0
2
4
6
(kms)
10 ohm-m
1 ohm-m
100 ohm-m
100 ohm-m
1 km
5
10
Depth (kilometers)

XBL786-1956

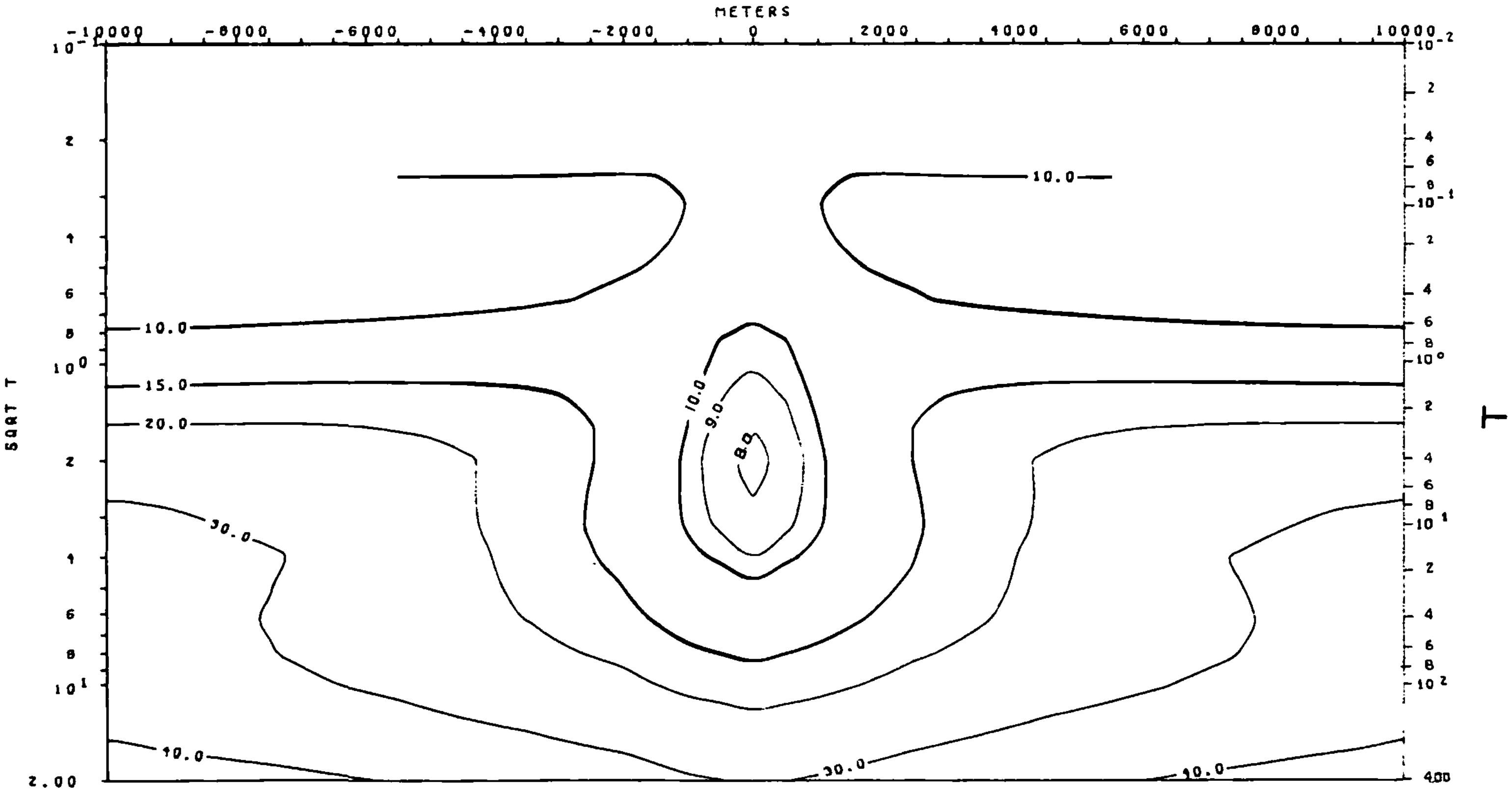

TE MODE
APPARENT RESISTIVITY VS. PERIOD (T)
MODEL 5-a

XBL 786-1927

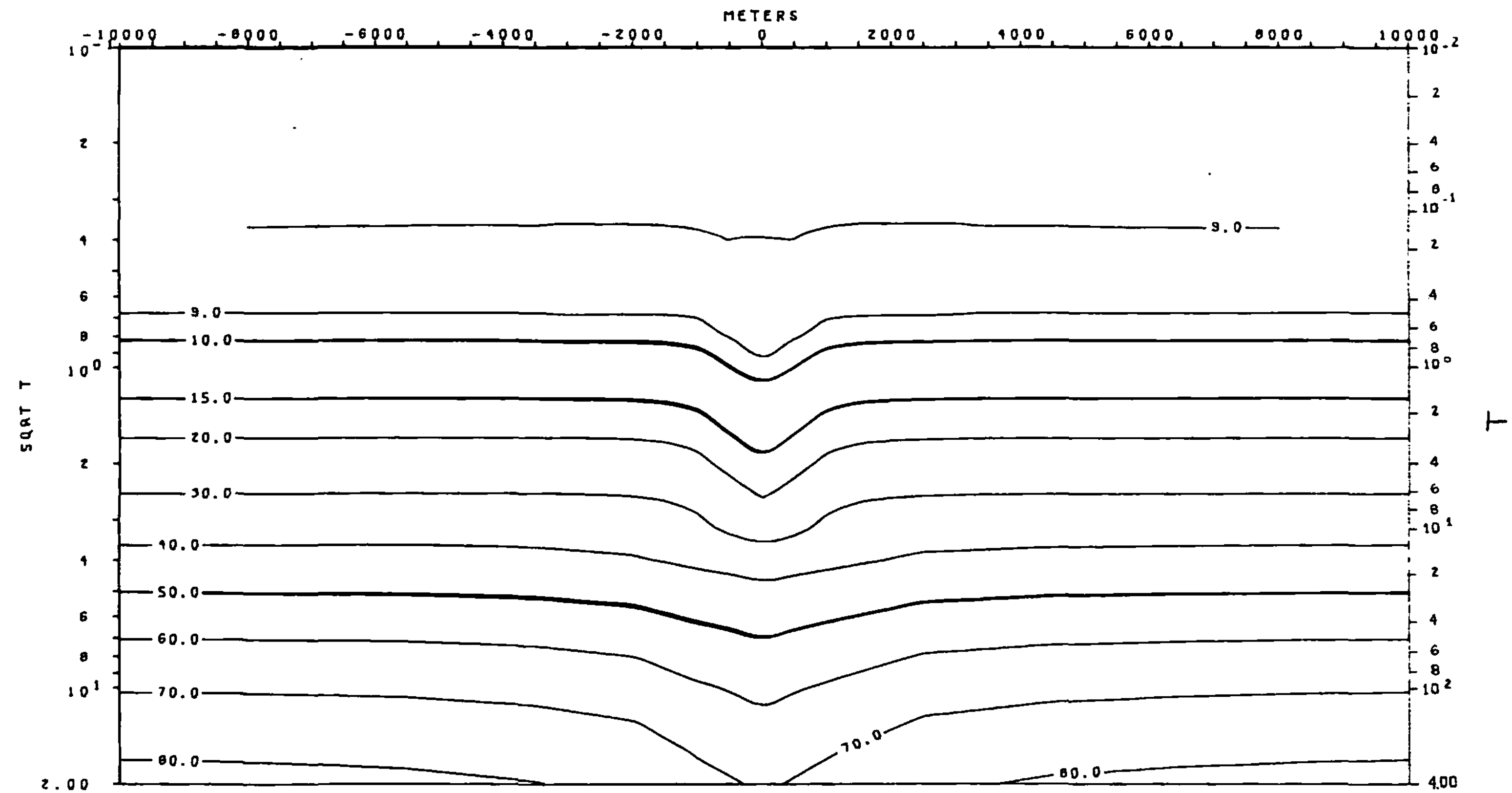

TM MODE
APPARENT RESISTIVITY VS. PERIOD (T)
MODEL 5-a

XBL 786-1914

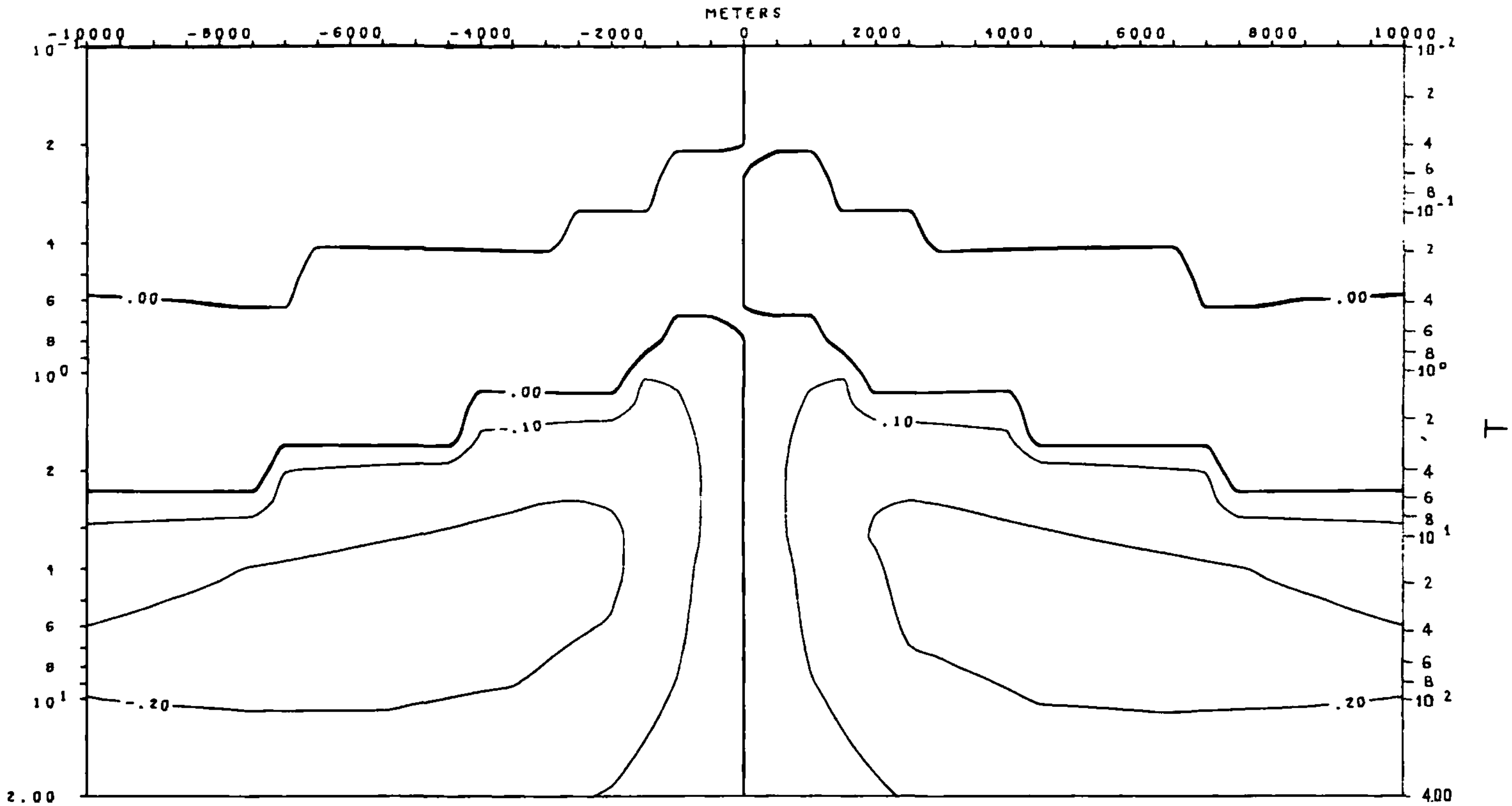

TIPPER VS. PERIOD (T)
MODEL 5-a

XBL 786-1899

Appendix 6

Model 6-a

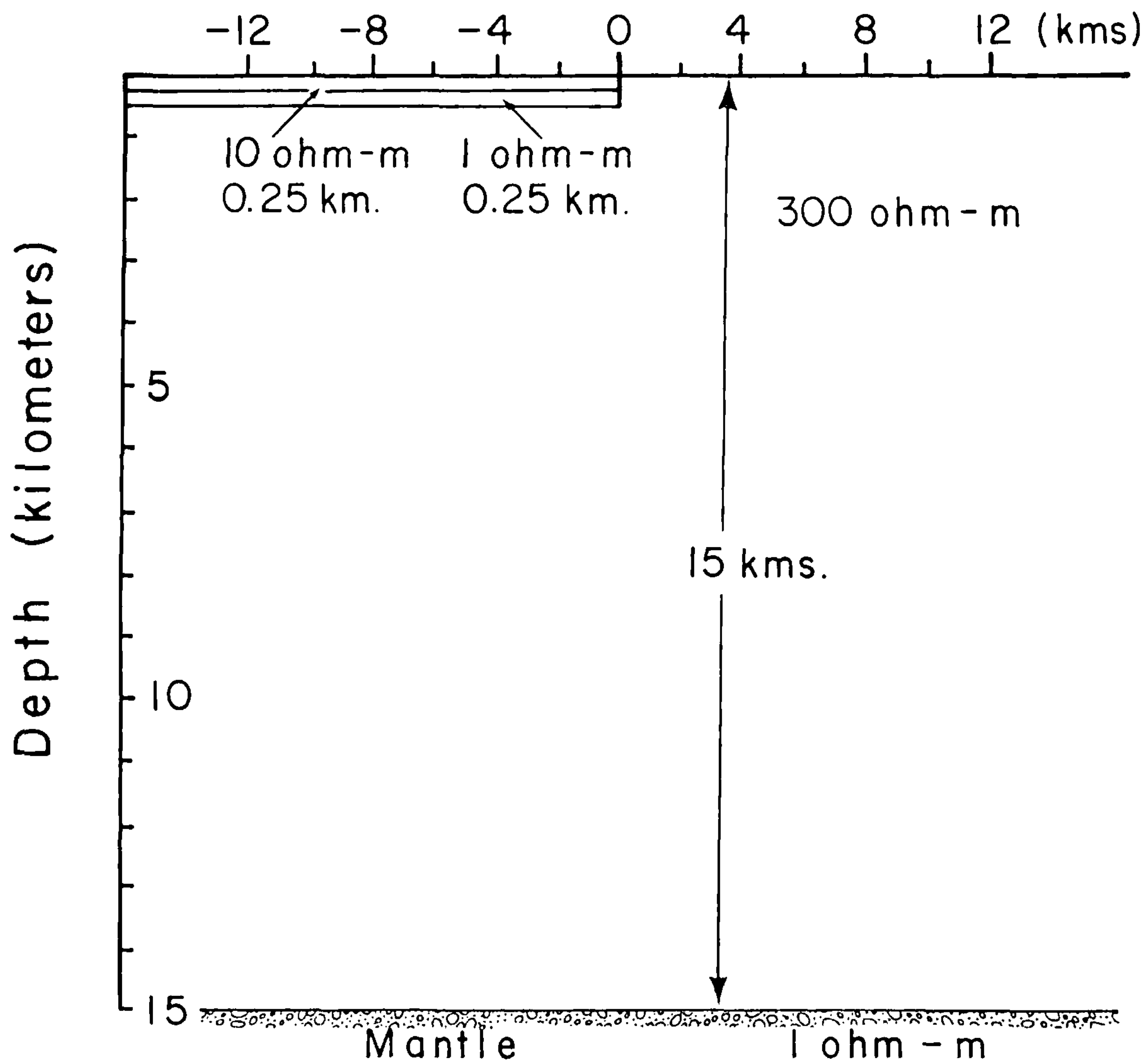

XBL 786-1955

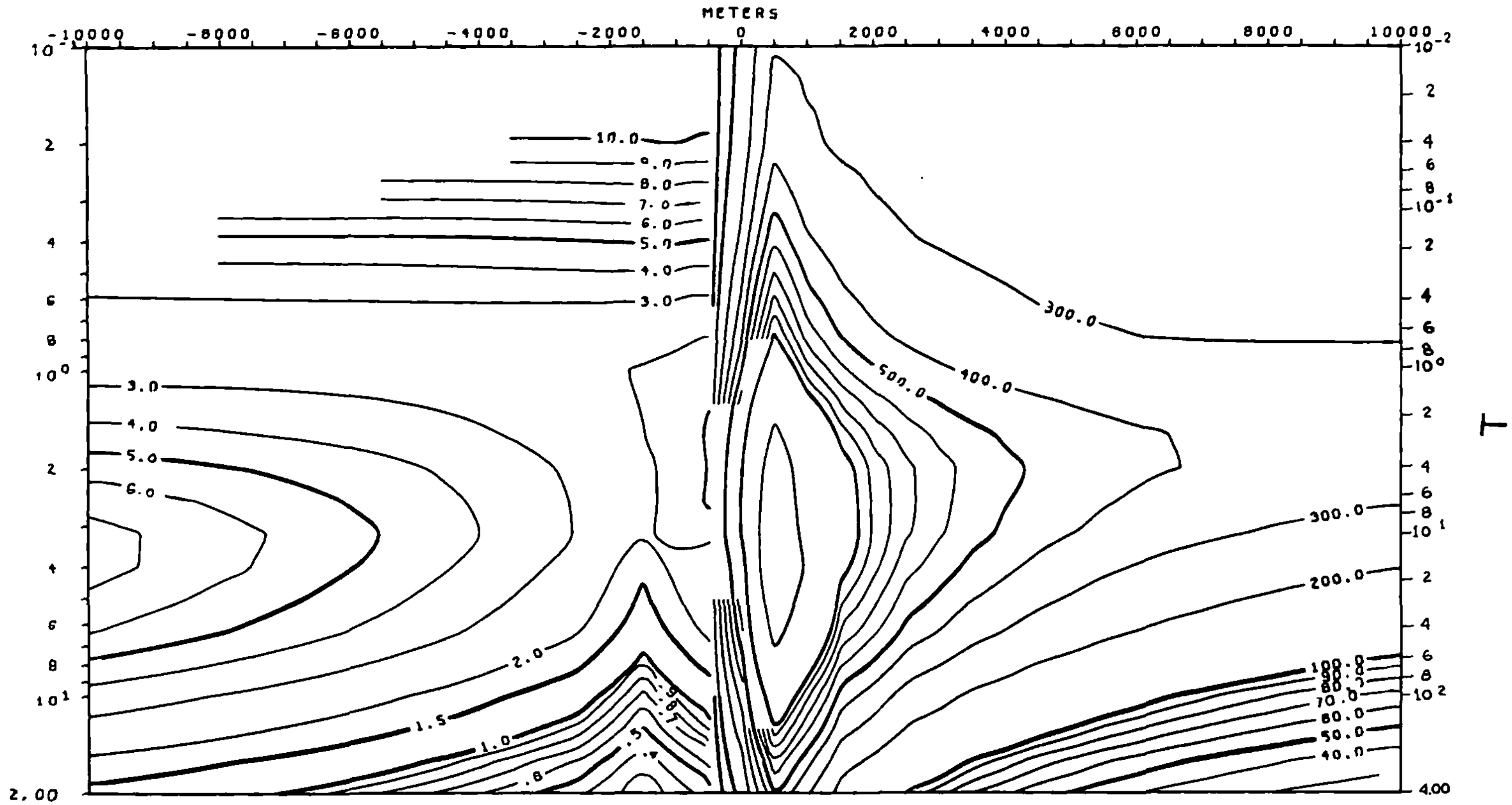

TE MODE
APPARENT RESISTIVITY VS. PERIOD (T)
MODEL 6-a

XBL 786-1942

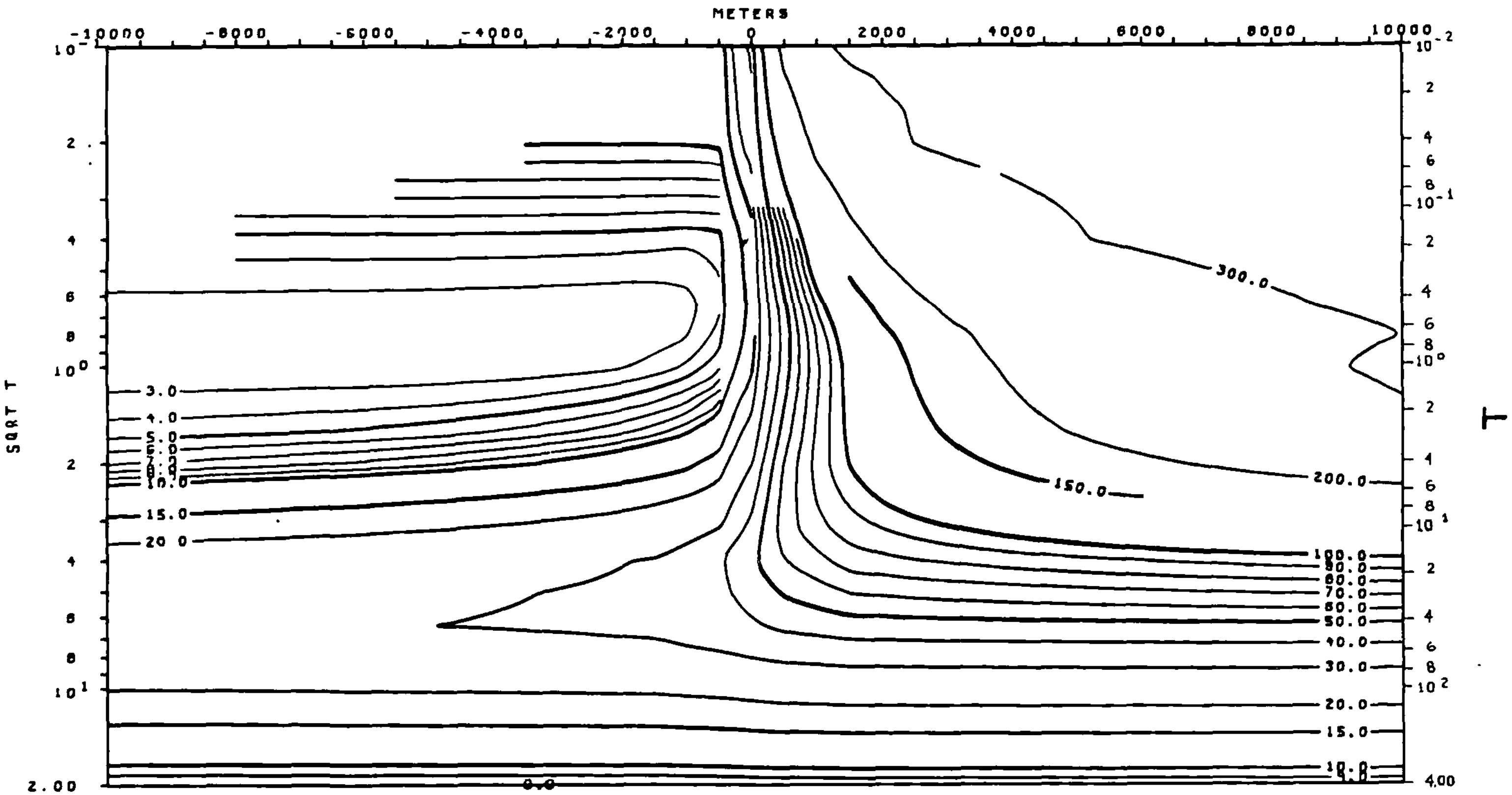

TM MODE
APPARENT RESISTIVITY VS. PERIOD (T)
MODEL 6-a

XBL 786-1938

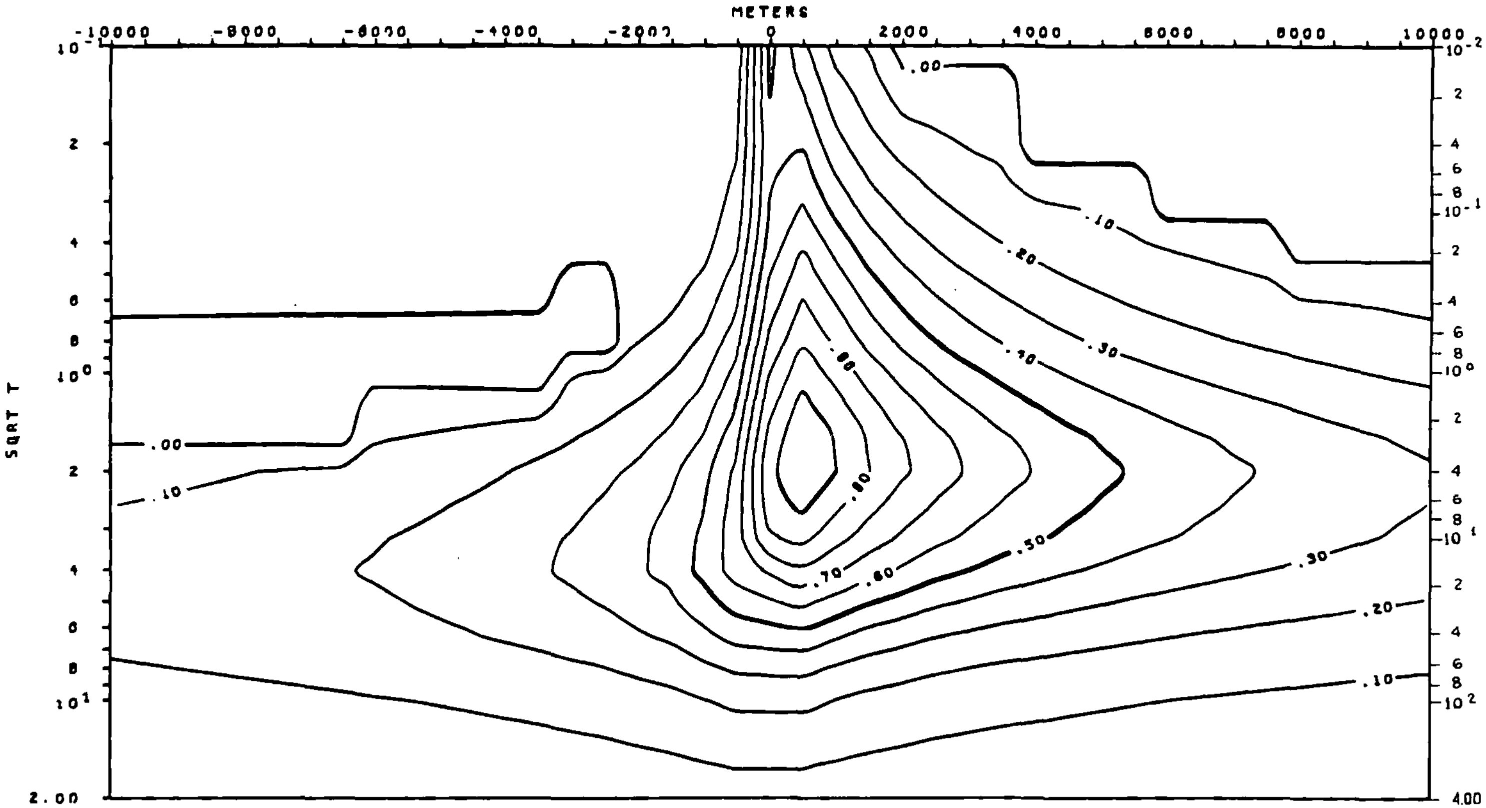

TIPPER VS. PERIOD (T)
MODEL 6-a

XBL 786-1920

Model 6-b

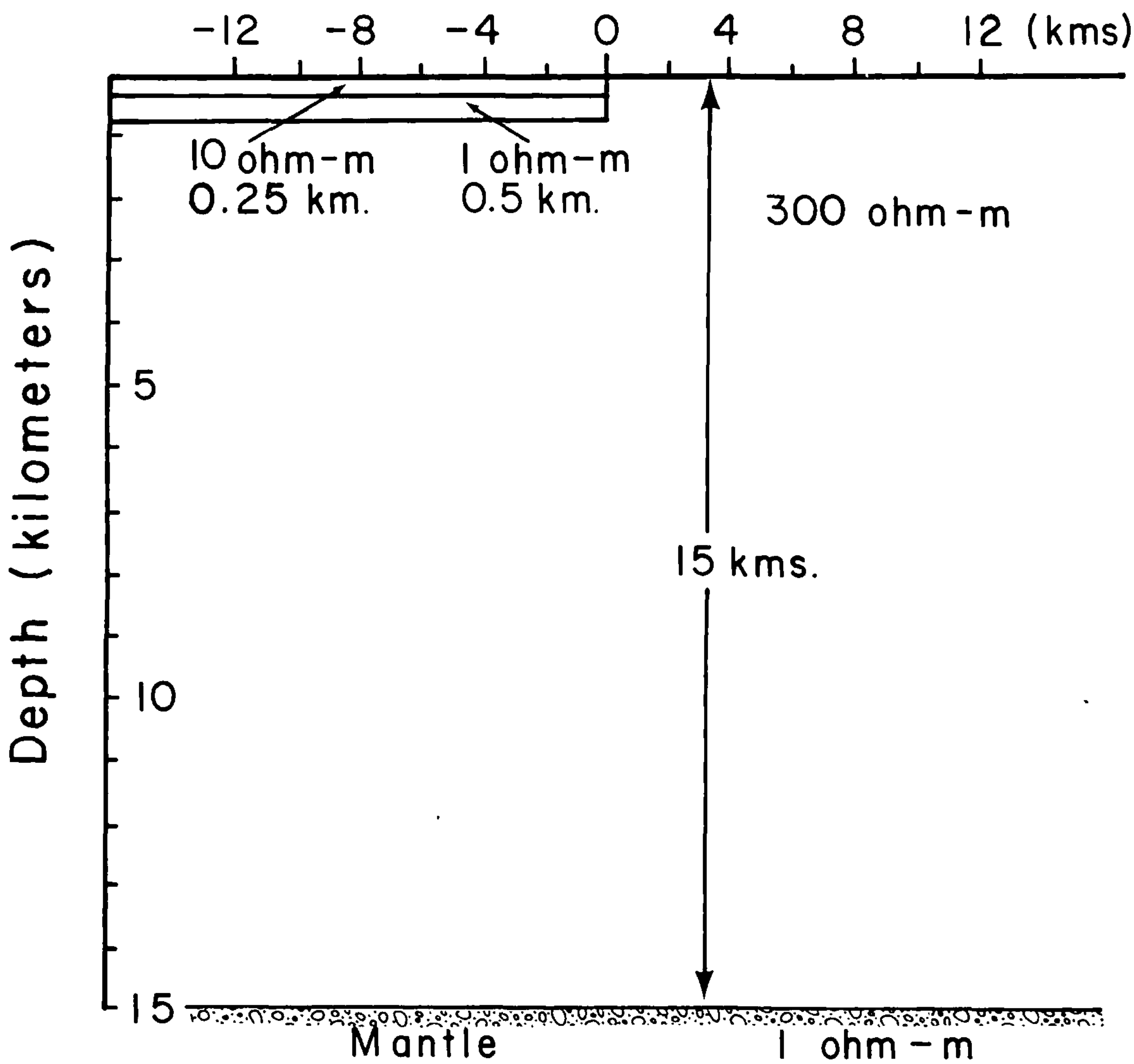

XBL 786-1960

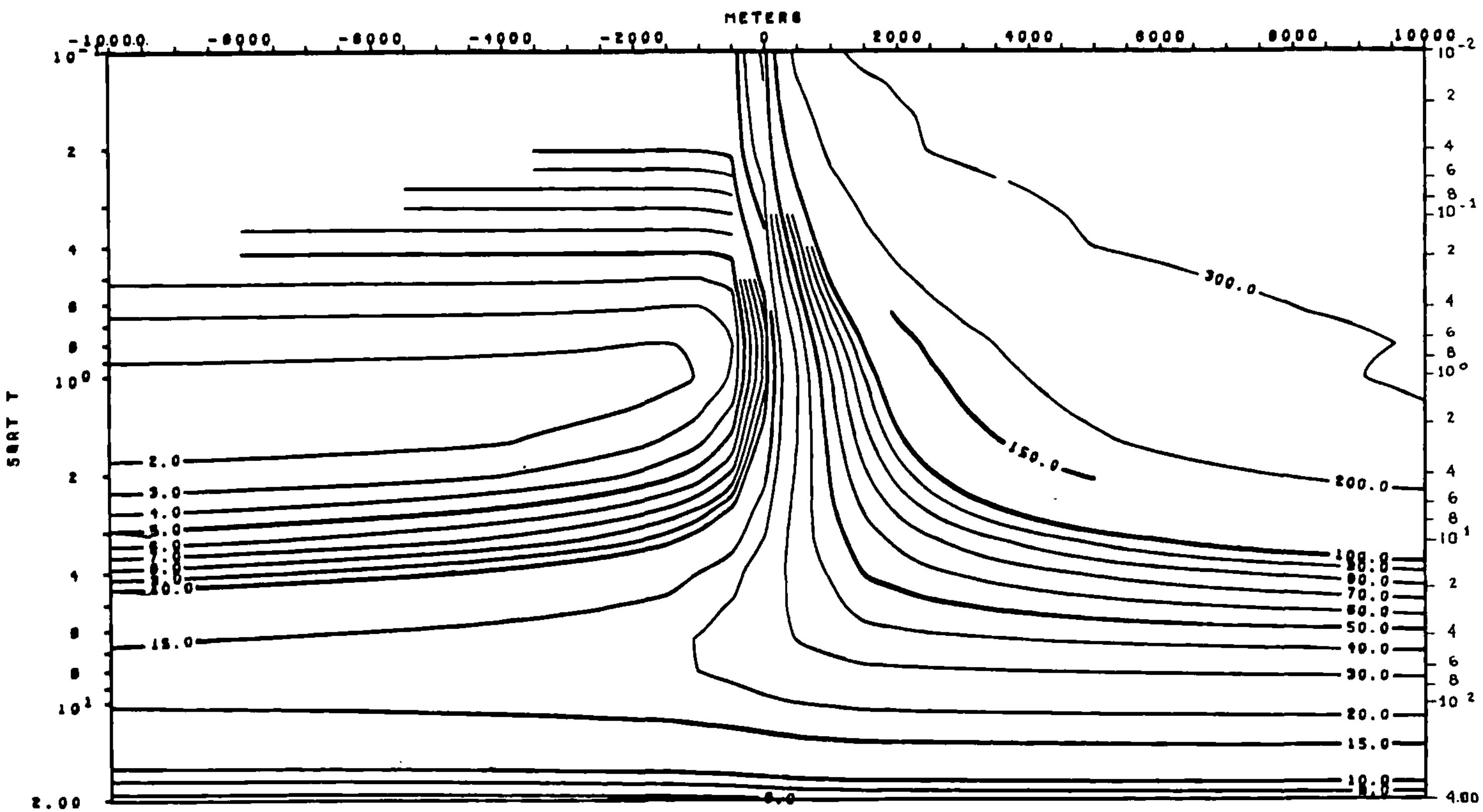

TE MODE
APPARENT RESISTIVITY VS. PERIOD (T)
MODEL 6-b

XBL 786-1921

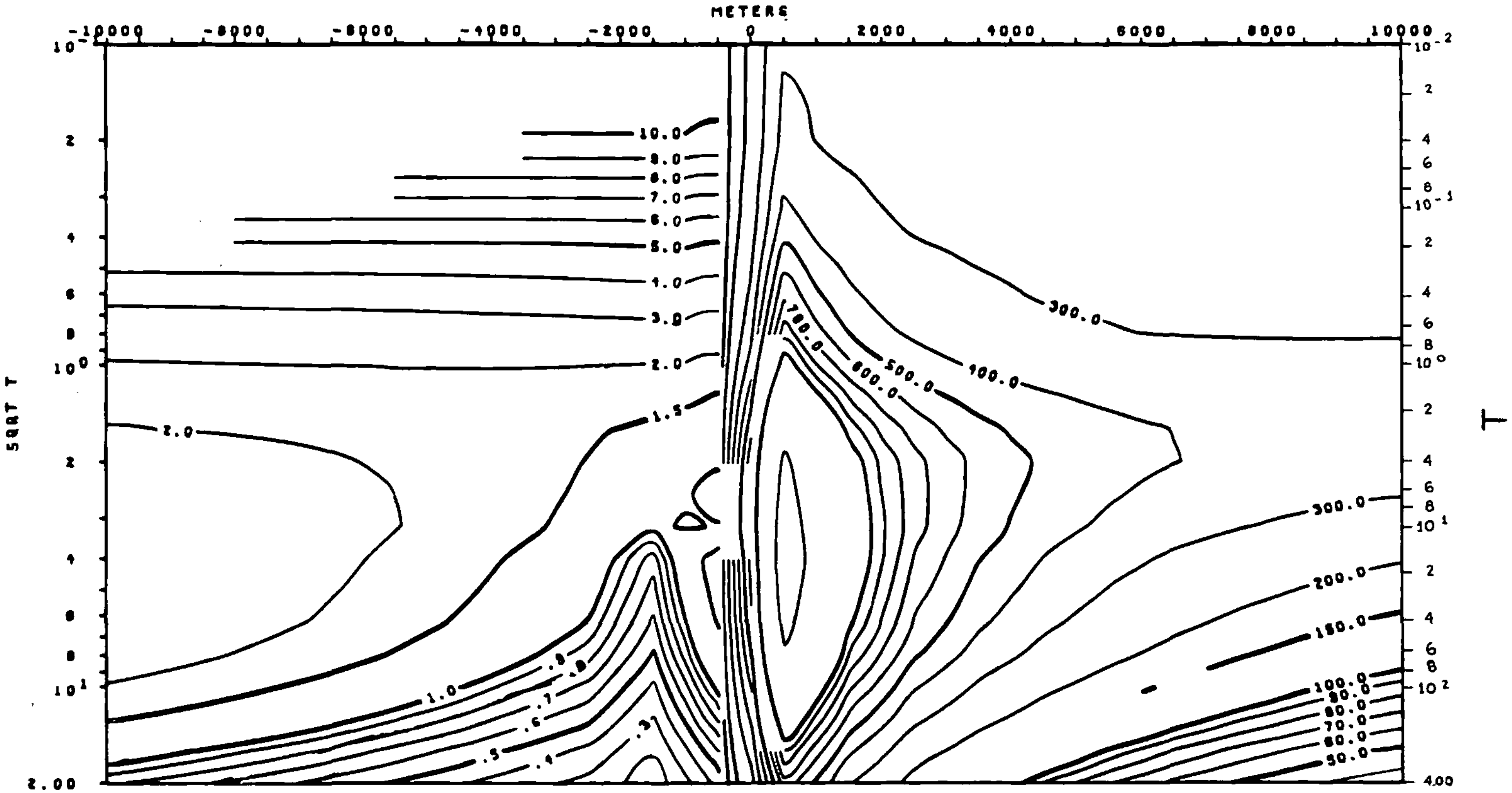

TM MODE
APPARENT RESISTIVITY VS. PERIOD (T)
MODEL 6-b

XBL 786-1922

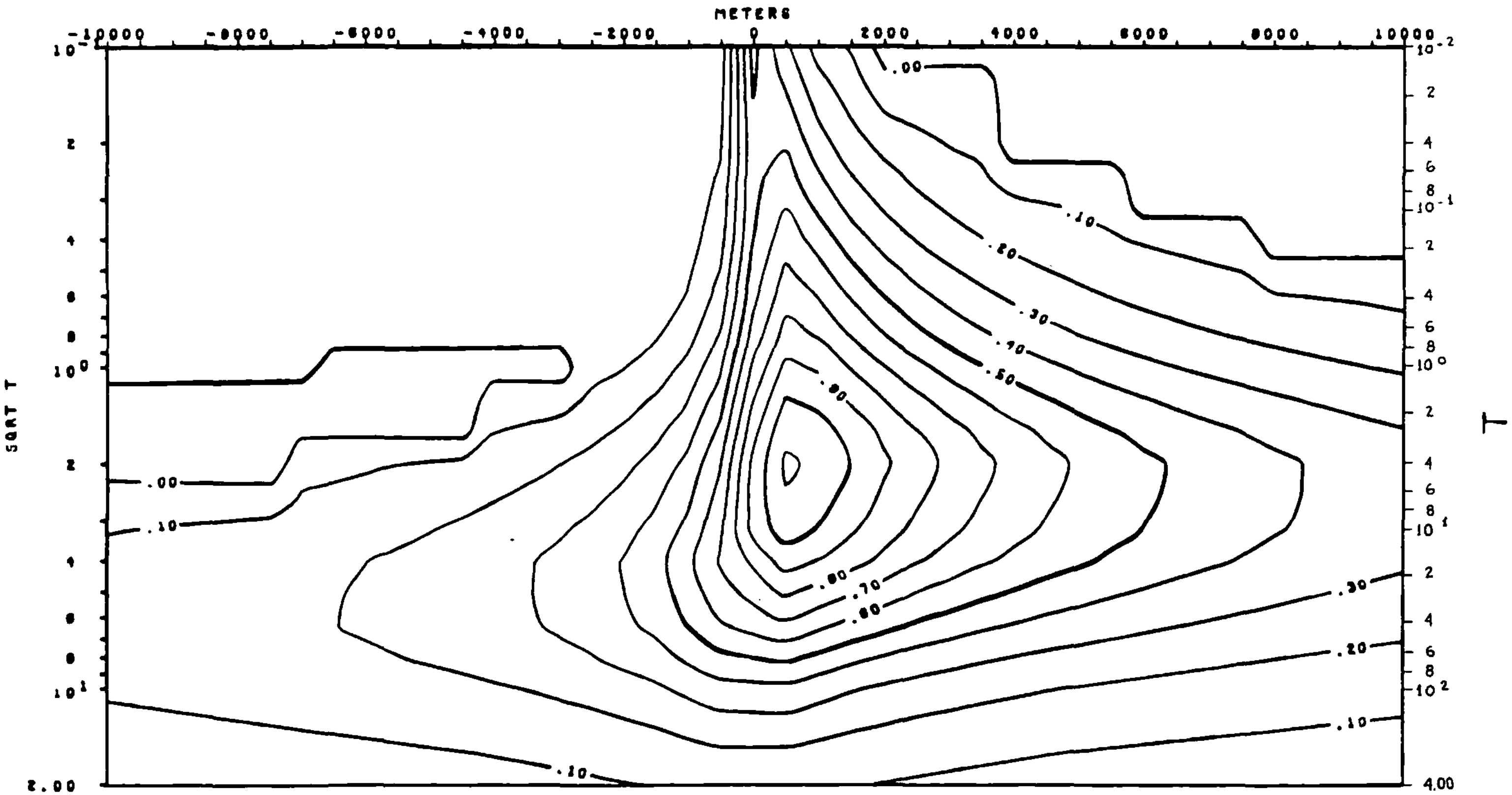

TIPPER VS. PERIOD (T)
MODEL 6-b

XBL 786-1939

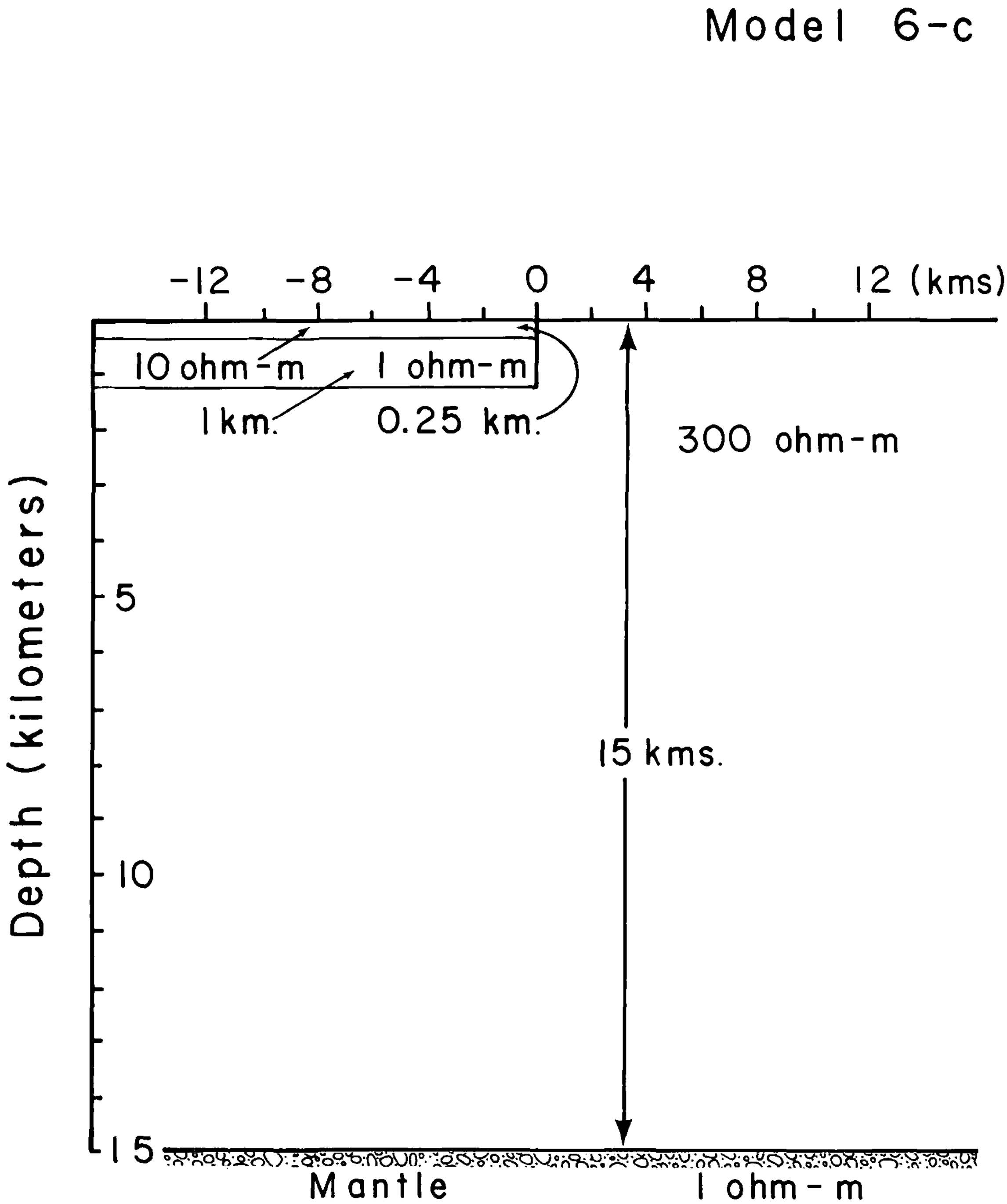
Model 6-c
-12
-8
-4
0
4
8
12 (kms)
10 ohm-m
1 ohm-m
1 km.
0.25 km.
300 ohm-m
Depth (kilometers)
5
10
15
15 kms.
Mantle
1 ohm-m

XBL 786-1961

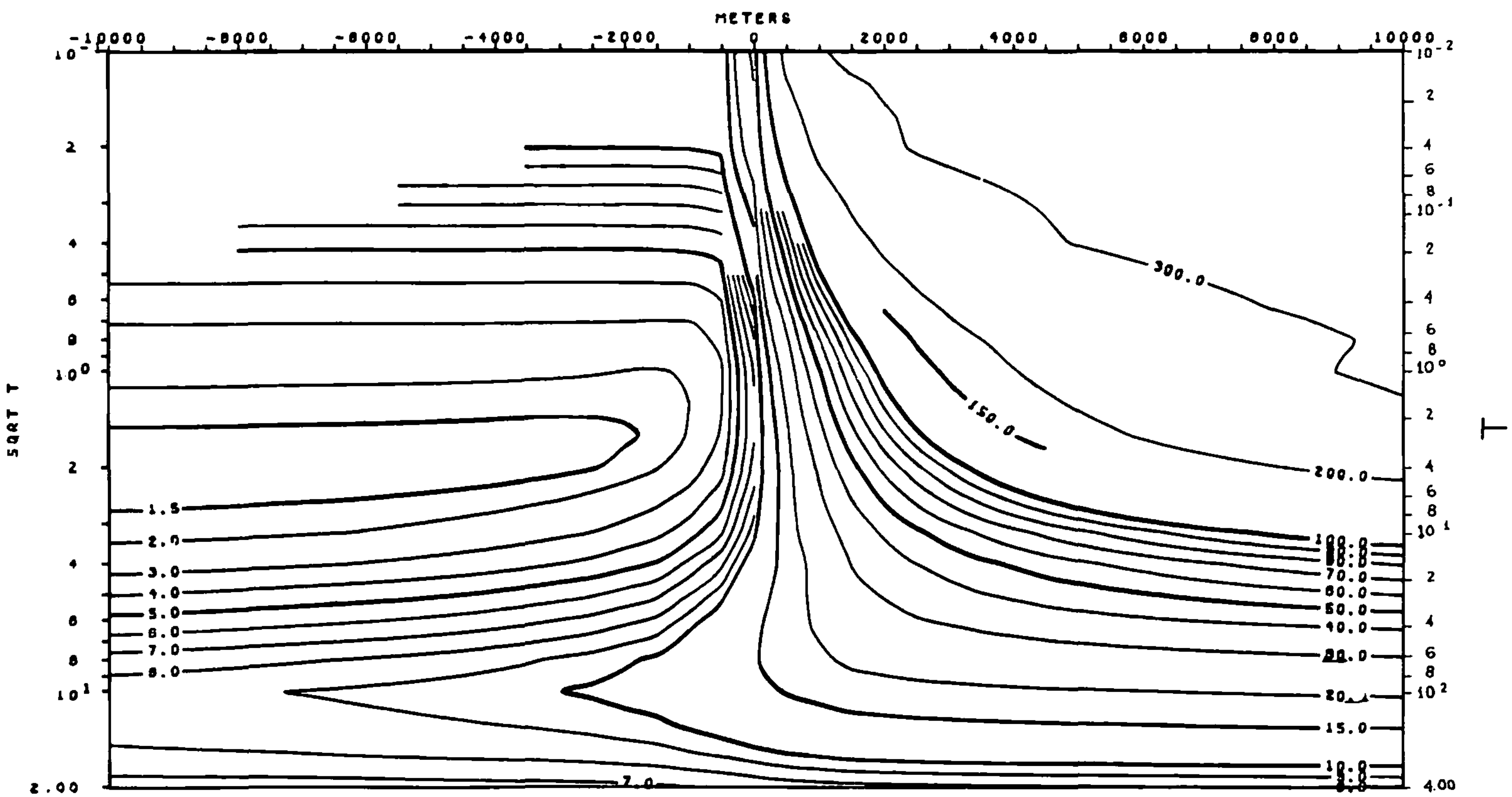

TE MODE
APPARENT RESISTIVITY VS. PERIOD (T)
MODEL 6-c

XBL 786-1940

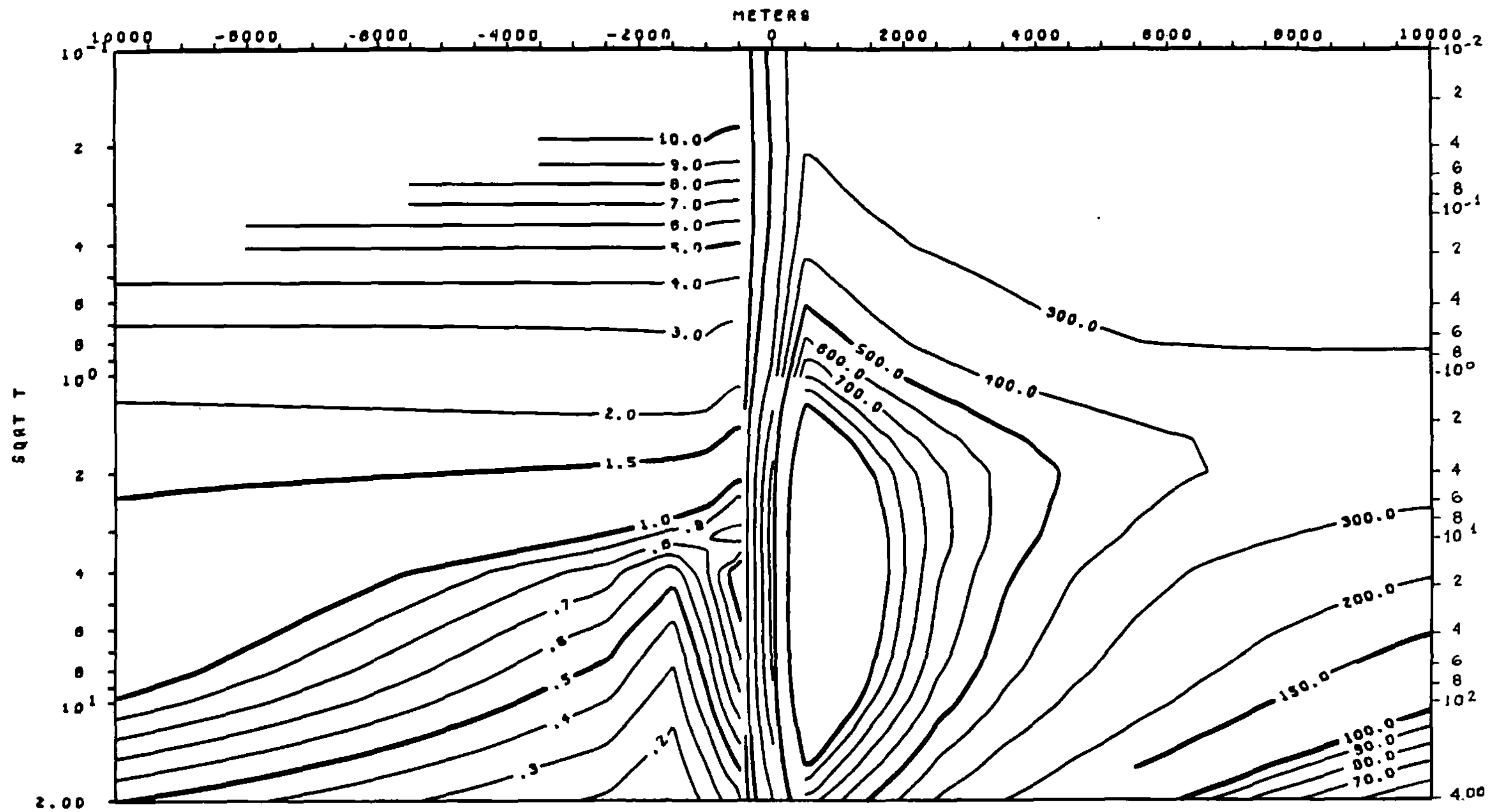

TM MODE
APPARENT RESISTIVITY VS. PERIOD (T)
MODEL 6-c

XBL 786-1924

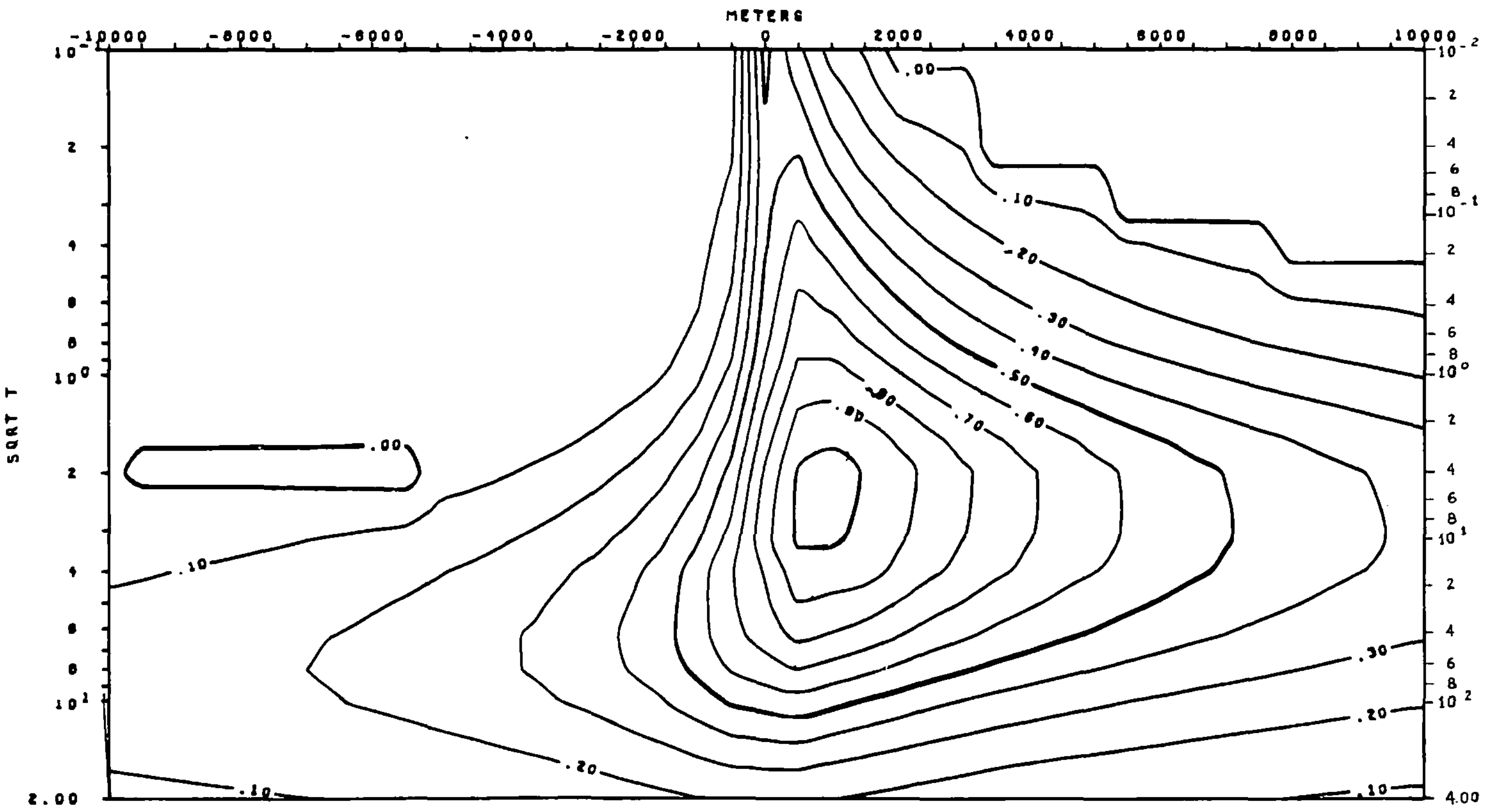

TIPPER VS. PERIOD (T)
MODEL 6-c

XBL 786-1941